MASTER'S THESIS

Spatial snow climatologies for Switzerland: Intercomparison and validation

Department of Environmental Systems Science, ETH Zurich
Institute for Atmospheric and Climate Science

Supervisors:
Dr. Stefanie Gubler, MeteoSwiss
Dr. Christian Steger, ETH Zurich
Dr. Sven Kotlarski, MeteoSwiss
Dr. Simon Scherrer, MeteoSwiss
Prof. Dr. Christoph Schär, ETH Zurich

Monika Göldi
16-934-283
Zurich, April 2021

Abstract

Snow is a key component in various environmental and economic sectors like winter tourism, hydrology, and ecology. Snow cover is an important part of the cryosphere and has a high albedo, which alters the surface energy fluxes. Therefore, snow data over Switzerland is important for monitoring the snow distribution and determining past snow changes. In this thesis two different reanalysis data sets (ERA5, COSMO-REA6), a land surface model (ERA5-Land), remote sensing data (AVHRR Uni Bern), two high resolution snow models (SNOWGRID, OSHD), and an observational data set provided by MeteoSwiss and the Swiss Federal Institute for Snow and Avalanche Research are used to analyse the Swiss snow climatology for the periods 1999-2019 and 1982-2019. Two versions of the OSHD exist, one with data assimilation and one without data assimilation. The gridded data sets have a horizontal resolution between 1 and 30 km. The performance of the data sets is assessed by comparing the gridded data sets against the observational data, and the high resolution snow model output of OSHD with data assimilation (OSHD_EKF). A spatio-temporal analysis for the snow indicators SWE, number of snow days, day of maximum snow, and snow cover fraction is conducted in 11 different regions of Switzerland and six elevation classes.

The mean SWE values for the period 1999-2019 shows that the high-resolution data sets have a very small bias and a high correlation with OSHD_EKF in all regions. For example, in the Engadine, SNOWGRID and OSHD_CL overestimate the mean SWE with a bias of 0.05 m SWE and 0.008 m SWE, respectively. The coarser data sets COSMO-REA6 and ERA5 show weak correlations and larger biases. In the Engadine, COSMO-REA6 has a poor performance with a bias of 0.1 m SWE. In all regions, the data sets show a negative SWE trend. A strong relative trend is found in the Valais, with OSHDCL, SNOWGRID and ERA5-Land having almost the same percentage decrease (-35%, -37%, -38%) and ERA5 having a slightly larger decrease (-58%). The analysis of altitude classes shows that the relative trend is strongest in the lower three altitude classes and weaker in the higher altitude classes. For example, in the southern part of Switzerland the relative trend of OSHD_CL is -84% for 0-500 m, -40% for 500-1000 m, -31% for 1000-1500 m, -19% for 1500-2000 m, -16% for 2000-2500 m, and -17% for >2500 m.

The analysis of the number of snow days showed that all data sets overestimate the number of snow days for all regions. For instance, the number of snow days of AVHRR in the Swiss Plateau is 16, OSHD_CL shows 51, OSHD_EKF 31, and SNOWGRID 28 snow days. A negative trend is found in all regions, the trends in the northern part of Switzerland are slightly stronger than in the southern part.

For the day of maximum snow, the high-resolution data sets show very similar results, whereas the coarse resolution data sets vary more amongst each other. A negative trend is found in all regions, meaning that the timing of the maximum snow occurs earlier with time. The day of maximum snow benefits from high spatial resolution. High resolution seems to be important to accurately predict the timing of maximum snow.

The analysis of the snow indicator snow cover fraction showed that all data sets overestimate the snow cover fraction in all regions compared to AVHRR. The 1 km data sets show biases of the same order of magnitude, whereas the other data sets have higher differences among them. A negative trend is detected in all regions, whereby SNOWGRID and OSHD_CL show similar trends in most regions (e.g. -17% in the southern part of Switzerland).

Contents

List of Figures

List of Tables

1 Introduction

1.1 General motivation

Snow plays a major socio-economic role in mountainous regions. The ecosystem is highly sensitive to changes in snow cover duration and snow depth. For example, earlier snowmelt influences the timing of vegetation onset (Pettorelli et al. 2007). Moreover, many alpine regions depend on winter tourism as a major source of income (Elsasser and Bürki, 2002). Ski tourism heavily relies on sufficient snow conditions, and there are substantial negative consequences during snow deficient winters (Koenig and Abegg, 1997). For example, in winter 2019/2020 only the altitudes above 1700 m had sufficient snow, while at medium and low altitudes the snow conditions were critical for winter tourism (Trachsel et al, 2020). Further, snowfall in winter contributes to river runoff in summer as snowpack stores water during spring, which is e.g. relevant for hydropower production (Anghileri et al., 2018). Hydropower is responsible for more than half of Switzerland's electricity production and is generally a major power production component in the alpine region (Anghileri et al., 2018; Bundesamt für Energie, 2020).

Due to climate change, the amount of snow has diminished, the zero-degree line has shifted upwards 300-400 m since the 1960s (CH2018, 2018), the number of snow days has decreased since the 1970s (CH2018, 2018), and a decline of snow water equivalent (SWE) was detected at elevations between 500 m and 3000 m (Marty et al., 2013). Consequently, many sectors will have to adapt to changing seasonal distribution of snow and water availability. For example, warming leads to less snowfall and earlier snowmelt, resulting in less available water in the spring and summer, requiring adaptation of the agricultural sector (Wu et al., 2015). Another example is the adaptation of the tourism sector. Here, the expected warming results in a shorter skiing season and a shift of the snow line to higher elevations (Abegg et al., 2007; Steiger, 2010) and adaptations include a higher production of artificial snow (Steiger, 2010).

Changes in snow coverage can be assessed by evaluating in-situ and modelled data sets. These data sets cover both different spatial scales and measured quantities, and can be used for adaption measurements and management strategies. However, little is known about their quality of representing spatio-temporal snow cover patterns in Switzerland. For these reasons, this master's thesis analyses various data sets to understand the Swiss snow climatology.

1.2 Background

1.2.1 Snow in the climate system

Snow is an important link between the atmosphere and the surface and has a large influence on the climate system (IPCC, 2013). For example, snow has a higher albedo than the underlying darker surface, and therefore reflects more radiation back to space (IPCC, 2013). This is known as the snow-albedo feedback, which is one of the most important positive feedbacks that alters the surface energy balance (IPCC, 2013; Hall, 2004). For instance, in Switzerland, the daily mean temperature in spring is on average around 0.4°C higher on a snow free surface compared to a snow covered surface at the same location (Scherrer et al., 2012). Moreover, snow has a low thermal conductivity, and can therefore have an insulating effect on the underlying ground, and the degree of insulation of the ground depends on the snow cover (Luetschg et al., 2008). A snow cover with a thickness above 60 cm insulates the ground and protects, for example, the permafrost from thawing when the air is warmer than the surface below the snow (Luetschg et al., 2008).

1.2.2 Spatial distribution of snow

Switzerland, the study region, is characterized by high topographic variability. It consists of the Alps, the Jura mountains, and the lowland Plateau. Around 50% of the country lies above 1000 metres above sea level (m a.s.l.) and around 25% is located at altitudes above 2000 m a.s.l. (Eidgenössische Forschungsanstalt WSL, 2012). On average, sites around altitudes of 1500 m a.s.l. receive 30% of their annual precipitation as snow, and sites above 2000 m.a.s.l receive even half of the precipitation as snow (Eidgenössische Forschungsanstalt WSL, 2012). Snow in alpine regions has a high spatio-temporal variability (Scherrer et. al, 2013). The formation of snow, deposition and redistribution of snow depends on many variables and physical processes that act on different scales. Variables that determine the formation of snow include temperature and precipitation. In Switzerland, one of the components that determines the distribution of precipitation is topography. In complex terrain, moist air masses that are blocked by mountains are forced to ascend. At higher altitudes the temperatures are cooler, and the saturation pressure is lower (Whiteman, 2000). When the saturation level is reached, clouds form and the precipitation starts. Moreover, the distribution of snow depends on temperature. The lapse rate describes how the temperature changes with altitude showing that the temperature decreases with increasing altitude, which favours the snow formation.

With the distribution of snow at different altitudes, it is found that snow depth increases with altitude up to a certain point, where the peak is reached, which is followed by a decrease at the highest altitudes (Grünewald et al., 2014). This shape is explained with a generally positive elevation gradient of snow fall, modified by the interaction of snow cover and topography. At lower elevations, only a part of the winter precipitation falls as snow due to higher temperatures, while total precipitation increases with elevation. (Eidgenössische Forschungsanstalt WSL, 2012). Moreover, the variability of snow depth is influenced by the surface roughness, whereby rougher surfaces are covered with less snow than smoother terrain as rougher terrains are steeper and have a higher wind exposure (Lehning et al., 2011). Wirz et al. (2011) found that steeper terrains have less snow than flatter terrains in the vicinity, which could be accounted to wind exposure, avalanching and higher irradiation.

Further, vegetation influences the snow depth. For example, in forests, the amount of snow on the ground changes within a short distance due to snow deposition on trees and due to the shading that lead to heterogeneous melting patterns (Stähli and Gustafsson, 2006). Observing a period of over 30 years, Stähli and Gustafsson (2006) found that the average maximum annual SWE and the SWE in forests is about half of that in open areas.

1.2.3 Temporal distribution of snow

In the Swiss Alps, strong negative snow trends were observed in the 1980s and 1990s (Laternser Schneebeli, 2003), which can be attributed mainly to local temperature increases, whereas precipitation is not the driving factor (Scherrer et al., 2004). These trends have a high altitudinal dependency, at high altitudes they are less pronounced than at low and medium altitudes (Laternser Schneebeli, 2003). The observed changes at the end of the 1980s in snow amounts are abrupt, and a significant step-like decrease for snow days was observed (Marty, 2008). Simultaneously, the European winter temperature shows a step-like increase at the end of the 1980s, which shows that the phenomena originates from a larger scale rather than on a regional scale (Marty, 2008). Sippel et al. (2020) suggest that the abrupt winter warming is caused by random atmospheric circulation variability superimposed upon a long-term and relatively homogenous warming trend, and no external cause or change of the underlying dynamics of the system is required. This could be explained by large scale flow patterns (Marty 2008), and no clear trend can be found after the regime shift.

Large-scale atmospheric circulation patterns such as the North Atlantic Oscillation (NAO) have an influence on the inter-annual snow cover variability. However, the influence of the North Atlantic Oscillation on snow variability is difficult to quantify in the Swiss Alps. It was identifed as the third major pattern of determining the snow pack variability (Scherrer and Appenzeller, 2006). Beniston (1997) showed that winters with little snow are linked to alpine high-pressure episodes. These persistent high-pressure systems are linked to the positive phase of NAO accompanied by positive temperature anomalies and below average precipitation. Scherrer and Appenzeller (2006) found that 50% of the Swiss alpine snowpack variability is related to the formation of atmospheric blocking patterns over Europe, and the relationship is not robust over several decades as it varies over time depending on the considered variable and altitude.

1.2.4 Applicability of existing snow data sets

For the analysis of the spatio-temporal variability and distribution of snow, various data sets such as observations or simulations are available. These data sets cover a wide range of horizontal resolutions, from coarse (> 30 km), intermediate (10-30 km), high (1-2 km) resolution to in-situ (point). The type of data sets includes e.g. measurements (ground and satellite), atmospheric reanalyses and high-resolution snow models. However, each data set has its own shortcomings, e.g. satellite data sets do not measure the amount of snow. In the following, a few examples of studies based on different data sets are shortly described with a focus on differences in the data sets in terms of resolution and parameterization. Dutra et al. (2011) investigated land surface model simulations and determined the impacts of horizontal resolution, parameterization of snow physics and atmospheric forcing on snow cover representation by running simulations at a horizontal resolution of 200, 80, and 25 km. The simulations were compared to station data, and the analysis showed how well the model simulated different snow characteristics, like the snow mass in Switzerland or the snow cover duration in Europe. They found a superior performance of high-resolution simulations for areas with complex terrain. In flat terrain, the impacts of snow physics and atmospheric forcing dominate snow characteristics. A study by Steger et al. (2013) compared regional climate models (RCM) with a spatial resolution of 25 km over Switzerland, driven both by reanalysis and global climate models (GCM), and found that RCMs in general reproduce the spatial and seasonal variability of snow cover well. However, the models underestimate the SWE at low altitudes and overestimate the SWE at high altitudes (Steger et al., 2013). They state that the results are limited by the low horizontal resolution of the data set as a 25 km RCM grid does not represent elevations above approximately 2700 m. Moreover, Terzago et al. (2017) analysed the greater alpine region using various remote sensing products of intermediate resolution and reanalysis products of low resolution. They found that different products show a heterogeneous picture of SWE distribution, meaning that the spatial and temporal distribution of snow is variable and is specific for each area. The knowledge of long-term variability at increased horizontal resolution is limited and Terzago et al. (2017) suggest that data sets with high resolution can better represent the snow processes and the topography.

1.2.5 Research gap

Various data sets have been used to analyse the snow distribution and other characteristics over Switzerland. However, there is no spatially high resolved data set at climatological scale and it is not clear which available data set reproduces which aspect of the Swiss snow climatology best. From previous studies, we know that coarse and intermediate scale products are not able to resolve small scale details. Therefore, we are rather interested in the overall performance of the coarse scale products, knowing that small scale processes are not resolved. These coarse scale products cover larger regions seamlessly, and it is interesting to asses their performance as they can be used to study snow on larger scales. Their performance of the spatio-temporal snow distribution in Switzerland is largely unknown. The mentioned studies suggest that higher resolution improves the general representation of topography and captures higher altitudes. Studies using high-resolution snow models and high-resolution reanalyses are less frequent. High-resolution snow models which produce the climatological snow cover over Switzerland exist but knowledge on their quality is not available. There is a knowledge gap regarding the ability of different spatial snow data sets to reproduce real snow distribution over Switzerland. This thesis will investigate various snow data sets and their performance, and thereby provide new insight on the Swiss snow climatology.

1.3 Research questions

In this study, we will investigate how various data sets of different resolution (i.e. point measurements to gridded data sets of 1 km to 30 km horizontal resolution) represent the Swiss snow climatology over the last 30 years. Therefore, we carry out a spatio-temporal analysis on different snow indicators in nine regions of Switzerland and six altitude classes. Through these analyses, we aim at answering the following research questions:

- Do existing data sets represent the spatio-temporal variability of Swiss snow cover, and to what extent do they agree or disagree with each other?
- Do certain products reveal superiorities or weaknesses in specific geographical regions, elevations, or seasons (e.g. during accumulation/ablation) in representing snow cover?
- Are high-resolution reanalyses suitable for snow monitoring in the alpine region in Switzerland?

2 Data and study region

2.1 Study region

The analysis is carried out for Switzerland, characterized by the Alps and the Jura, which form areas with more complex terrain, and the lower laying Swiss Plateau. Based on the 149 warning regions of the Swiss Federal Institute for Snow and Avalanche Research (SLF), Switzerland is divided into the following nine regions: Northern flanks of the Alps (western, central and eastern part), Valais, northern and central Grisons, central part of the southern flank of the Alps, Engadine/eastern part of the southern flank of the Alps, Jura and the Swiss Plateau (Figure 1). These regions are further merged into northern and southern Switzerland. The regions are chosen due to their geographic and climatological characteristics.

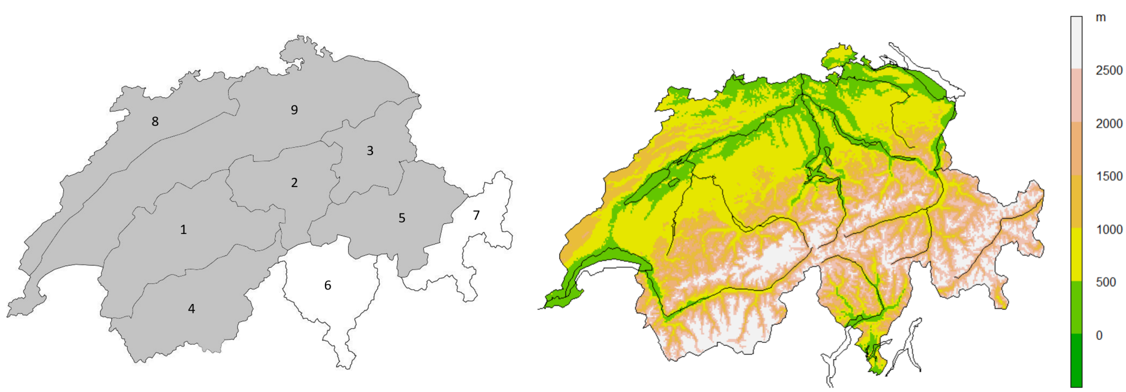

(a) Regions (b) Topography

Figure 1: Map of Switzerland. (a) The nine study subregions are shown: 1. Western part of the northern flank of the Alps, 2. Central part of the northern flank of the Alps, 3. Eastern part of the northern flank of the Alps, 4. Valais, 5. northern and central Grisons 6. Central part of the southern flank of the Alps, 7. Engadine/eastern part of the southern flank of the Alps, 8. Jura, 9. Swiss Plateau. Subregions 6 and 7 are joined into southern Switzerland (white), the remaining subregions merge into northern Switzerland (grey). (b) The topography of Switzerland at a 1 km horizontal resolution is shown.

2.2 Data sets

The analyses are based on observational data, reanalysis, remote sensing, a land surface model and two high-resolution snow models. In the following, each data set is described, and an overview of the horizontal resolution and the temporal data availability can be found in Table 1 and Figure 3, respectively. AVHRR and OSHD_EKF serve as reference data sets because AVHRR is an observational data set and OSHD_EKF has station measurements as input data. Therefore, they are believed to be the most accurate.

2.2.1 Observational data

In-situ observations

The in-situ observations are provided by MeteoSwiss and SLF. Two data sets, which consist of daily total snow depth (cm) and SWE (m.w.e.) are available: one contains 139 stations measuring continuously since 1999, and the second one contains 27 stations measuring since 1982 (Figure 2). A limitation of the data set is temporal inhomogeneities, which might affect trend analyses. Further, in-situ snow depth measurement are only representative for a larger surrounding in relatively flat homogeneous terrain. In complex terrain, it is difficult to find such an area, and thus the point scale snow measurements are only representative for the narrow vicinity of the observation sites. This is the reason why many snow measurements are made in flat terrain, which is more predisposed to snow accumulation (due to wind and topographic effects), and thus tends to overestimate the amount of snow. Moreover, the observation sites are not evenly distributed across the elevations. Higher elevation sites are underrepresented due to the often difficult access.

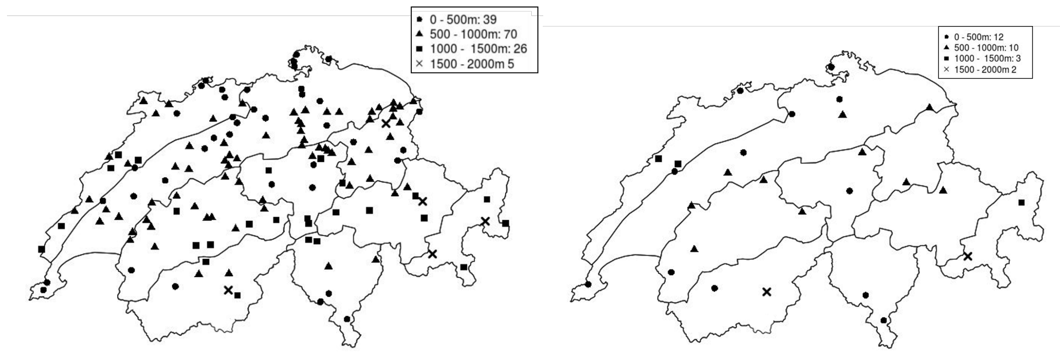

(a) Regions (b) Topography

Figure 2: Station distribution over Switzerland for the period 1999-2019 on the left (a), and for the period 1972-2019 on the right (b). A circle denotes stations between 0 - 500 m, triangle stations between 500 - 1000 m, square stations between 1000 – 1500 m and cross stations between 1500 - 2000 m. The number next to the symbols are the numbers of stations that fall within that altitude category.

Remote Sensing Data set: AVHRR
Remote sensing data can be used to analyse the spatio-temporal snow cover variability as it covers large and also remote areas. Optical remote sensing gives no information about the actual snow depth and only says whether a grid cell is covered by snow or not. In this thesis, the remote sensing product Advanced Very High Resolution Radiometer (AVHRR) of the University of Bern will be used. It covers the European Alps for the time period 1991 - 2016 at a horizontal resolution of 1 km (Hüsler et al., 2014). Limitations of the data sets are due to cloud cover that blocks the surface view and clouds being misclassified as snow. Moreover, it is difficult to detect snow below dense vegetation. Due to too large data gaps some years were dropped for this analysis.

2.2.2 Model data

Model data is available for different variables and resolutions. If required atmospheric forcing data is available. Models can produce data over a consistent spatial and temporal resolution over multiple decades. However, models do not fully represent reality as they are only an abstraction of reality and underlie systematic and random errors. Model uncertainties arise from the simplified representation of physical processes, spatio-temporal discretisation and limited resolution, and uncertainty in the input and model parameters.

Reanalysis
Climate reanalyses produce a record of the climate on a gridded field by combining a numerical weather prediction model with observations (ECMWF, 2020). The reliability of reanalyses depends on the chosen location, time period, and variable as the spatial density and types of assimilated observational data sets varies. In this thesis, the following reanalysis products will be evaluated:

- ERA5 is the 5th generation atmospheric reanalysis produced by European Centre for Medium-Range Weather Forecasts (ECMWF) (Copernicus Climate Change Service, 2018). It has a global horizontal coverage at a resolution of 30 km and a temporal coverage from 1979 to present. ERA5 provides hourly estimates of atmospheric, land and oceanic climate variables. The data is available on the Copernicus Climate Change Service (C3S) Climate Data Store.

- COSMO-REA6 is a high-resolution regional reanalysis product produced by the Hans-Ertel Centre for Weather Research and the German Weather Service (Hans-Ertel-Zentrum für Wetterforschung, 2020). The development of COSMO-REA6 is based on the numerical weather prediction model COSMO (consortium for small-scale modelling). It covers the European continent at a horizontal resolution of 6 km for the period 1995 - 2019, and it is driven with ERA-Interim at lateral boundaries.

Land surface model
Land surface models (LSM) provide a consistent record of land variables for the past decades. In this thesis, the ERA5-Land product, which has a global coverage and is available for the period 1981 to present (Copernicus Climate Change

Service, 2019), will be used. ERA5-Land is a re-run of the ECMWF ERA5 Land component with a finer horizontal resolution of 9 km. Information about surface variables is produced at hourly temporal resolution and available for 1981 to present from C3S.

High resolution snow models

The snow models are run as a temperature-index model which calculates the melt rates of snow from air temperature. The available input data consist of gridded temperature and precipitation data. To run a calculation of a full climatological surface energy balance for Switzerland further input data like humidity, wind speed, radiation fluxes, etc. are needed. No data sets for these other atmospheric variables are available for Switzerland, hence temperature-index models have to be applied. Here, we evaluate two high resolution snow models (HRSM):

- SNOWGRID-CL is the climatological version of SNOWGRID that was developed by the Austrian weather service (ZAMG) (Olefs, 2019). In its climatological version, it is based on a temperature-index model and uses temperature and precipitation as input data. The data sets for Switzerland consist of daily snow depth (cm) and SWE (m.w.e.) for the period 1971 - 2019 at a horizontal resolution of 1 km. Hereafter, SNOWGRID-CL is referred to as SNOWGRID.

- OSHD is the operational snow-hydrological model produced by SLF (SLF, 2020). The climatological version of the OSHD is based on a temperature-index model, which uses the same precipitation and temperature data as SNOWGRID to estimate snow quantities and melting rates. It produces daily SWE (m.w.e) over Switzerland at a horizontal resolution of 1 km. Two versions are available:

  - OSHD_EKF: spans the period from 1998 to present. In this version, snow observations are assimilated using an extended Kalman filter, which adjusts the model output to the snow depth observations of the stations in Figure 2. OSHD_EKF is used as a reference data set.
  - OSHD_CL: spans the period 1961 – 2019, no data assimilation was applied.

Table 1: Overview of the data sets with type and horizontal resolution. RS denotes remote sensing, HRSM high resolution snow model, and RA reanalysis.

Name	Type	Horizontal Resolution
ERA5	RA	30 km
ERA5-Land	LSM	9 km
COSMO-REA6	RA	6 km
SNOWGRID	HRSM	1 km
OSHD_CL	HRSM	1 km
OSHD_EKF	HRSM	1 km
AVHRR	RS	1 km
Station observation	in-situ	point

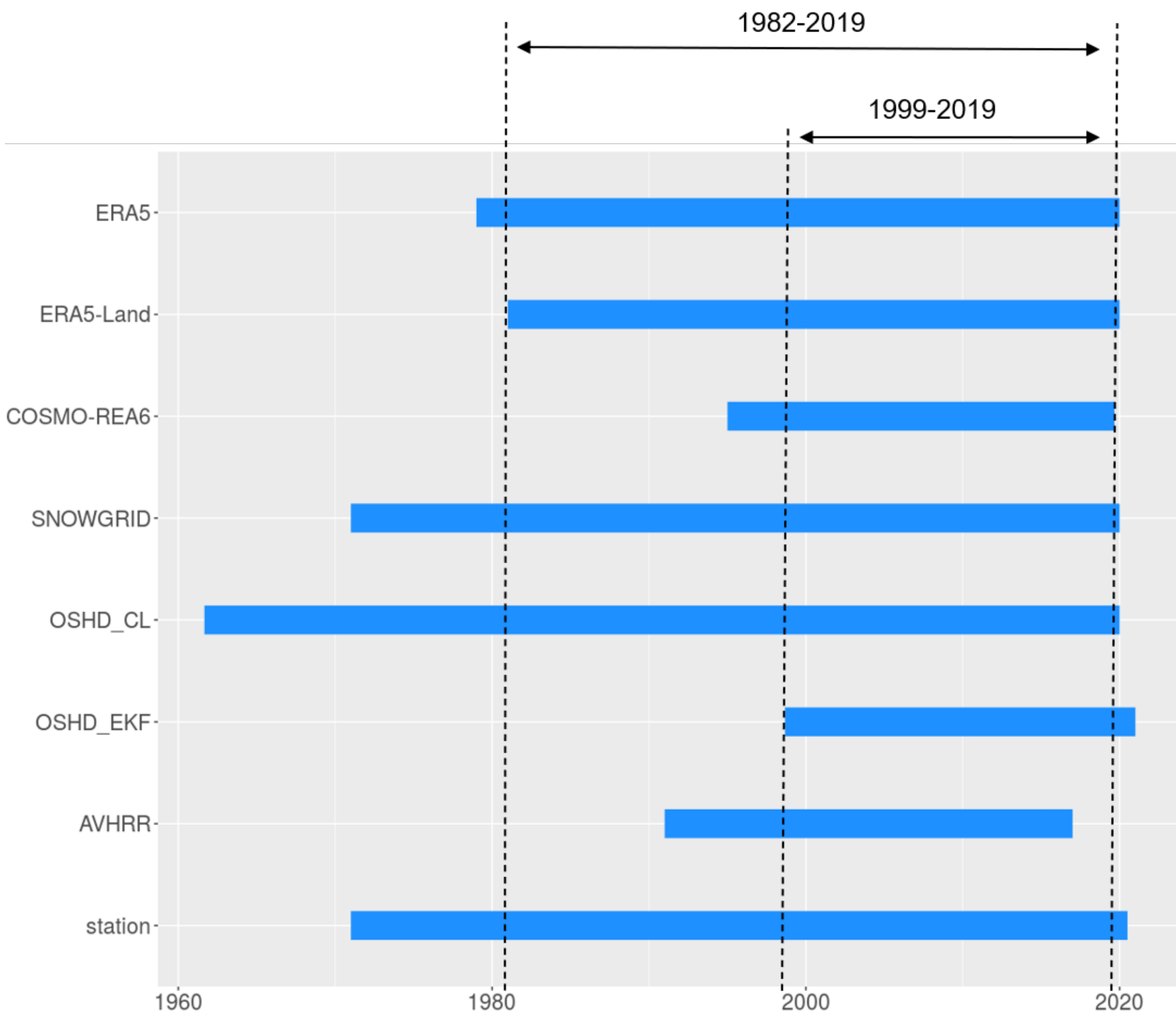

Figure 3: Time periods of all data sets. Time spans from 1961 to 2020. The data sets are sorted from lowest to highest resolution (from top to bottom). The dashed vertical lines indicate two time periods, one from 1999-2019 to compare climatologies for all data sets and the longer period 1981-2019 for trend analysis.

3 Methods

This chapter introduces the data pre-processing, which includes the identification of snow accumulating grid cells and the temporal gap-filling of AVHRR data. Subsequently, the calculation of the yearly and monthly climatology and trends are presented. Finally, the definition and computation of the snow indicators are described.

3.1 Data pre-processing

Before the spatial and temporal analysis can be performed, the snow data must be pre-processed due high-elevated grid cells in the models that exhibit perennial snow accumulation. Due to the lack of a sub-grid parameterization and the proper treatment of snow on glaciers, snow output from these grid cells must be pre-processed. Snow accumulation over several years is a realistic phenomenon, which happens above the Equilibrium Line Altitude in glaciated areas. However, glaciers are, due to the lack of representing relevant processes and the coarse horizontal model resolution, not captured. Accumulated SWE values are thus somewhat arbitrary and largely depend on the previously modelled temporal interval.

In the OSHD and the SNOWGRID model run, the amount of snow on September 1 is set to 0 because the available quantity of water for the year is of interest. For consistency and to avoid accumulating grid cells, the same procedure is applied for the model output of ERA5 and COSMO-REA6. Thereby, we assure that the models represent snow accumulation for each year separately and that there is no snow from the previous year.

ERA5-Land reveals grid cells that have a minimum SWE threshold above zero for the entire time period, and a seasonal cycle is modelled on top of that threshold. The seasonal SWE cycle modelled on top of the minimal threshold is not realistic and too small compared to neighboring grid cells, potentially due to contamination of glacier points during the interpolation to the regular 0.1x0.1 grid. Therefore, grid cells with a minimum SWE threshold above zero, i.e.grid cells in which SWE does not drop below 1 cm for more than 5 years, are masked out and not implemented in the analysis. So, one must be careful comparing the regions Valais, Engadine, and Central part of the Northern flank of ERA5-Land with the other data sets, as not the same area is used. The masking is only applied for SWE quantities and not snow cover days or snow cover fraction.

Some grid cells of the remote sensing product AVHRR display missing values or clouds values, which leads to gaps in the time series. To obtain a more complete time series, a temporal filter was applied that determines a substitute value in each grid cell without a snow value, a substitute value is sought. For this, we look if a snow value is available seven days into the future and past at a specific gridcell. If a ground observation exists within these 14 days, then the missing value is replaced by the value closest in time. So, if in this 14 day period a snow day is detected, the missing day becomes a snow day. No spatial interpolation is performed. Despite this gap filling, there are still some years that exhibit substantial gaps. Therefore, these years, i.e. 2000, 2001, 2012, and 2013, are not considered in the analysis.

3.2 Snow indicators

Snow cover can be described by snow depth, snow density and SWE. These variables are all connected with each other as the SWE can be determined by snow density and snow depth. The snow model OSHD returns SWE as output, so this variable is used. From the quantity SWE, various snow indicators to characterize snow cover can be derived. In this thesis the following indicators are used:

- SWE: SWE is the depth of water if all snow is melted and its unit is meter water equivalent (m.w.e.). SWE is the output for all models. The station observations are given in snow depth, therefore, a transformation from snow depth to SWE assuming a density was necessary. The mean SWE value for each year or month is calculated as described in section 3.3.
- Number of snow days: For models and station data, a snow day is defined as a day with at least 0.01 m.w.e. The remote sensing product AVHRR has a binary output (snow day/no snow day) and no threshold must be defined. Snow days are summed up over a year.
- Day of maximum snow: The day of maximum snow of a grid cell is the day with the maximum amount of SWE throughout the year.
- Snow cover fraction: The snow cover fraction is defined as the percentage of the gridcells that indicate a snow day.

All indicators can be calculated for all data sets, except the remote sensing product AVHRR and the in-situ observations. AVHRR cannot provide the mean SWE and the day of maximum snow, while a calculation of snow cover fraction in a region is obviously not possible with in-situ observations.

3.3 Spatio-temporal data aggregation and trend calculation

The presented analyses are based on the hydrological year instead of the calendar year. In this thesis, a hydrological year lasts from September 1 of the previous year to August 31 of the year in consideration. For example, the hydrological year 1999 is composed of the months September to December of the year 1998 and the months January to August of the year 1999. This definition is chosen to record the annual balance of the precipitation that has fallen in the previous calendar year in late autumn and winter, and that has been stored as snow during the winter months. The impact of the stored precipitation will only become effective as meltwater in the following year when snow starts to melt. Therefore, it is used in the analysis instead of the calendar year. Hereafter, the hydrological year as defined above is referred to as ”year”.

For each region, the data is aggregated to get a climatology. The yearly/monthly averages of SWE are calculated as follows: for each gridcell the SWE of each year/month over the entire time period are averaged. To obtain the yearly/monthly average over the whole time period of an entire region, the yearly/monthly means of all gridcells are averaged. For instance, the mean of January in the period 1999-2019 for one region is calculated by averaging all values in January over 20 years for each gridcell. To obtain a regional value, these averages of the grid cells within this region are averaged once more.

The number of snow days per region is calculated similarly, the number of snow days per year is counted per grid cell and the regional number of snow days is defined as the spatial median number of snow days of all grid cells in a region. The climatology of the day with maximum snow is determined by first summing up the SWE of all grid cells in a region for each day. Then the day with the highest sum is defined as the day of maximum snow for the region.

To calculate trends in a time series, a simple linear regression (ordinary least squares) is used for continuous variables and a logistic regression is used for indicators that use count data.

3.4 Elevation classes

For SWE, the climatology and trend are calculated for six different elevation classes. These elevation classes are defined as: 0-500 m, 500-1000 m, 1000-1500 m, 1500-2000 m, 2000-2500 m and >2500 m. The data sets show a different distribution of grid cells per elevation class (Figure 4). OSHD_CL and OSHD_EKF have the same elevation profile. ERA5 does not have grid cells above 2500 m in any region.

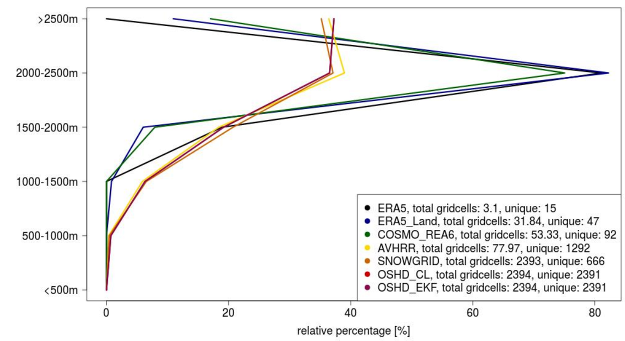

(a) Engadine

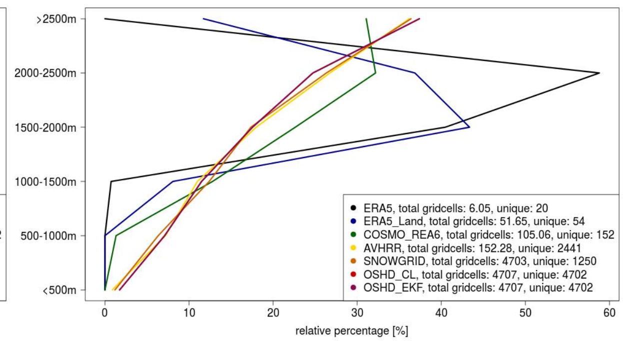

(b) Valais

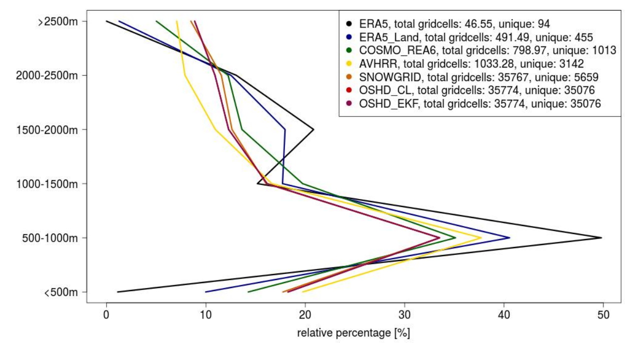

(c) North

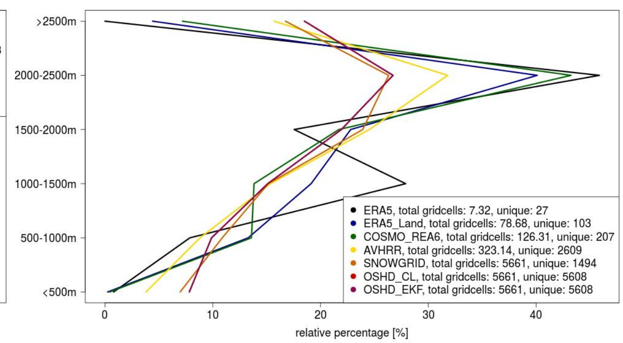

(d) South

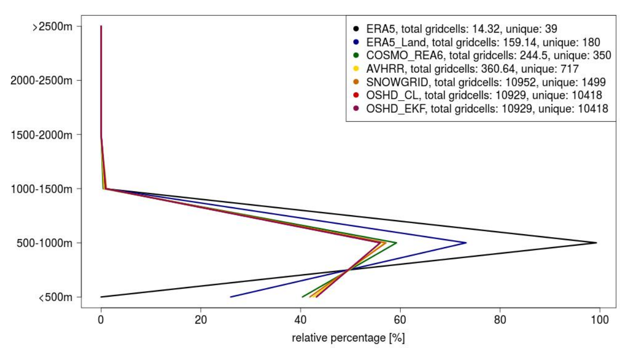

(e) Swiss Plateau

Figure 4: The distribution of grid cells at the six elevation classes for the regions (a) Engadine, (b) Valais, (c) Northern Switzerland, (d) Southern Switzerland, and (e) the Swiss Plateau. Each color represents a data set.

3.5 Nearest grid cell for station

For the snow indicator SWE, a comparison of the 1 km data sets and the station observations are made. As these observations are point data, the nearest grid cell with the smallest difference in elevation is chosen for the comparison. To identify this nearest grid cell, the grid cell in which the station is located and the eight neighbouring grid cells are evaluated for the smallest difference in height. The height difference between the stations and the nearest grid cell is selected to be minimal, nevertheless deviations occur. In Table 2, the biggest elevation differences are shown for OSHD_CL, the remaining stations have small elevation differences. The largest difference is found at the station Kronberg with 103 m.

Table 2: Elevation difference between station and nearest grid cell of OSHD_CL. In the first column, the station abbreviation of the station with the largest elevation difference is given. The second column shows the elevation of the station, the third column the elevation of OSHD_CL, and the fourth column shows the difference between the station and the nearest grid cell. The unit is meter.

[m]	Station elevation	OSHD_CL elevation	Difference
AIR	1139	1216	77
BAS	316	335	19
BSG	280	250	30
KRO	1652	1549	103
KUA	894	942	29
NEU	485	514	29
OBP	687	640	47
OTL	366	410	44

The regions are composed of stations and not all regions contain the same number of stations. The Swiss Plateau has the largest number of stations with 57, followed by the Jura with 18, the eastern northern flank of the Alps with 15, the western northern flank of the Alps with 14, the central northern flank of the Alps with 11, Grisons with 8, the central southern flank of the Alps with 7, the Valais with 6 stations and the Engadine with the least stations of all with 4. To calculate a mean for the region, all stations and their nearest grid cell are averaged.

4 Results

4.1 Mean SWE

In the following sections, different aspects of the mean SWE are described. First, the climatology, variability, and seasonal cycle are shown. Then the anomalies, the deviation of products from the reference data set, the trend, and the distribution in height classes are shown. And afterwards, the comparison btweeen the station observations and the nearest grid cell is shown.

4.1.1 Climatology, variability, and seasonal cycle

The calculated mean SWE over the 20 winters (1999-2019) is displayed in Figure 5 for each data set. Topographical features determine the distribution of snow, higher (lower) altitudes have higher (lower) SWE values. The higher the resolution, the more detail is visible. ERA5 shows the lowest mean SWE in all regions except in the Swiss Plateau (Table 3). Differences between the 1 km data sets are apparent, e.g. OSHD_CL shows more snow in the lower lowland than both OSHD_EKF and SNOWGRID. This is also well reflected in the mean SWE values over the entire period with OSHD_CL showing a mean SWE of 0.008 m in the Swiss Plateau. Whereas OSHD_EKF and SNOWGRID both show 0.003 m SWE. COSMO-ERA6 shows the lowest mean SWE of 0.0024 m, ERA5-Land is close to OSHD_CL with 0.01 m SWE, and ERA5 shows a mean SWE of 0.005 m in the Swiss Plateau (Table 3).

In the Engadine, COSMO-REA6 has more snow than the other data sets. The mean SWE over the entire 20 year period shows that COSMO-REA6 has a mean SWE of 0.26 m, ERA5 0.08 m SWE, ERA5-Land 0.19 m SWE, SNOWGRID 0.18 m SWE, and OSHD_CL and OSHD_EKF both show a mean SWE of 0.13 m SWE. COSMO-REA6 shows double the amount of SWE as OSHD_CL and OSHD_EKF. When comparing the northern part of Switzerland, SNOWGRID and ERA5-Land show the highest mean SWE values with 0.1 m SWE, OSHD_CL and OSHD_EKF show less with 0.08 m SWE and 0.07 m SWE, respectively. COSMO-REA6 has a slightly smaller mean SWE than OSHD_EKF with 0.065 m SWE and ERA5 shows the smallest mean SWE with 0.047 m SWE. To obtain more details such as inter- and intraannual variability, the mean SWE is shown for several regions (Engadine, Valais, north, south, and Swiss Plateau) per year.

Table 3: Mean SWE over the period of 1999-2019 for each region.

[m SWE]	ERA5	ERA5-Land	COSMO-REA6	SNOWGRID	OSHD_CL	OSHD_EKF
Jura	0.003	0.007	0.012	0.018	0.029	0.015
Plateau	0.005	0.010	0.002	0.003	0.008	0.003
Engadine	0.081	0.186	0.260	0.180	0.134	0.126
Grisons	0.083	0.193	0.164	0.149	0.133	0.116
East. northern flank	0.051	0.134	0.054	0.092	0.091	0.087
West. northern flank	0.071	0.139	0.070	0.124	0.102	0.091
Cent. northern flank	0.069	0.155	0.079	0.126	0.112	0.101
Cent. southern flank	0.061	0.122	0.090	0.119	0.107	0.077
Valais	0.102	0.240	0.153	0.284	0.210	0.194
North	0.046	0.099	0.064	0.096	0.082	0.072
South	0.070	0.148	0.162	0.145	0.118	0.096

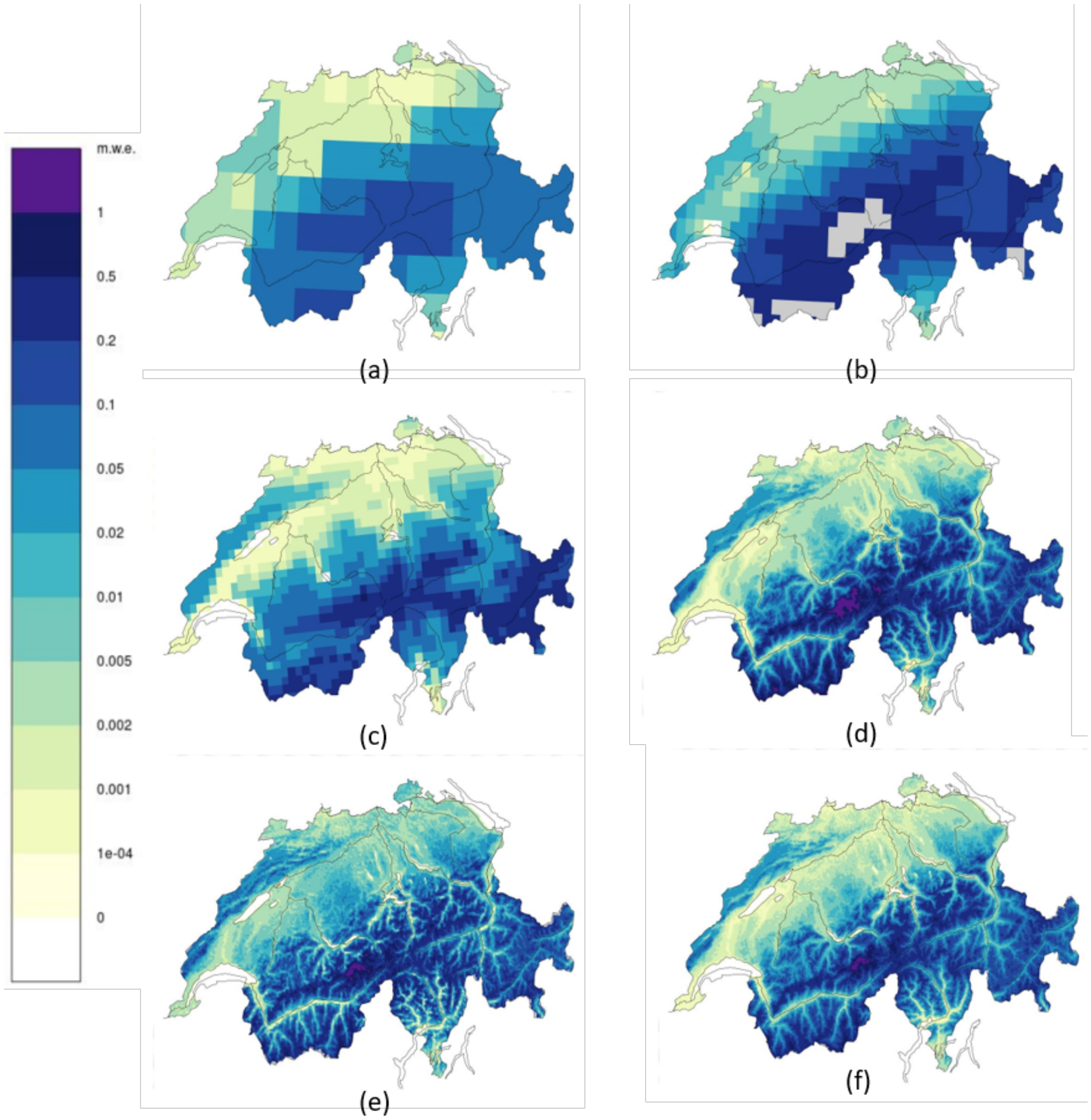

Figure 5: Climatology of mean SWE for the period 1999-2019 for (a) ERA5, (b) ERA5-Land, (c) COSMO-REA6, (d) SNOWGRID, (e) OSHD_CL, (f) OSHD_EKF. Darker colours indicate higher SWE and grey indicates that no data is available since the respective grid cells were masked out (see Chapter 3.1).

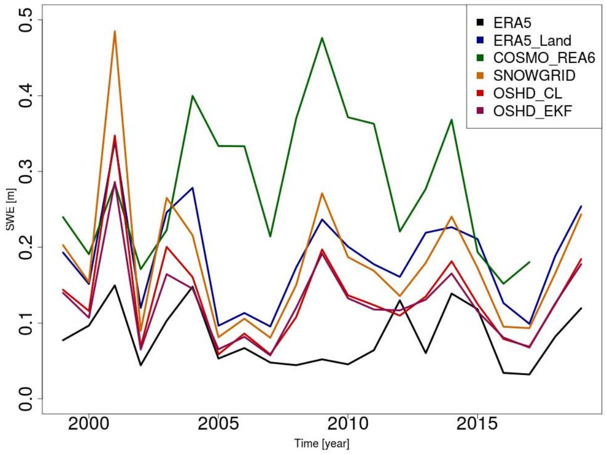

(a) Engadine

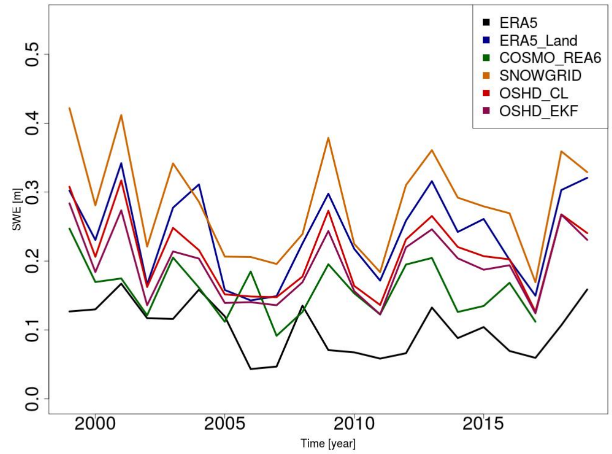

(b) Valais

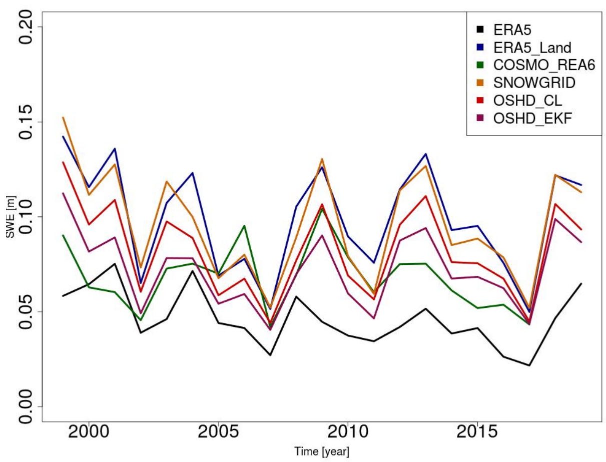

(c) North

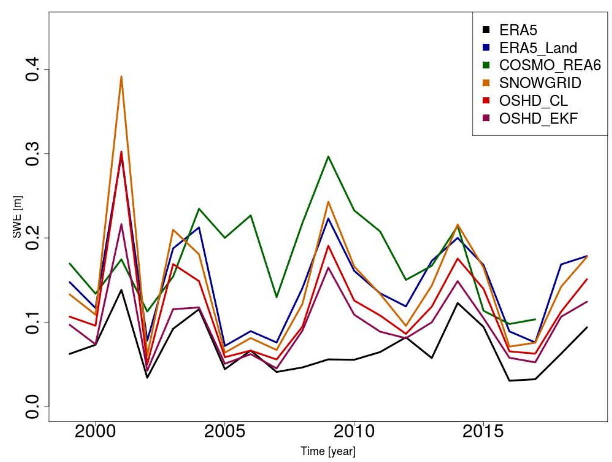

(d) South

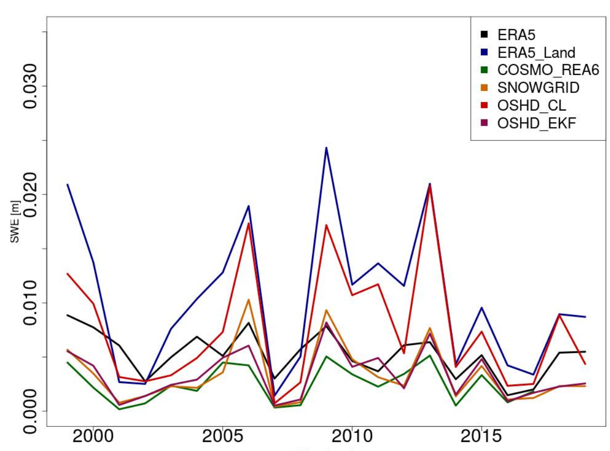

(e) Swiss Plateau

Figure 6: Mean SWE for the period 1999-2019 for the regions (a) Engadine, (b) Valais, (c) Northern Switzerland, (d) Southern Switzerland, and (e) the Swiss Plateau. Each color represents a data set. Note the variable y-axis range.

In the Engadine (Figure 6), as shown before on the map, COSMO-REA6 is most biased with 0.1 m SWE to the reference data set OSHD_EKF. At the beginning COSMO-REA6 shows the same behaviour as the other data sets, but from 2003 on the deviation is much larger. The 1 km resolution data sets have a high correlation of 0.99 with OSHD_EKF (Figure 7a) and their interannual variability is very similar. With a bias of 0.05 and 0.008 (Figure 7b), respectively, SNOWGRID and OSHD_CL overestimate the mean SWE compared to OSHD_EKF. The coarser resolution data set ERA5-Land has a bias of 0.06 m SWE and has a correlation of about 0.9 with the high-resolution data sets. ERA5 underestimates the mean SWE compared to OSHD_EKF and has the lowest SWE of all the data sets. This is likely due to the low-lying grid cells in this region.

A similar pattern of data sets is found in the Valais. However, here COSMO-REA6 shows an underestimation of the mean SWE (bias: -0.04 m SWE). Furthermore, all data sets except COSMO-REA6 and ERA5 overestimate the quantities of snow, with SNOWGRID showing the highest and OSHD_CL the smallest overestimation. Once again, the correlation of the 1 km data sets is the highest and COSMO-REA6 shows a low correlation with the reference data set.

In larger regions, e.g., northern Switzerland, there is a high agreement of year-to-year variability between the 1 km data sets and ERA5-Land. Consistent with the other regions, ERA5 shows an underestimation (bias: -0.03). On the other hand, OSHD_CL and SNOWGRID show an overestimation as well as a much stronger correlation than ERA5 and COSMO-REA6. COSMO-REA6 has a very low bias of -0.008, but a correlation of only 0.24 with OSHD_EKF. In the southern part of Switzerland a similar behaviour as in the Engadine is found. COSMO-REA6 has the highest deviation from the other data sets, and ERA5 has the lowest absolute SWE values.

Across all regions, the high-resolution data sets are more stable in terms of variability. Coarse data sets show less snow in higher regions because the resolution does not represent grid cells at high elevations and therefore temperatures are higher, and snow is not formed. In addition, COSMO-REA6 and ERA5 show the lowest correlations with OSHD_EKF and the 1km data sets and ERA5-Land the highest (Figure 7a). The mean values for the shown regions can be found in Table 3. Overall, SWE values in the northern and southern part are similar, ERA5 has the lowest values, and the 1 km data sets are alike in many regions.

In the Swiss Plateau, there are greater differences among the data sets, with OSHD_CL and ERA5-Land showing the highest mean SWE. SNOWGRID has a very small positive bias and a very high correlation to OSHD_EKF.

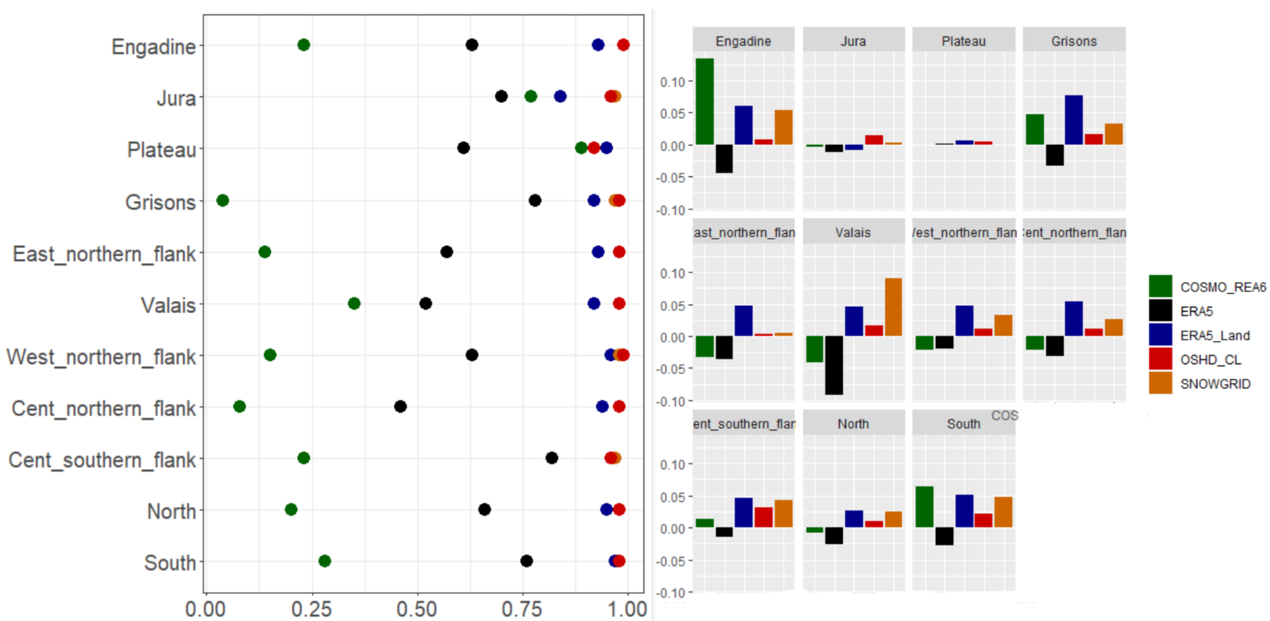

(a) Correlation

(b) Bias (m SWE)

Figure 7: (a) shows the temporal mean SWE correlation of the data sets ERA5 (black), ERA5-Land (blue), COSMO-REA6 (green), SNOWGRID (orange), and OSHD_CL (red) with OSHD_EKF for each region is plotted. On the right (b), the bias to OSHD_EKF is illustrated.

Figure 8 shows the monthly climatology of SWE. In general, it can be seen that snow accumulation starts early and melting starts late at high elevations. In particular the high-resolution data sets peak at the same time. In the Engadine, COSMO-REA6 accumulates swiftly, has an earlier and stronger peak than the other data sets and at the end of the year all snow has melted. In the Valais, similar behaviour is observed, but the high-resolution data sets do not reach zero. As seen before, OSHD_CL and OSHD_EKF are very close, SNOWGRID overestimates the SWE, and ERA5 has the lowest values. At lower elevations, as in the Swiss Plateau, the mean SWE is lower and the transition from peak to melting is more abrupt. Moreover, ERA5, ERA5-Land, and OSHD_CL overestimate the mean SWE compared with OSHD_EKF. SNOWGRID has high agreement with the reference data set, as in the other regions.

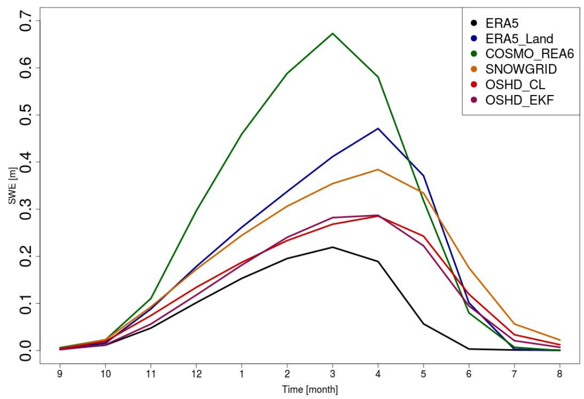

(a) Engadine

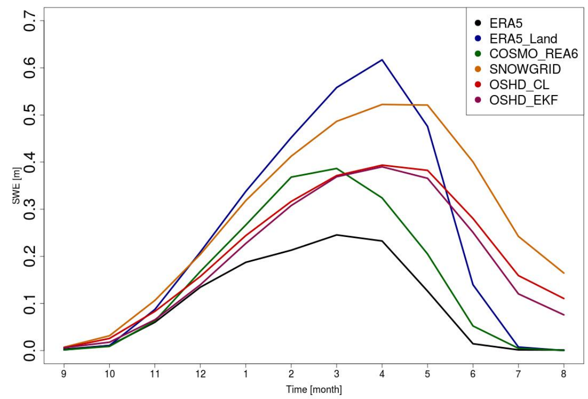

(b) Valais

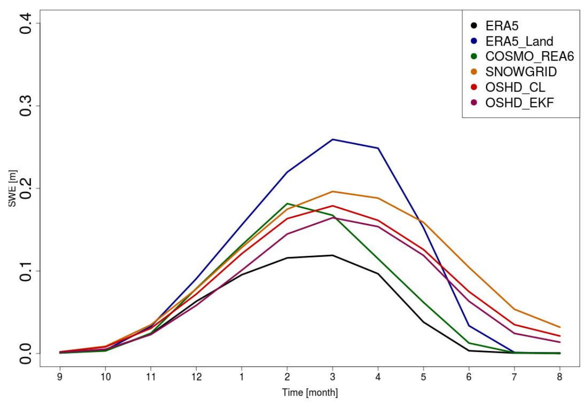

(c) North

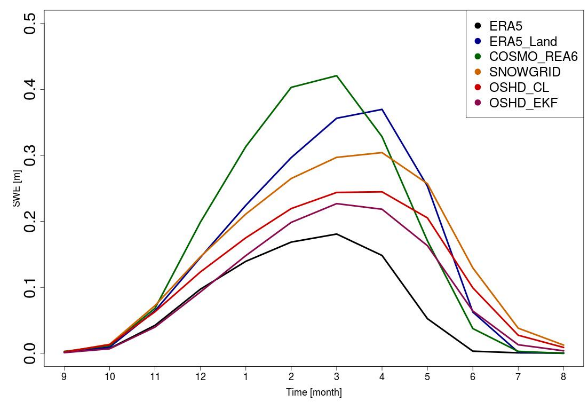

(d) South

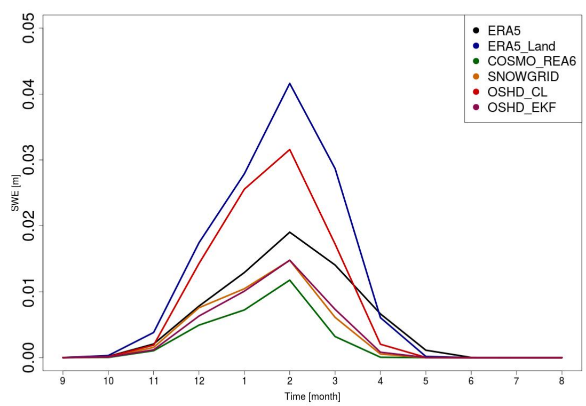

(e) Swiss Plateau

Figure 8: Monthly climatology over the period of 1999-2019 for the regions (a) Engadine, (b) Valais, (c) Northern Switzerland, (d) Southern Switzerland, and (e) the Swiss Plateau. The data sets ERA5 (black), ERA5-Land (blue), COSMO-REA6 (green), SNOWGRID (orange), OSHD_CL (red), and OSHD_EKF (purple) are illustrated.

4.1.2 Anomalies

Anomalies were calculated for the yearly mean SWE. Here, the years 2007 and 2009 are presented as examples. In 2007, all data sets show a strong negative deviation from the long-term mean (1999-2019) over the entire country (Figure 9a). Figure 9b and Figure 9c depict an increase of SWE starting in November, which indicate the late onset of snowfall in both the north and the south of Switzerland. Further, the snow maximum was reached in March, and then in April the snowmelt proceeded rapidly. On the other hand, 1999 shows a positive deviation from the mean in all regions except the central part of the southern flank of the Alps (Figure 10). It starts snowing early, the amount of snow increases strongly in February and the melting takes a long time. The SWE values peak in April and the absolute values are higher than in 2007. The variability between the data sets is larger in 1999 than in 2007. COSMO-REA6 shows a different behaviour in the south than the other data sets in both years.

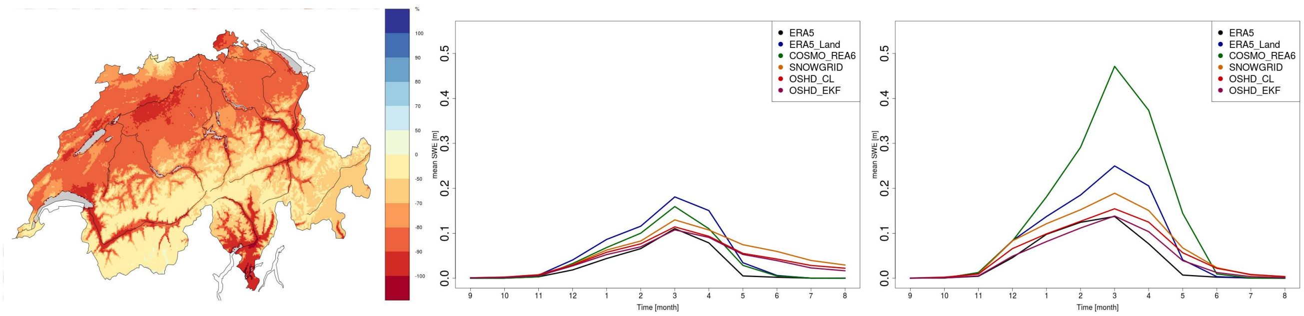

(a) 2007 (b) North (c) South

Figure 9: (a) The deviation of the year 2007 from the long-time mean (1998-2019) of OSHD_EKF, (b) seasonal cycle of SWE in 2007 of the northern, and (c) southern part of Switzerland. In subfigures (b) and (c), the data sets ERA5 (black), ERA5-Land (blue), COSMO-REA6 (green), SNOWGRID (orange), OSHD_CL (red), and OSHD_EKF (purple) are illustrated.

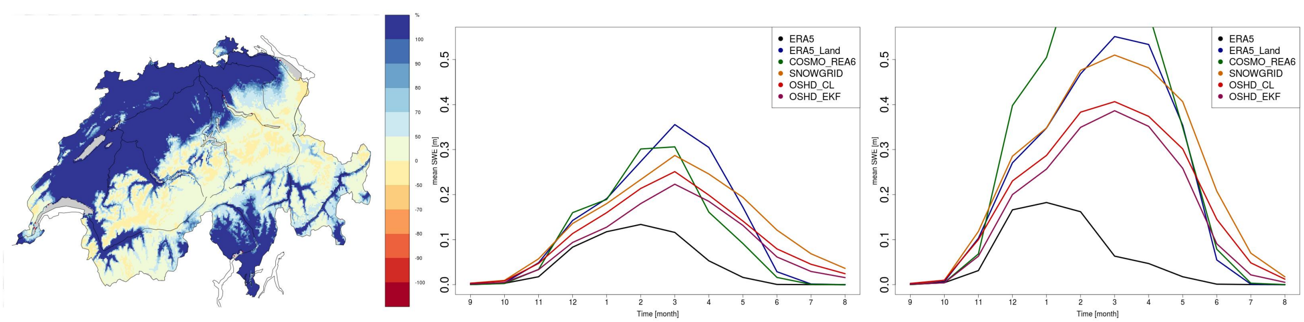

(a) 2009 (b) North (c) South

Figure 10: (a) The deviation of the year 2009 from the long-time mean (1998-2019) of OSHD_EKF, (b) seasonal cycle of SWE in 2009 of the northern, and (c) southern part of Switzerland. In subfigures (b) and (c), the data sets ERA5 (black), ERA5-Land (blue), COSMO-REA6 (green), SNOWGRID (orange), OSHD_CL (red), and OSHD_EKF (purple) are illustrated.

In Figure 11, the deviation from the mean is shown for the period 1999-2019 for the regions Valais and the Swiss Plateau. It can be observed that the percentage deviation is smaller in the Valais than in the Swiss Plateau. This is due to the fact that small amounts of snow in a region like the Swiss Plateau, where there is not much snow, cause large differences. For example, in a region with a lot of snow, a difference of 1 mm SWE does not make a big difference, but in a region with little snow, it is significant. In addition, the variability between data sets is greater in the Swiss Plateau than in the Valais. In both regions it is the case that the 1 km data sets agree very well and the more coarsely resolved ones show deviations in the other direction in many years (e.g. ERA5 in 2004).

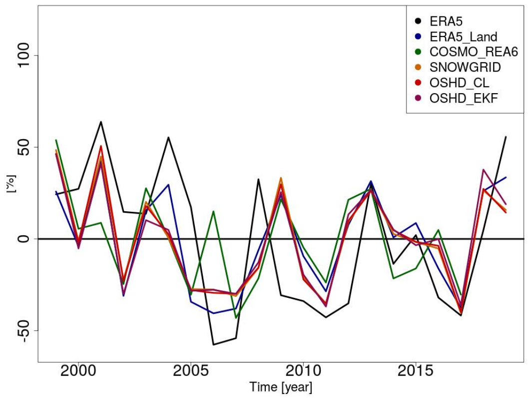

(a) North

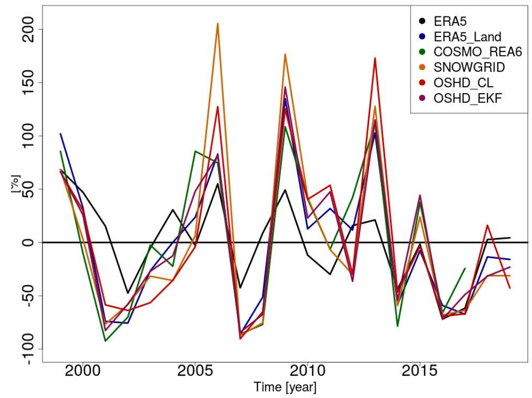

(b) South

Figure 11: Percentage deviation of SWE from the mean (1999-2019) for (a) the northern and (b) the southern part of Switzerland. The data sets ERA5 (black), ERA5-Land (blue), COSMO-REA6 (green), SNOWGRID (orange), OSHD_CL (red), and OSHD_EKF (purple) are illustrated. Note the variable y-axis range.

4.1.3 Deviation of products from the reference data set OSHD_EKF

The data sets deviate to varying degrees from OSHD_EKF (not shown). Across all regions, we see that OSHD_CL and SNOWGRID have the smallest percentage deviations from the mean SWE over the entire period, followed by COSMO-REA6, ERA5 and ERA5-Land. The strongest deviations are observed in the Swiss Plateau with up to 250% deviation by ERA5-Land and the region with the smallest deviation is the eastern part of the northern flank, which shows deviations between 5% (SNOWGRID) and 60% (ERA5-Land).

4.1.4 Trend

The trend is calculated from 37 winters (1982-2019). The results of the linear regression are shown in Figure 13, illustrating the climatology, and Figure 14, illustrating the relative trend. All data sets show a negative trend in all regions. In the Engadine, the relative trend is rather weak, it ranges from -17% to -7%, and the weakest relative trend is seen from ERA5-Land. A strong relative trend is found in the Valais, with OSHD_CL, SNOWGRID and ERA5-Land having almost the same percentage decrease (-35%, -37%, -38%) and ERA5 having a slightly larger decrease (-58%).

An even stronger relative trend is found in the Swiss Plateau, here all data sets show a similar value, apart from ERA5-Land, which showing a weaker trend. Comparing the northern and southern part of Switzerland, the northern part shows a stronger trend than the southern part. It is important to note that the residual analysis revealed that the data is not normally distributed (Figure 12). Different transformations, i.e. log- and square-root transformation, were tested. But the normal distribution was not achieved and in the end no data transformation was applied. Therefore, extrapolation into the future is erroneous as SWE would reach values below zero at sometime in the future, which is unphysical.

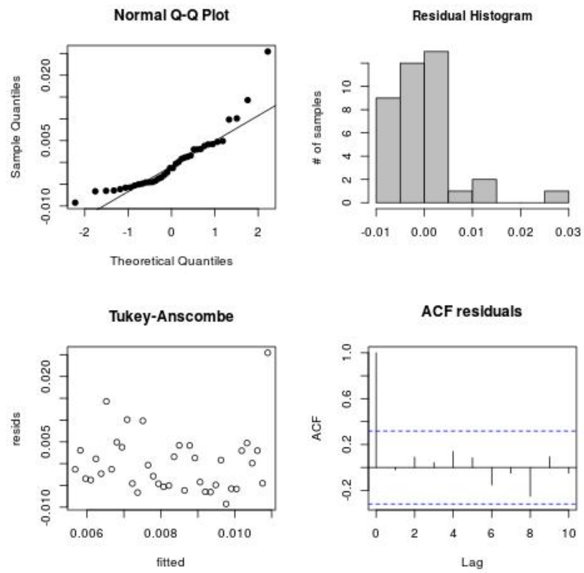

Figure 12: Residual analysis of SWE from OSHD_CL for the Swiss Plateau during the period of 1982-2019.

Figure 15 and Figure 16 show the mean SWE per year for the period 1971-2019 for OSHD_CL and SNOWGRID, respectively. The interannual variability and years with heavy (e.g. 1982, 1999) or light (e.g. 1990, 2007) snowfall can be recognized very well. Furthermore, it can be seen that the winters in recent years have less snow than the winters 30 years ago The two snow model show very similar results, however, regional differences, such as OSHD_CL having less snow in the Swiss Plateau than SNOWGRID are visible.

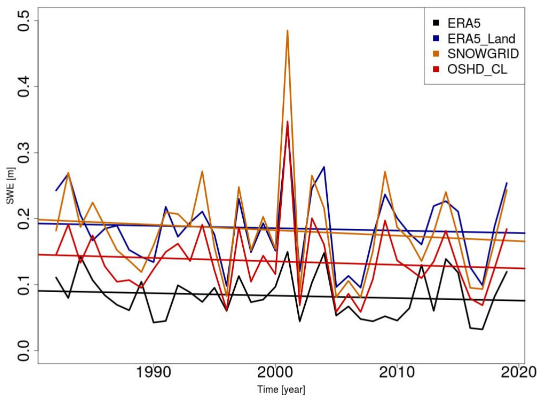

(a) Engadine

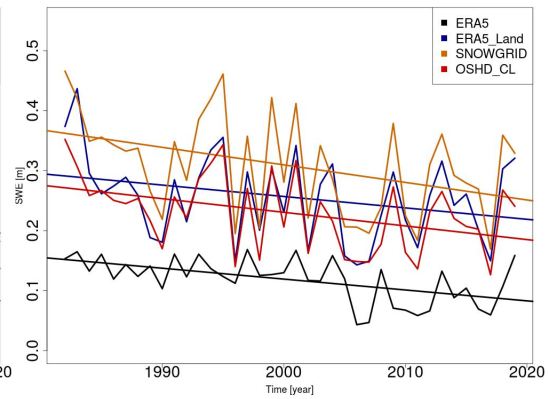

(b) Valais

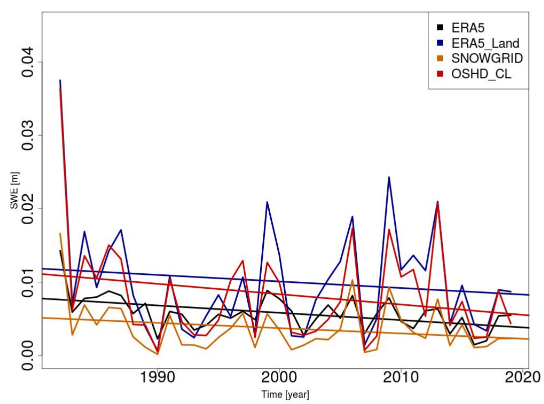

(c) Swiss Plateau

Figure 13: Mean SWE with calculated trend line for the period 1982-2019 for the regions regions (a) Engadine, (b) Valais, and (c) Swiss Plateau. The data sets ERA5 (black), ERA5-Land (blue), SNOWGRID (orange), and OSHD_CL (red) are shown.

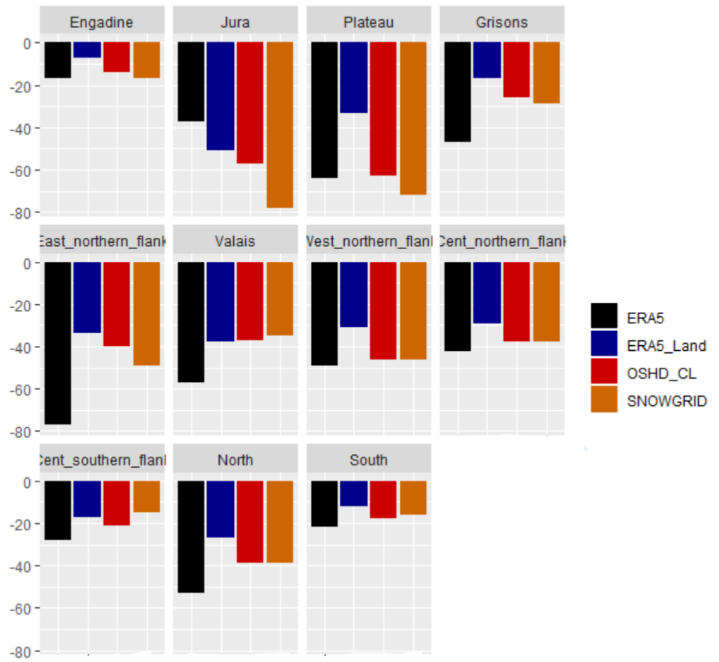

Figure 14: Relative trend in percent of SWE over the period of 1982-2019 for all regions. The data sets ERA5 (black), ERA5-Land (blue), SNOWGRID (orange), and OSHD_CL (red) are shown

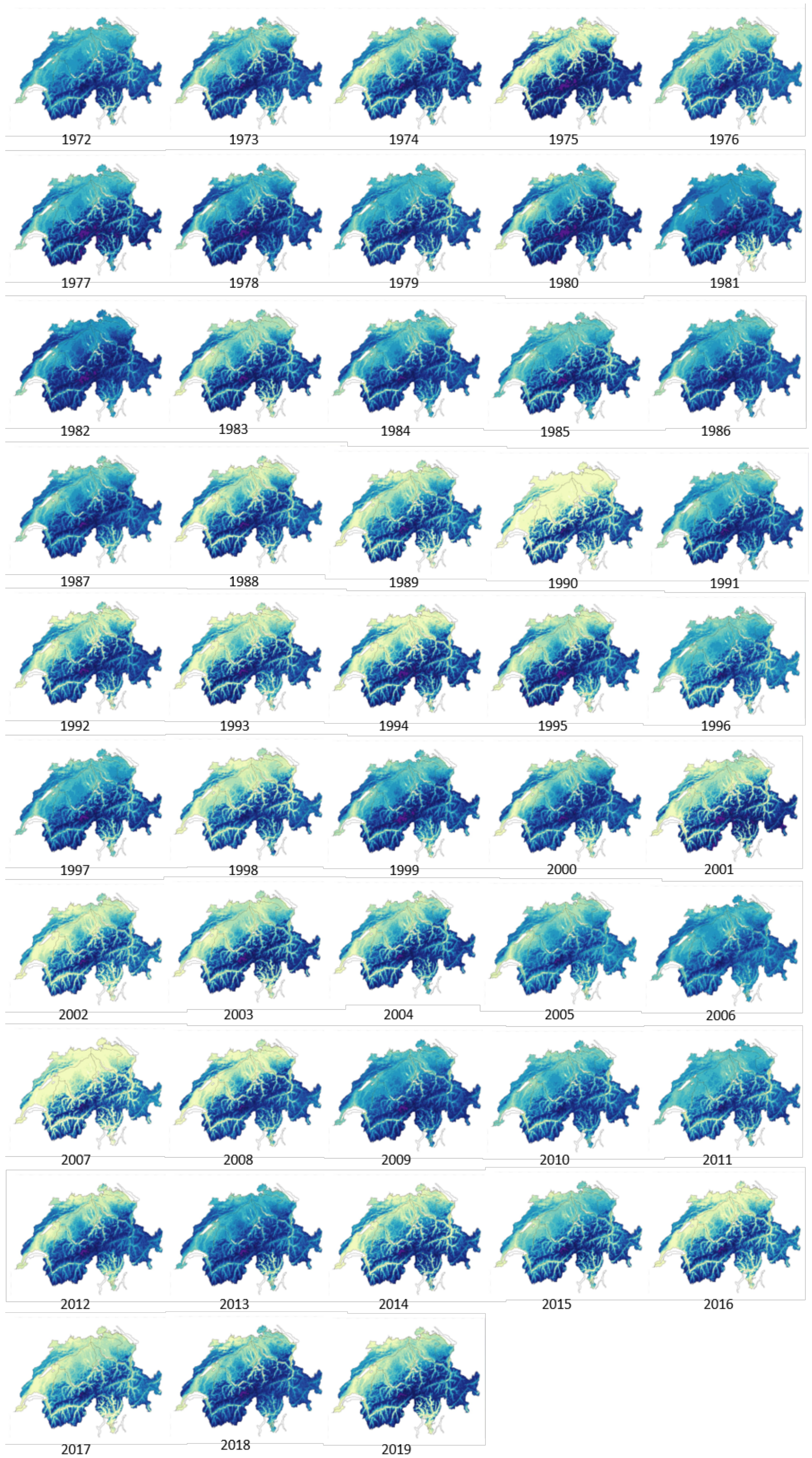

Figure 15: Map of Switzerland. Mean SWE of OSHD_CL for each year in the period of 1972-2019.

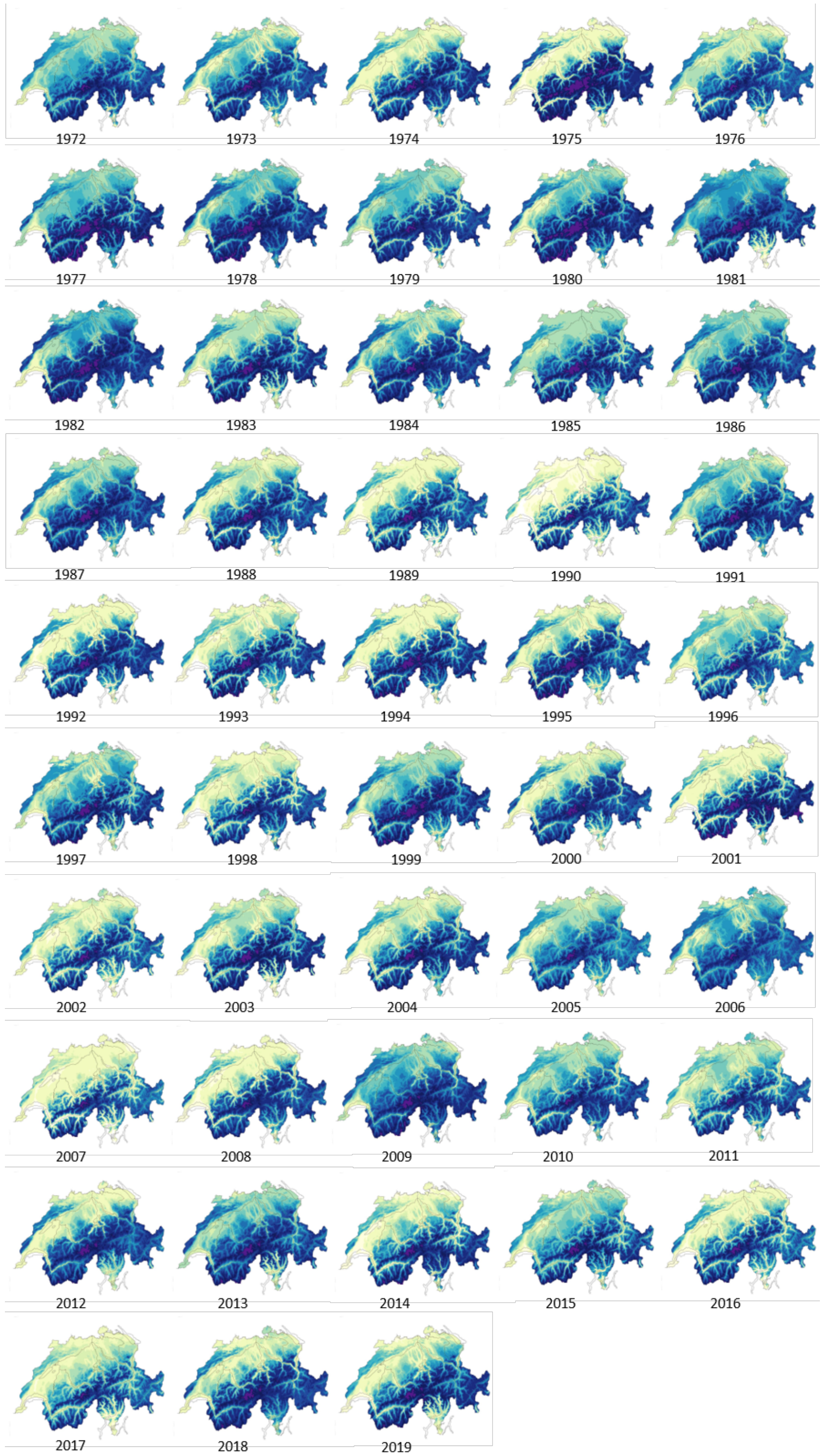

Figure 16: Map of Switzerland. Mean SWE of SNOWGRID for each year in period of 1972-2019. Darker colours indicate higher SWE.

4.1.5 SWE distribution in height classes

In Figure 17, the mean SWE at different elevation classes is shown for the Engadine. Here, no grid cells are present at the lowest altitude level, while at the second (500-1000 m) the high-resolution have grid cells. The SWE values vary between 0 and 0.04 m SWE, with OSHD_EKF having the lowest values and SNOWGRID deviating the most from it. In some years, like 2009 or 2014, the deviation is very strong. At the third altitude class (1000-1500 m), ERA5 land is also included, displaying the highest SWE values. As before, OSHD_EKF and OSHD_CL show very similar behaviour, and SNOWGIRD shows a surplus in some years. Here the data sets reach snow values up to 0.3 m SWE. At 1500-2000 m, all data sets hold grid cells and they all show a large variability among one another. The highest SWE values are shown by COSMO-REA6 and ERA5-Land. ERA5 underestimates the snow quantity and shows similar behaviour to the other data sets during the first couple of years, but from 2008-2011 SWE values are significantly lower. In 2012 and 2013 SWE values increase, although all other data sets see an intensification. As in the other elevation classes, SNOWGRID has higher values as OSHD_EKF and OSHD_CL, but the 1 km data sets agree well. Here the SWE values reach up to 0.35 m SWE. For the fifth altitude level (2000-2500 m), all data sets are available. Looking at the data, it can be seen that ERA5-Land is in the same range as the 1 km data sets. While COSMO-REA6 is within the same range as the other data sets for the first five years, but afterwards it shows a strong deviation. Here the SWE reaches up to 0.7 m and never reaches no snow. At the highest level (¿2500 m), all data sets have grid cells except ERA5. Like the last elevation class, ERA5-Land and the high-resolution data sets coincide well. COSMO-REA6 also shows the same behaviour as before. The SWE values never reach zero and range up to 0.75 m.

In the Valais (see Appendix), there are grid cells at the lowest altitude class (0-500 m) for the 1 km data sets. Only the 1 km data sets have grid cells in this category. The data sets agree nicely, none of the data sets over- or underestimate in all years. The values range between 0 and 0.02 m SWE. At the second altitude class, both the 1 km data sets and COSMO-REA6 have grid cells. The data sets agree well, COSMO-REA6 has the most snow of all the data sets. Among the 1 km data sets SNOWGRID has the highest values, in some years this is very pronounced (e.g. 2009, 2014). Furthermore, OSHD_CL has higher values than OSHD_EKF. On the whole, all data sets behave similarly and vary between 0 and 0.045 m SWE. At 1000-1500 m, all data sets are represented. ERA5-Land stands out, as it shows large SWE values compared to the other data sets. OSHD_EKF and OSHD_CL are very similar in pattern and magnitude. SNOWGRID and COSMO-REA6 both have higher SWE values than OSHD_EKF and OSHD_CL. However, the pattern through the years is similar. ERA5 shows an overestimation at the beginning, with time it resembles SNOWGRID and COSMO-REA6 increasingly, but the pattern is differently. The SWE values go from 0 to 0.3 m SWE. On the 5th height class (2000-2500 m), all data sets except ERA5 are represented. Here, the high-resolution data sets show more snow than the coarser resolution data sets. Of the 1 km data sets, SNOWGRID shows the highest amount of snow, followed by OSHD_CL. OSHD_EKF and OSHD_CL are in very good agreement. COSMO-REA6 and ERA5-Land both show less snow than OSHD_EKF, and ERA5-Land follows the pattern of OSHD_EKF more closely than COSMO-REA6.

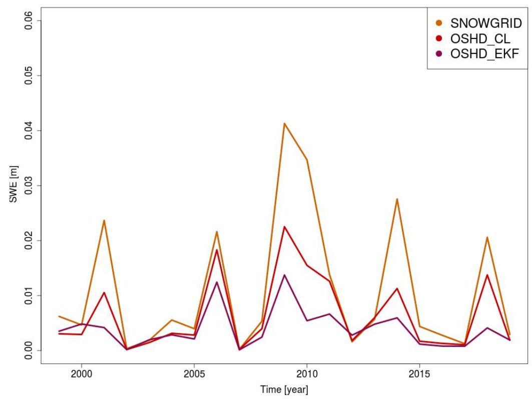

(a) Engadine: 500-1000 m

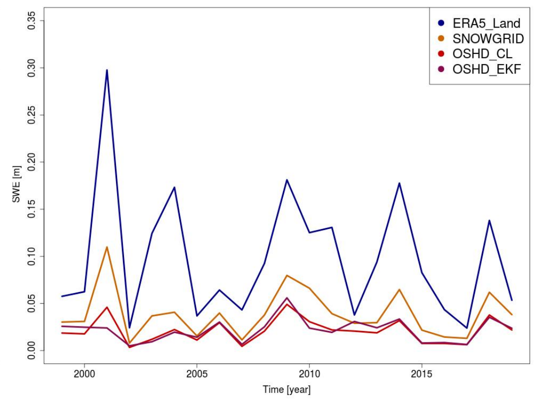

(b) Engadine: 1000-1500 m

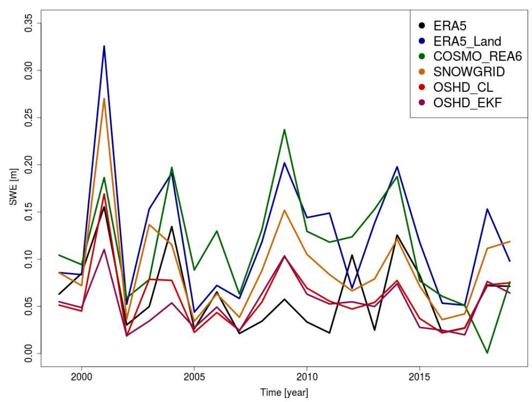

(c) Engadine: 1000-1500 m

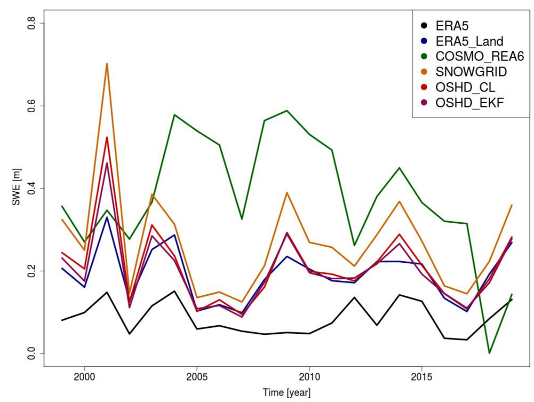

(d) Engadine: 1500-2000 m

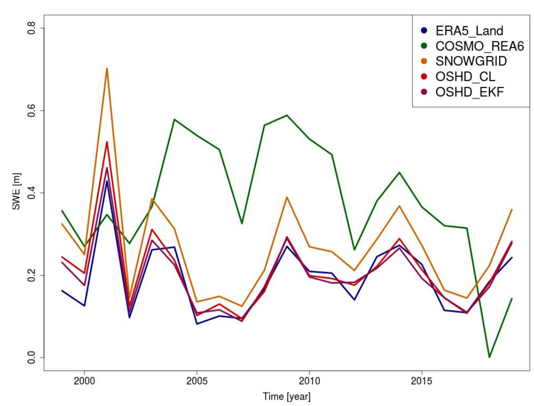

(e) Engadine: >2500 m

Figure 17: Mean SWE in the Engadine at different elevation classes (a) 500-1000 m, (b) 1000-1500 m, (c) 1500-2000 m, (d) 2000-2500 m, and (e) >2500m.

In low-altitude regions (see appendix), such as the Swiss Plateau, only the first three elevation classes are covered. At 0-500 m, all data sets except ERA5 are available. The snow amounts vary between 0 and 0.01 m SWE. ERA5-Land and OSHD_CL show the highest amount of snow and COSMO-REA6 the lowest. OSHD_EKF and SNOWGRID display a high agreement, SNOWGRID shows only higher SWE in a few instances (e.g. 2006). The variability of OSHD_EKF, COSMO-REA6 and SNOWGRID increases with time. At 500-1000 m, all data sets are represented and the behaviour is very similar to before: OSHD_CL and ERA5-Land show the largest amount of snow, SNOWGRID, OSHD_EKF, COSMO-REA6 and ERA5 display snow in the same order of magnitude and with the same year-to-year variability. At this height, the data sets reach up to 0.03 m SWE. At 1000-1500 m all data sets are available and attain values up to 0.1 m SWE. Compared with the previous altitude classes, the data sets show high variability. No data set shows the lowest or highest SWE values across all years. The closest to the OSHD_EKF is SNOWGRID.

Larger regions such as the northern part of Switzerland (not shown) cover all elevation classes. At the first elevation class (0-500 m), all data sets display a small variability and reach values up to 0.012 m SWE. SNOWGRID and OSHD_EKF are similar, ERA5 and COSMO-REA6 show lower values, and OSHD_CL and ERA5-Land show the highest values. Like the first elevation class, the data sets show similar behaviour for the second altitude class (500-1000 m). The variability is small, ERA5-Land shows the highest values (up to 0.04 m SWE), and the remaining data sets have a similar SWE range. In the 3rd class (1000-1500 m), the variability among the data sets is more pronounced. The SWE values go up to 0.2 m SWE and again ERA5-Land shows the highest values. SNOWGRID and OSHD_CL have similar SWE values as OSHD_EKF, but in some years the peaks are higher (e.g. 2014). COSMO-REA6 is within the same magnitude as the 1 km data sets and shows the same year-to-year variability. During the first years ERA5 shows an exceedance compared to the 1 km data sets, but from 2005 on it is in the similar magnitude as the high-resolution data sets and COSMO-REA6. At 1500-2000 m, the data sets show a large variability and the SWE values range from 0.05 to 0.3 m SWE. The year-to-year variability is similar among the data sets, again ERA5-Land shows the highest values and the 1 km data sets have a similar pattern and snow values. Only in year 2003 OSHD_EKF shows a less pronounced peak than the other two. At the beginning, ERA5 has a different pattern and stronger peaks than the high-resolution data sets, and from 2009 to 2012 displays a flat pattern with almost no year-to-year variability. COSMO-REA6 shows similar variability to the 1 km data sets, but in some years has either too much or too little snow. At 2000-2500 m, the data sets again exhibit greater variability and obtain values between 0.05 to 0.4 m SWE. Larger differences exist between the 1 km data sets, with SNOWGRID showing more snow than the other two. ERA5 and ERA5-Land have the same pattern over the years, but the values of ERA5 are low and ERA5-Land is high, e.g. the year-to-year variability is very small in some years (2005-2006). COSMO-REA6 has higher values than the 1 km data sets and does not show peaks in the same years (e.g. 2001). On the 6th elevation class (>2500 m) all data sets are available except ERA5. The variability is large and the SWE values ranges from 0.18 to 0.8 m SWE. SNOWGRID has the highest SWE values, followed by OSHD_CL and OSHD_EKF. COSMO-REA6 and ERA5-Land underestimate the snow compared to OSHD_EKF.

All altitude classes are found in the southern part of Switzerland (see appendix). At the lowest altitude, OSHD_CL and SNOWGRID have the most snow and correlate well with each other. OSHD_EKF shows lower values and a smaller interannual variability, which is especially pronounced in the later years. ERA5 and COSMO-REA6 have lower snow values than OSHD_EKF and show a small year-to-year variability throughout the entire time. ERA5-Land is within the same magnitude as OSHD_EKF but does not consistently show an over- or underestimation. Values range from 0 to 0.025 m SWE. On the 2nd elevation class (500-1000m), the data sets show a greater variability and the SWE values go up to 0.085 m SWE. ERA5 shows the lowest values in most years. SNOWGRID, OSHD_CL, and ERA5-Land are in the same order of magnitude and estimate larger amounts of snow than OSHD_EKF. COSMO-REA6 is close to OSHD_EKF in many years, but in some years it also shows quite different behaviour such as in 2012. At 1000-1500 m the 1 km data sets show the same order of magnitude and ERA5-Land for many years has more snow than the other data sets, but none of the data sets always display the low-est value. COSMO-REA6 is good in terms of the order of magnitude, but the pattern does not always coincide, e.g. in 2013. On the 5th altitude class (2000-2500 m), the values range between 0.1 and 0.8 m SWE. ERA5 shows the lowest values. Among the 1 km data sets and ERA5-Land, SNOWGRID shows the highest values and ERA5 the lowest. COSMO-REA6 displays similar values to the other data sets in the first five years, but afterwards it overestimates the snow amounts compared to OSHD_EKF. In 2012 and 2013, COSMO-REA6 shows almost the same snow amounts as SNOWGRID. The highest elevation class shows very similar behaviour like the 5th elevation class (2000-2500 m).

The trend analysis shows that the higher altitude classes undergo a smaller change over time. Figure 18 depicts the relative trend in percent in the Engadine at all elevation classes. It can be seen that the trends of OSHD_CL and SNOWGRID are highest at 1000-1500 m, and decrease with height. The same altitudinal decline can be observed for ERA5 and ERA5-Land. Across all regions (for Figures see appendix section 7.1.2), OSHD_CL and SNOWGRID show trends of similar magnitude, ERA5 shows the strongest relative trend throughout all altitude classes, and the trends at higher elevations are smaller.

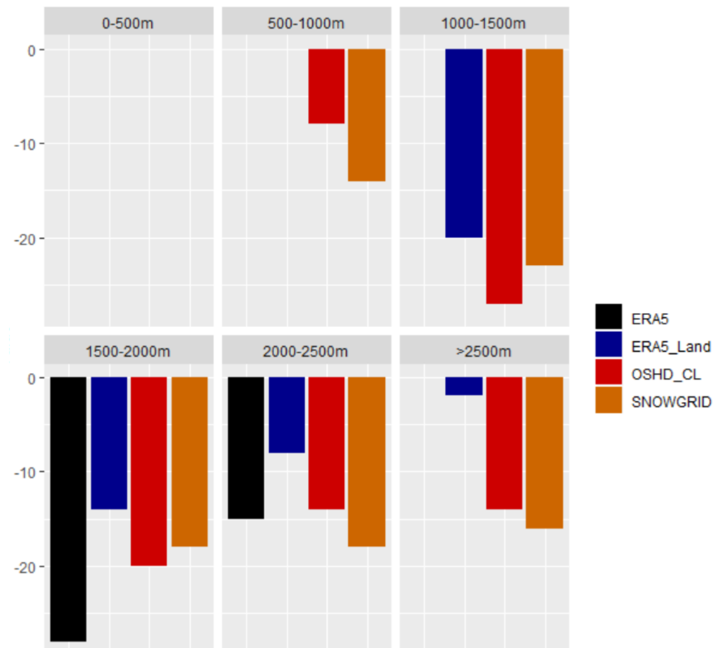

Figure 18: Trend at different altitudes in the Engadine for the period 1999-2019. The unit is m SWE.

4.1.6 Comparison station and nearest gridcell

The SWE climatology of the stations and the nearest grid cell of the 1 km data set is shown in Figure 19, and the bias with respect to the station is shown in Figure 20. Considering all regions, the smallest bias is seen in OSHD_EKF. Since station data are assimilated in this data set, it is not surprising that this bias is the smallest. Furthermore, it can be observed that SNOWGRID shows higher snow amounts in most regions and has the strongest bias.

Figure 20 shows that the Engadine has the largest bias, with OSDH_CL deviating the most. In the Valais, SNOWGRID overestimates the snow amounts, and OSHD_CL and OSHD_EKF both underesti-mate the snow amounts in comparison to the station. In the Swiss Plateau, the data sets show a larger variability than in the other regions. Here, all data sets overestimate the station values, most strongly by SNOWGRID.

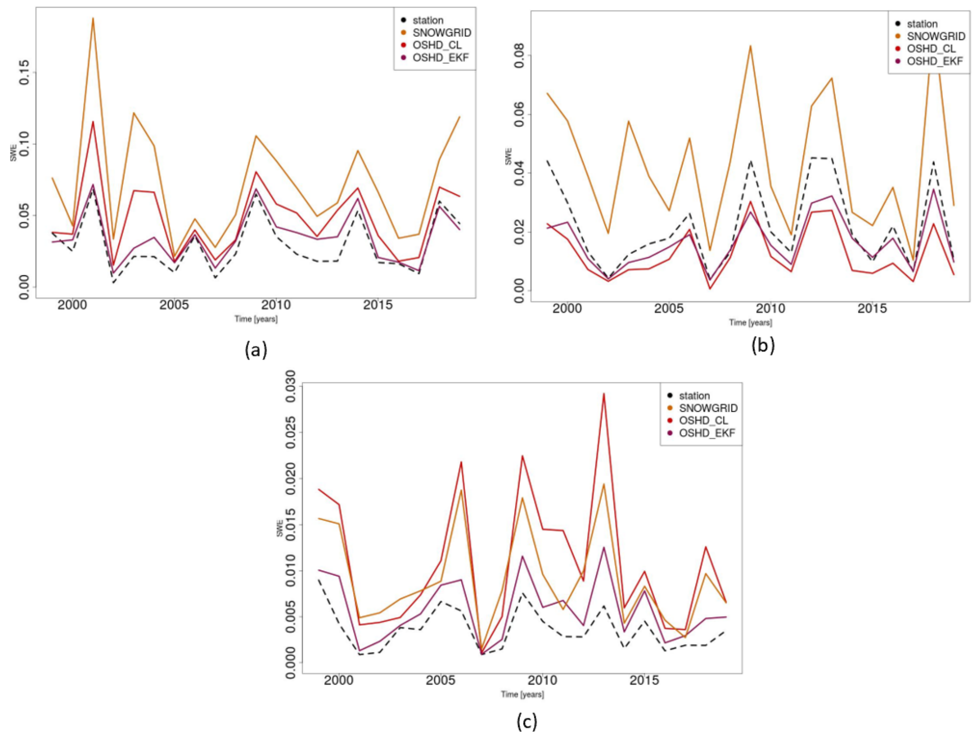

Figure 19: Mean SWE of the stations and the nearest gridcells for the regions (a) Engadine, (b) Valais and (c) Swiss Plateau. The station data is shown in black, SNOWGRID in orange, OSHD_CL in red, and OSHD_EKF in purple. Note the different y-axis range for the Engadine.

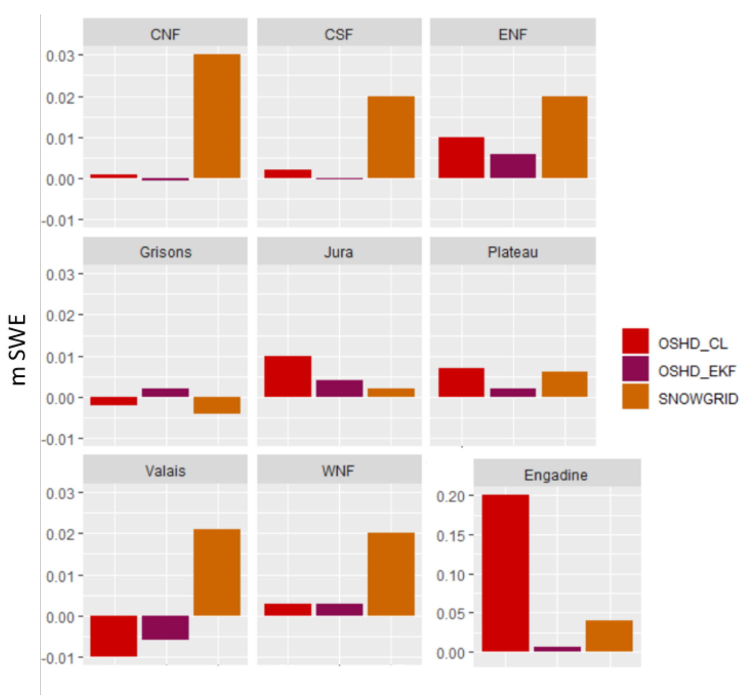

Figure 20: Bias of the nearest grid cells of snow models OSHD_CL (red), OSHD_EKF (purple), and SNOWGRID (orange) to station data. One plot for each region. CNF denotes central part of the northern flank, CSF the central part of the southern flank, ENF the eastern part of the northern flank, and WNF the western part of the northern flank. Note the different y-axis range for the Engadine.

Figure 21 shows data from two stations, Scoul and Sion, for one year as an example to illustrate the unprocessed time series of individual stations and their corresponding grid cells. The maximum of all data sets is reached approximately at the same time in 1999. In Scoul, the end of the snow cover is reached later by OSHD_EKF and OSHD_CL than by the station and SNOWGRID. In Sion the models display much more snow at the beginning than measured at the station.

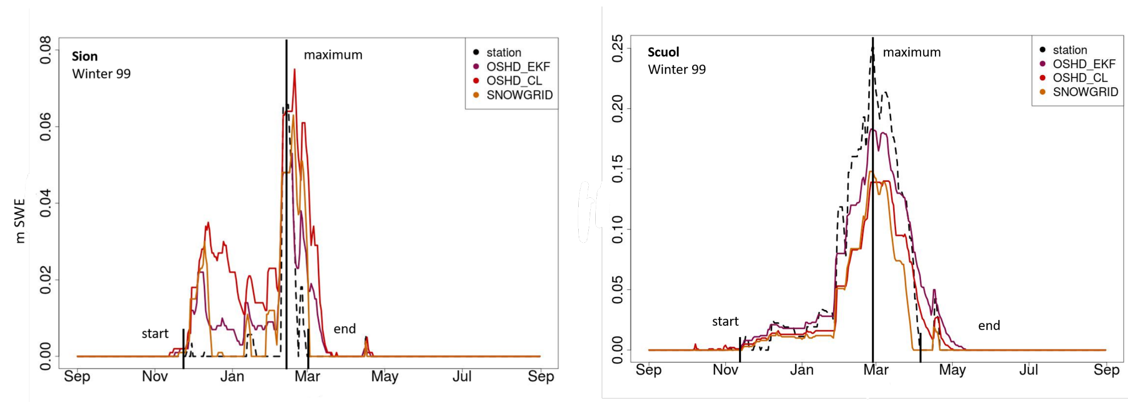

(a) Sion

(b) Scoul

Figure 21: SWE of the winter 1999 for the station Scuol on the left and the station Sion on the right. Plotted are the station data in black, the nearest gridcells of OSHD_CL in red, OSHD_EKF in purple and SNOWGRID in orange. The start, end and the maximum of SWE are indicated by black lines.

4.2 Number of snow days

In the following sections, different aspects of the number of snow days are described. First, the climatology and then the anomaly and deviation of products from the reference data set, and lastly, the results of the trend analysis are shown.

4.2.1 Climatology

In this section, the results of the number of snow days for the period 1999-2016 are presented. The climatology is shown in Figure 22 for the data sets ERA5, ERA5-Land, COSMO-REA6, SNOWGRID, OSHD_CL, OSHD_EKF, and AVHRR. Due to the gaps in AVHRR, some years (i.e. 2000, 2001, 2012, and 2013) were discarded. At higher elevations, snow is found throughout the year, which can be seen in AVHRR. ERA5 shows no grid cells, which are covered with snow all year round. There are also differences among the 1 km data sets: In comparison with AVHRR, the other high-resolution data sets show too many snow days in the low-altitude areas.

In Table 4 the mean number of snow days for the entire period is given. The lowest number of snow days is found in the Swiss Plateau (17-63 snow days) and in the Jura (25-98 snow days). The regions with the highest number of snow days are the Engadine with 202-245 snow days, the Valais with 188-238 snow days, and Grisons with 168-232 snow days. Followed by the central part of the northern flank showing 92-201 snow days, the western part of the northern flank with 97-197 snow days, eastern part of northern flank with 99-191 snow days, and the central part of the southern flank with 77-187 snow days. Dividing Switzerland into the northern and southern part shows that the southern part experiences more snow days (158-228 snow days) than the northern part (49-156 snow days).

Table 4: Mean number of snow days over the period of 1999-2016 for each region.

[#snow days]	ERA5	ERA5-Land	COSMO-REA6	AVHRR	SNOWGRID	OSHD_CL	OSHD_EKF
Jura	25	53	53	38	64	98	68
Plateau	17	63	16	26	28	51	31
Engadine	202	245	234	205	231	235	227
Grisons	195	232	182	168	197	213	207
East. northern flank	141	191	113	99	131	152	148
West. northern flank	183	197	124	97	132	153	152
Cent. northern flank	190	201	122	92	144	163	162
Cent. southern flank	171	187	143	77	135	148	148
Valais	207	238	188	201	223	226	221
North	156	155	88	49	91	113	105
South	187	228	190	158	187	193	184

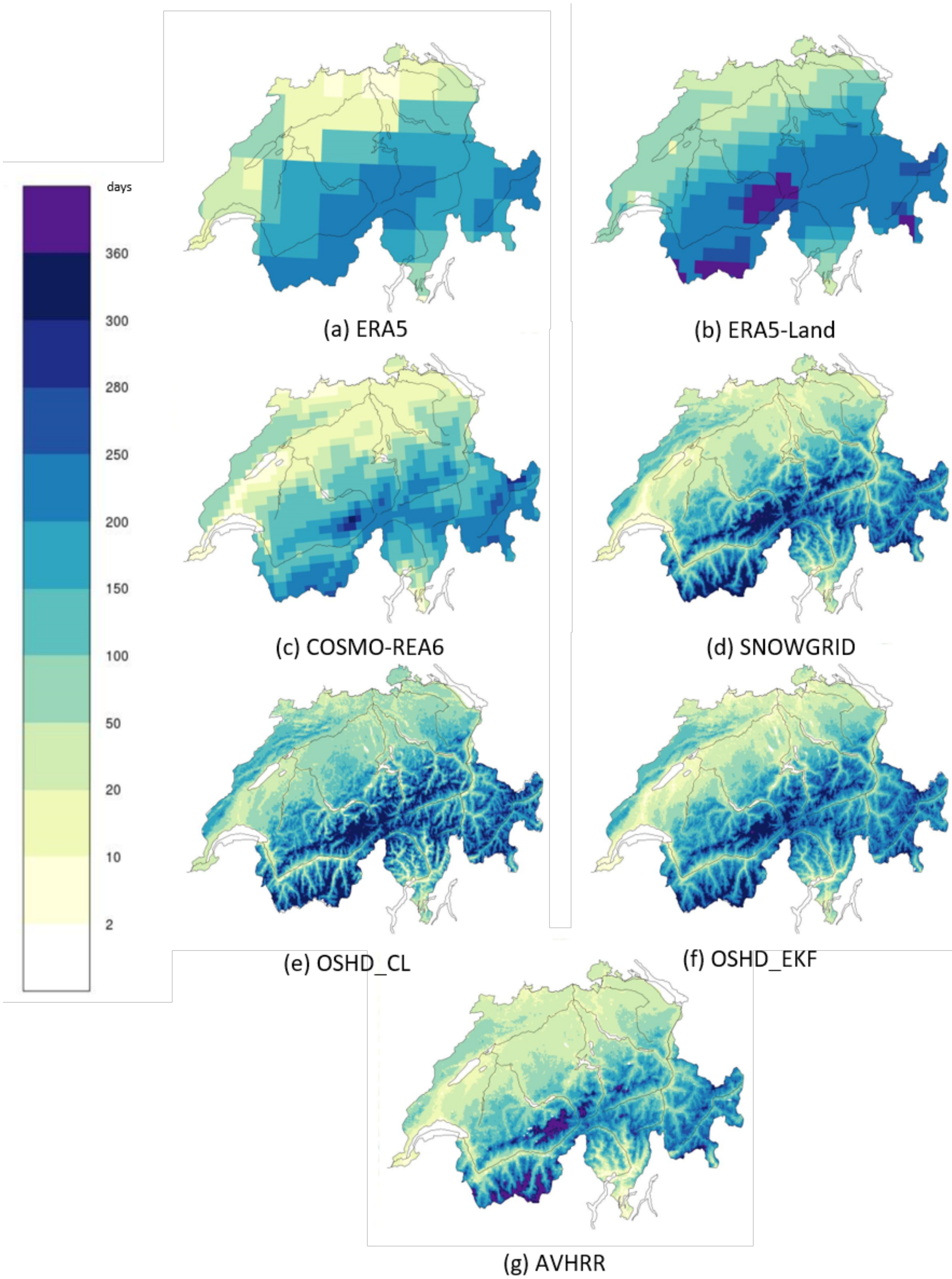

Figure 22: Climatology of snowdays for the period 1999-2016 for (a) ERA5, (b) ERA5-Land, (c) COSMO-REA6, (d) SNOWGRID, (e) OSHD_CL, (f) OSHD_EKF, and (g) AVHRR.

Figure 23 shows the evolution of the number of snowdays and Table 6 shows the mean number of snow days for five regions from 1999-2016. In the Engadine all data sets except ERA5 overestimate the number of snowdays relative to AVHRR. All data sets have a positive correlation with AVHRR, the highest with 0.93 belongs to SNOWGRID. Next come OSHD_CL and OSHD_EKF with 0.78 and 0.8, respectively. ERA5 has the lowest correlation with AVHRR at 0.52 and ERA5-Land a correlation of 0.68. COSMO-REA6 behaves differently in the first five years with less year-to-year variability compared to the other data sets. But afterwards the behaviour is quite similar and the correlation over the whole period is 0.71.

In the Valais (Figure 23b), a similar pattern is found again with the 1 km data sets and ERA5-Land counting more snow days than AVHRR. The correlations with AVHRR are worse than in the Engadine and range from 0.27 to 0.35. In the north, all data sets overestimate the number of snow days, with the strongest being ERA5 and ERA5-Land. COSMO-REA6 has the highest correlation with 0.66, followed by SNOWGRID (0.43), OSHD_CL and OSHD_EKF (both 0.3), ERA5-Land (0.27) and ERA5 (0.12).

In the south (Figure 23c), the variability of the data sets is smaller, and all data sets record more snow days than AVHRR. ERA5-Land shows the most snow days and the other data sets all show lower but approximately the same number of snow days. The correlation in the south is higher, SNOWGRID shows the best correlation with 0.88. Close to it are OSHD_EKF (0.86) and OSHD_CL (0.85). The coarser resolved products have a lower correlation with a range from 0.61 to 0.69.

In the Swiss Plateau (Figure 23d), the variability of the data sets and the year-to-year variability is large. Compared with AVHRR, the 1 km data sets show a small positive and ERA5-Land a large positive bias, and COSMO-REA6 and ERA5 show a small underestimation of the number of snow days (Figure 24). All data sets show a positive correlation with AVHRR, SNOWGRID was found to have the highest correlation at 0.71, followed closely by ERA5-Land and OSHD_EKF both at 0.69. Next at 0.58 is COSMO-REA6, then OSHD_CL at 0.52 and ERA5 at 0.5.

The correlation is not positive in all regions, e.g. COSMO-REA6 in the central flank of the southern Alps shows a negative correlation. Across all regions, SNOWGRID has the highest correlation, followed by COSMO-REA6, OSHD_CL and OSHD_EKF. ERA5 and ERA5-Land correlate poorest with AVHRR.

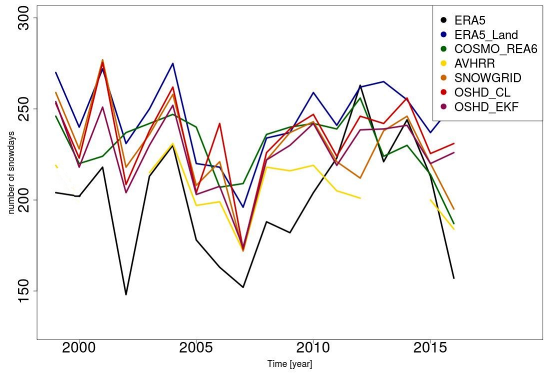

(a) Engadine

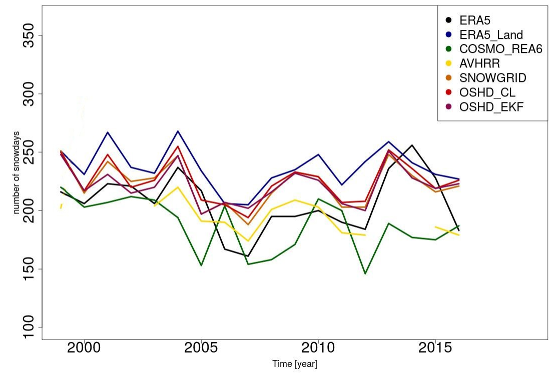

(b) Valais

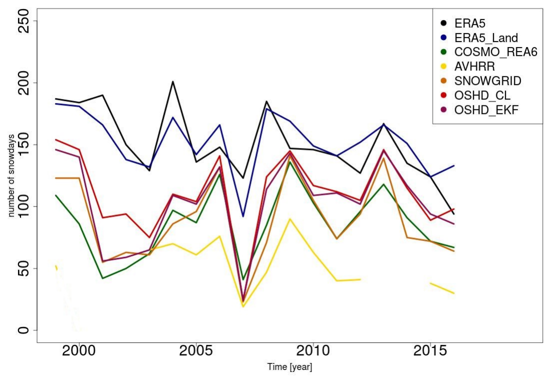

(c) North

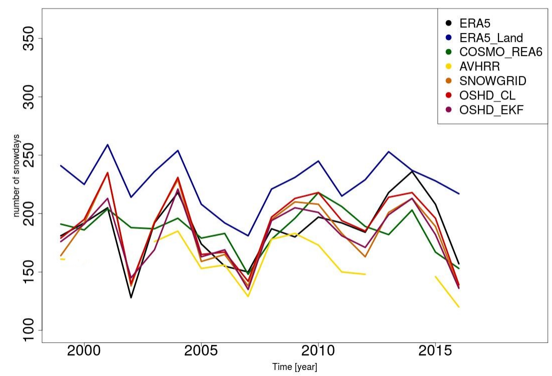

(d) South

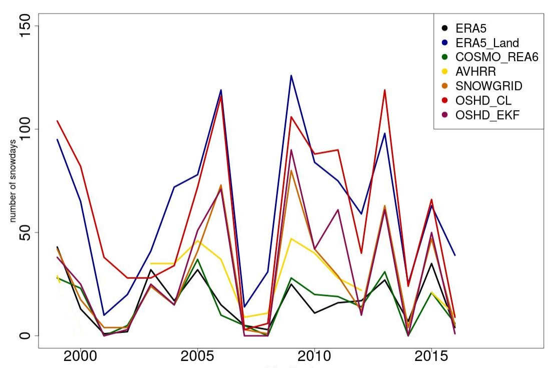

(e) Swiss Plateau

Figure 23: Climatology of snow days for the period 1999-2016 for (a) Engadine, (b) Valais, (c) Northern Switzerland, (d) Southern Switzerland, and (e) the Swiss Plateau. The data sets ERA5 (black), ERA5-Land (blue), COSMO-REA6 (green), SNOWGRID (orange), OSHD_CL (red), OSHD_EKF (purple), and AVHRR (yellow) are illustrated. Note the variable y-axis range.

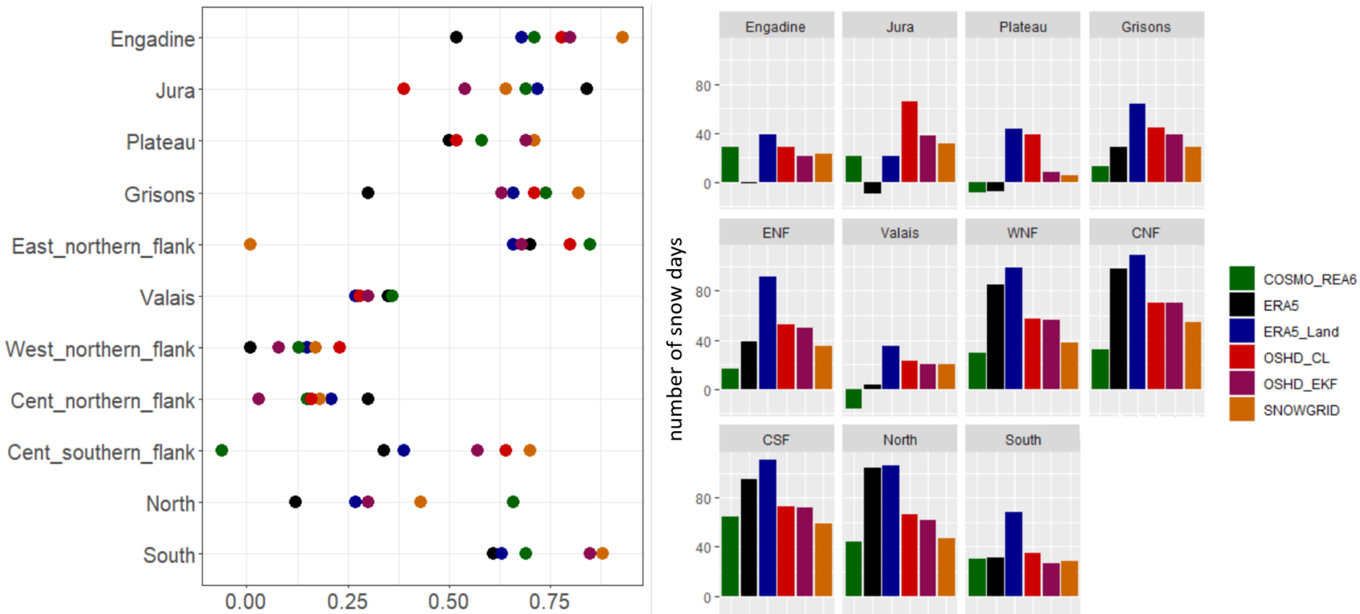

(a) Correlation

(b) Bias

Figure 24: On the left, the temporal correlation of the number of snow days of the data sets ERA5 (black), ERA5-Land (blue), COSMO-REA6 (green), SNOWGRID (orange), OSHD_CL (red), and OSHD_EKF (purple) with AVHRR for each region is plotted. On the right, the bias to OSHD_EKF is illustrated and some regions are abbreviated: CNF denotes central part of the northern flank, CSF the central part of the southern flank, ENF the eastern part of the northern flank, and WNF the western part of the northern flank.

4.2.2 Anomaly

The data sets show the same deviation in percent during the same time period and are in good agreement with the AVHRR deviation (e.g. northern and southern part of Switzerland (Figure 25)). Only in the Engadine and in the Valais COSMO-REA6 shows a different interannual variability of the deviation. Considering all data sets, the deviation is small in many years, which can be observed for OSHD_EKF in 2010 (Figure 26c). In the years where a larger deviation is detected, predominantly the Swiss Plateau is affected. For example, there was a negative deviation in 2007 (Figure 26a) and a positive one in 2009 (Figure 26b). These deviations are consistent within all data sets and the magnitude of change is the same.

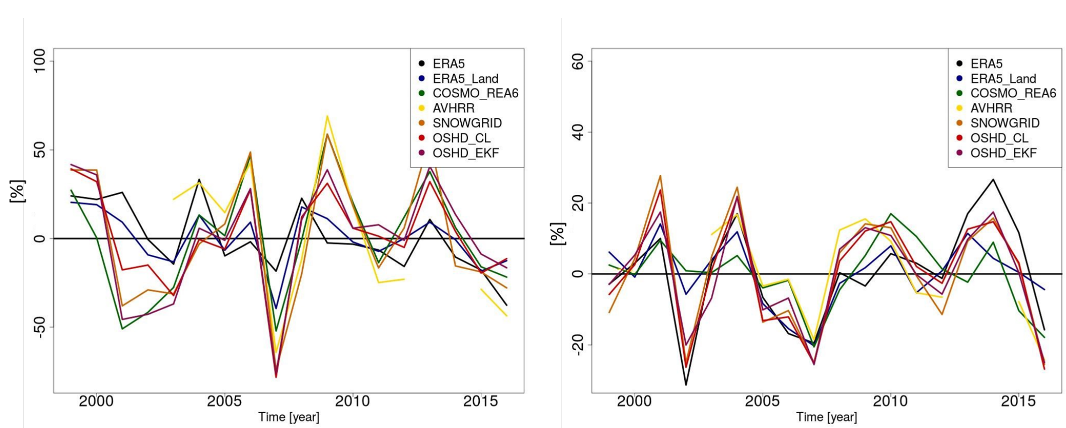

(a) North

(b) South

Figure 25: Percentage deviation from the mean number of snow days (1999-2016) for the northern and southern part of Switzerland. Note the variable y-axis range.

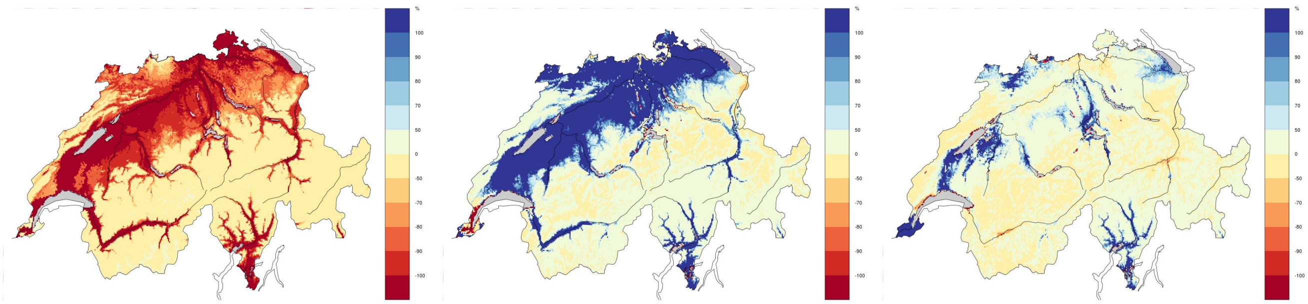

(a) 2007 (b) 2009 (c) 2010

Figure 26: Percentage deviation of OSHD_EKF from the mean number of snowdays (1999-2016) for the years 2007, 2009 and 2010. Red indicates less and blue indicates more snow days than on average.

4.2.3 Deviation of products from the reference data set AVHRR

The data sets tend to overestimate the number of snow days in all regions except the Swiss Plateau and the Jura. In the Jura, ERA5 underestimates the snow days while in the Swiss Plateau ERA5 and COSMO-REA6 both underestimate the snow days (Figures not shown). The largest percentage deviation with up to 150% is also found in these two regions. The regions with the smallest deviation are the western part and the southern part of the northern flank. Considering all regions, SNOWGRID and COSMO-REA6 show the smallest percentage deviation, followed by OSHD_EKF, OSHD_CL, ERA5 and ERA5-Land. Of course, this is highly dependent on the selected threshold. A threshold above 1 cm SWE would lead to different results.

4.2.4 Trend

The relative trend of the number of snow days was calculated for the period 1982-2019. During this period, a negative trend is detected in all regions. The variability between data sets is greatest at lower elevations, while higher elevations are more stable.

For example, ERA5 shows the strongest trend in the Swiss Plateau with an 83% decrease in snow days (Figure 28). However, SNOWGRID has only half the trend (42%), OSHD_CL has a 27% decrease, and ERA5-Land has a 6% decrease. The range of the relative trend in the Engadine and Valais is more consistent, ranging from -6% to -14% and -16% to -18%, respectively. Northern Switzerland experiences a larger reduction in snow days than the southern part. Across all regions, ERA5-Land has the lowest trend, OSHD_CL and SNOWGRID are of the same order of magnitude, with SNOWGRID showing a slightly stronger trend in more regions. ERA5 shows a more pronounced trend in the Jura and eastern part of the northern flank than the other data sets. However, in all other regions it is of the same order of magnitude.

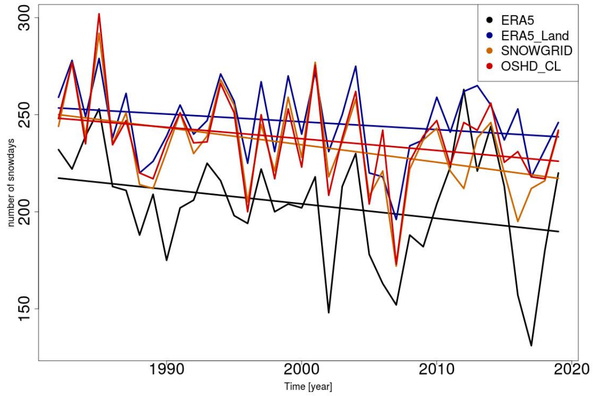

(a) Engadine

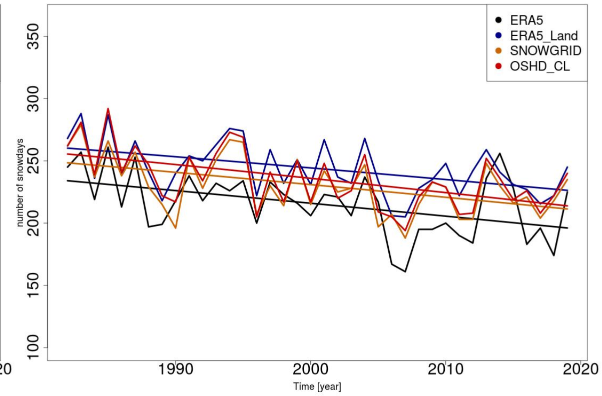

(b) Valais

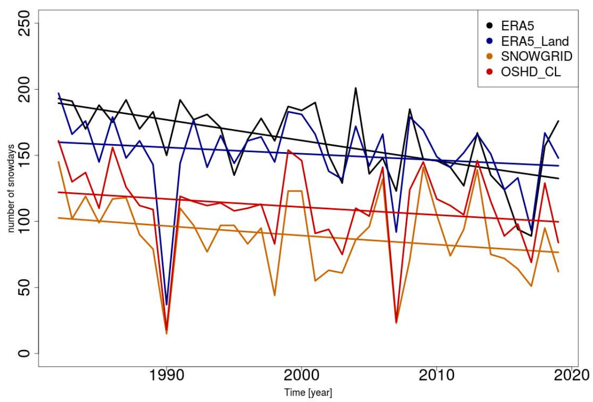

(c) North

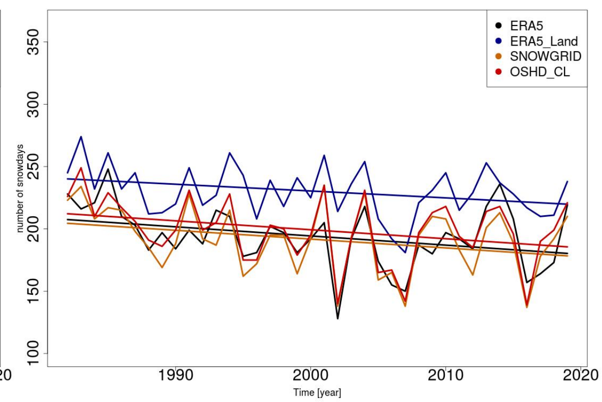

(d) South

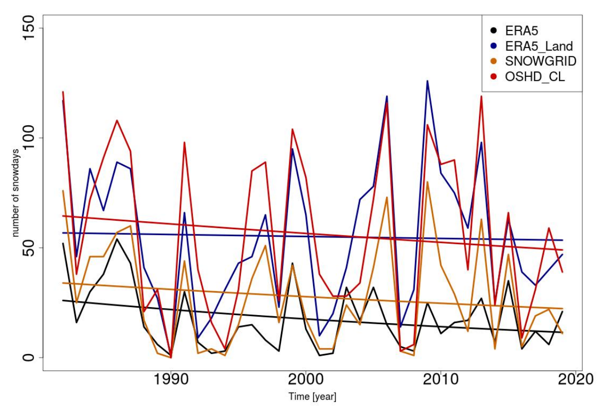

(e) Swiss Plateau

Figure 27: Mean number of snowdays with trend line for the period 1982-2019 for the regions regions (a) Engadine, (b) Valais, (c) Northern Switzerland, (d) Southern Switzerland, and (e) the Swiss Plateau. The data sets ERA5 (black), ERA5-Land (blue), COSMO-REA6 (green), SNOWGRID (orange), OSHD_CL (red), and OSHD_EKF (purple) are plotted. Note the variable y-axis range.

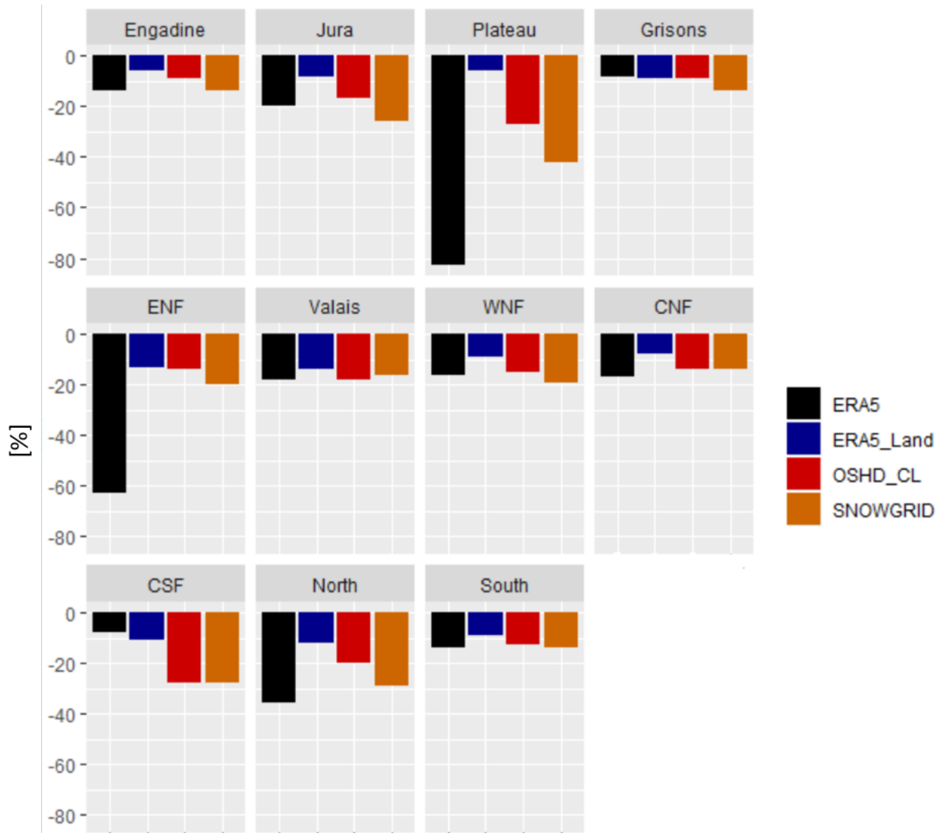

Figure 28: Relative trend in percent over the period 1982-2019 for each region are shown. The data sets ERA5 (black), ERA5-Land (blue), SNOWGRID (orange) and OSHD_CL (red), OSHD_EKF (purple) are displayed. Some regions are abbreviated: CNF denotes central part of the northern flank, CSF the central part of the southern flank, ENF the eastern part of the northern flank, and WNF the western part of the northern flank.

4.3 Day of maximum snow

In the following sections, different aspects of the day of maximum snow are described. First, the climatology, then the anomaly and deviation of products from the reference data set, and lastly, the results of trend analysis are shown.

4.3.1 Climatology

The climatology of the day with maximum snow is shown in Figure 29. In general, the lower-lying regions reach their maximum earlier than the higher-lying regions. In some data sets, in the highest altitude regions of the Alps, snow accumulates throughout the year. As the models set the snow to zero on September 1, the maximum in these accumulation-only grid cells occurs always at the end of the year (August 31). Hence, the grid cells with continuous accumulation are masked out and the maximum is considered as undefined in these regions. In Figure 29 these grid cells are marked in grey. ERA5-Land, SNOWGRID, OSHD_CL and OSHD_EKF contain such grid cells. Small differences can be observed among the 1 km data sets, the most distinctive difference being the later maximum in the Swiss Plateau for OSHD_CL than for the other two data sets.

Table 5 shows the average date at which the the maximum is found for each region and data set. It displays that COSMO-REA6 simulates the day of the maximum the earliest most regions. In the regions Jura and Swiss Plateau, OSHD_CL finds the maximum the latest. There are very small differences among the high-resolution data sets for most regions, the largest difference of 14 days (betweeen SNOWGRID and OSHD_CL) is found in the Swiss Plateau.

In the Jura, the maximum snow is reached at the end of February according to the 1 km data sets, whereas the coarse resolution data sets find the maximum at the beginning of February (Table 5). In the Swiss Plateau, all data sets except COSMO-REA6 agree that the maximum is found on the beginning of February. COSMO-REA6 finds the maximum already at the end of January. The more elevated the region, the later the maximum is simulated. In the Engadine, ERA5 and COSMO-REA6 find the maximum in the middle of March, whereas the remaining data sets find it much later in April. In Grisons, the range among the data sets is larger. The 1 km data sets agree on a maximum at the end of March, while the coarser data sets vary between end of February and the middle of March. For the northern flanks of the Alps (western, central and eastern part), the 1 km data sets show the maximum in the middle of March. Once again, the other data sets vary between end of February and end of March. The latest detection of the maximum is found in the Valais. Here all data sets except COSMO-REA6 exhibit the maximum at the end of March/beginning of April. For COSMO-REA6 the day of maximum snow occurs at the beginning of March. In the Southern part of Switzerland, the day of maximum snow is found later than in the northern part.

Table 5: Mean day of maximum snow over the period of 1999-2019 for each region. The unit is the date (day.month)

[date]	**ERA5**	**ERA5-Land**	**COSMO-REA6**	**SNOWGRID**	**OSHD_CL**	**OSHD_EKF**
Jura	3.2	5.2	9.2	24.2	26.2	21.2
Plateau	8.2	10.2	20.1	1.2	15.2	6.2
Engadine	16.3	27.4	10.3	17.4	14.4	6.4
Grisons	9.3	18.3	24.2	30.3	27.3	30.3
East. northern flank	23.3	23.3	10.2	13.3	13.3	14.3
West. northern flank	17.3	27.3	17.2	11.3	12.3	13.3
Cent. northern flank	16.3	27.3	14.2	21.3	14.3	25.3
Cent. southern flank	18.3	3.4	17.2	20.3	27.3	26.3
Valais	24.3	21.4	3.3	3.4	31.3	4.4
North	18.3	31.3	17.2	11.3	6.3	13.2
South	11.3	13.4	27.2	5.4	30.3	29.3

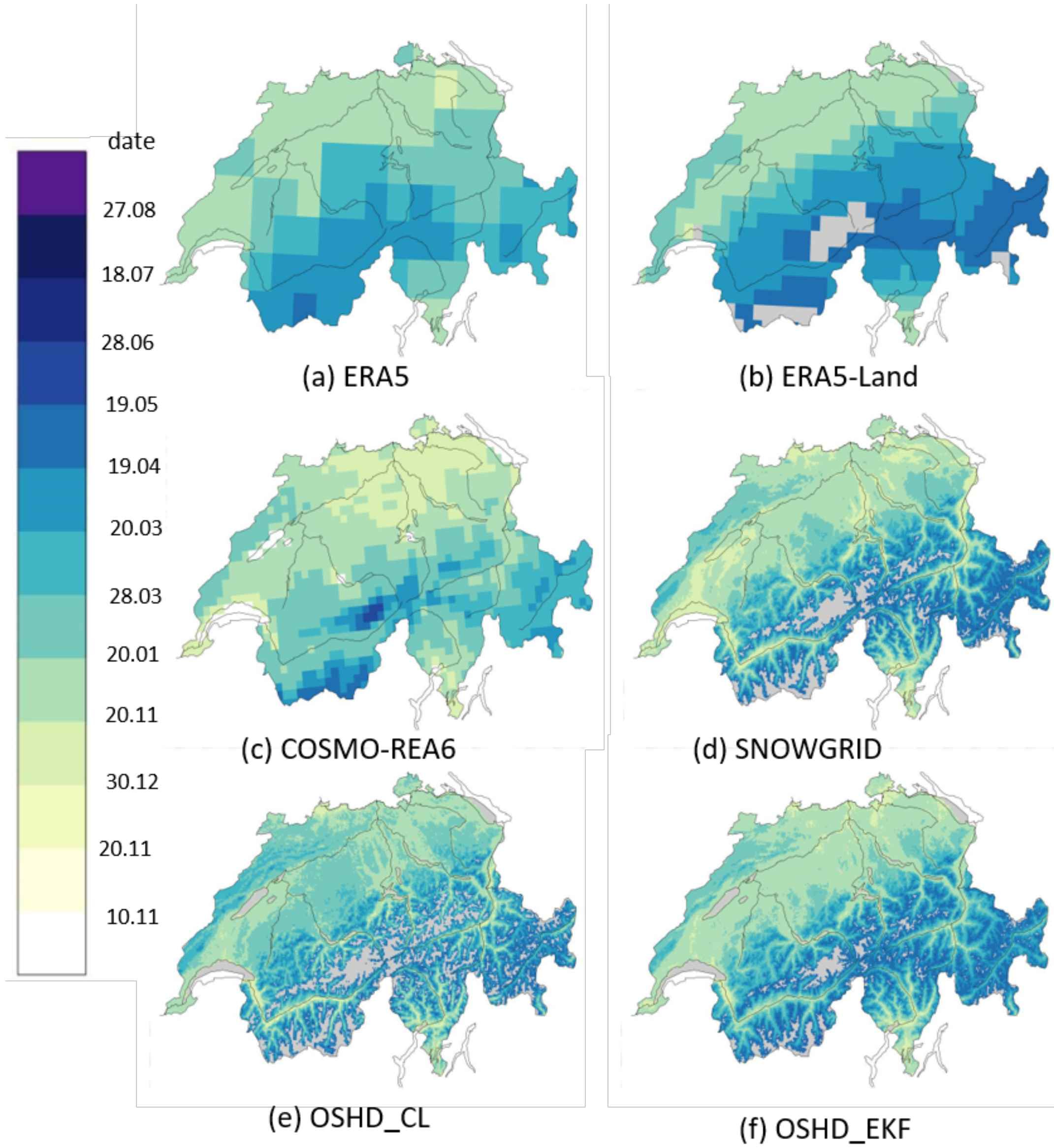

Figure 29: Climatology of the day with maximum snow for the period 1999-2019 for (a) ERA5, (b) ERA5-Land, (c) COSMO-REA6, (d) SNOWGRID, (e) OSHD_CL, and (f) OSHD_EKF. The legend shows the date and the grey area denotes masked grid cells.

Figure 30 depicts the day of maximum snow per region. The maximum per region is defined as the day with the highest mean SWE over the entire region. As mentioned earlier, the maximum is not defined in some grid cells. Therefore, caution must be taken when comparing data sets in these regions.

In the Engadine and Swiss Plateau, the data sets have different interannual variability and the variability between data sets is most pronounced for the coarse resolution data sets, while the 1 km data sets have little variability among themselves. Furthermore, the maximum in the Engadine is later (end of March/beginning of April) than in the lowlands (between January and February) and the coarse resolution data sets simulate the maximum earlier. For example, in the Engadine, ERA5 reaches the maximum earliest in most years, since it does not represent the very high grid cells, which reach their maximum later. In the Swiss Plateau, the agreement between the data sets is high, the largest discrepancy is found from 2012-2016, and in some years (e.g. 2009) COSMO-REA6 shows larger discrepancies.

In the Valais, the variability among the data sets is large and all data sets show the day of the maximum later than in the lower lying regions. COSMO-REA6 tends to simulate the maximum the earliest in many years and ERA5-Land the latest. The 1 km data sets are very similar, especially in recent years. ERA5 does not consistently show an earlier or later maximum compared to the other data sets and in some years (e.g. 2015) it is not far off the 1 km data sets.

In the northern and southern part of Switzerland, the 1 km data sets agree well with each other and the coarse resolution data sets show higher variation. COSMO-REA6 reaches the SWE maximum earlier than OSHD_EKF, whereas ERA5 and ERA5-Land show a later SWE maximum in many years. In the south, COSMO-REA6 shows an earlier maximum as well. ERA5 also detects the maximum earlier and ERA5-Land later in many years.

In Figure 31, the bias to OSHD_EKF is illustrated. It shows that ERA5 has by far the largest bias, it simulates the day of maximum snow earlier. COSMO-REA6 also shows an earlier detection than OSHD_EKF in all regions, but the bias is much smaller. The remaining data sets show much smaller biases and do not consistently detect an earlier or later occurrence of the maximum.

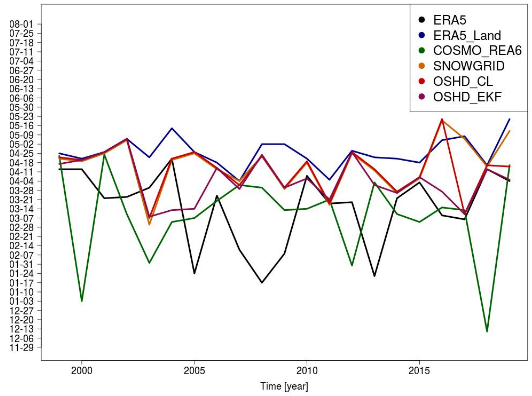

(a) Engadine

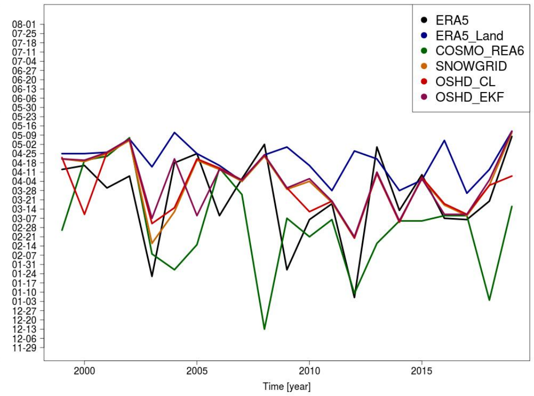

(b) Valais

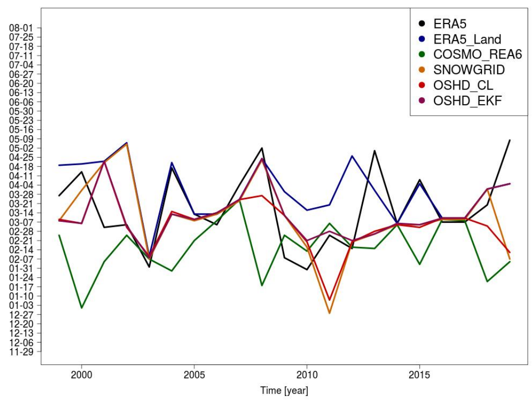

(c) North

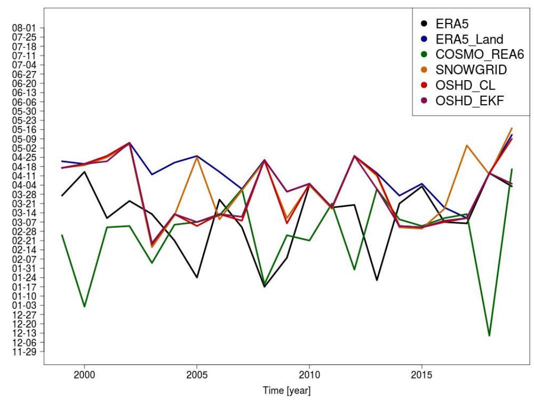

(d) South

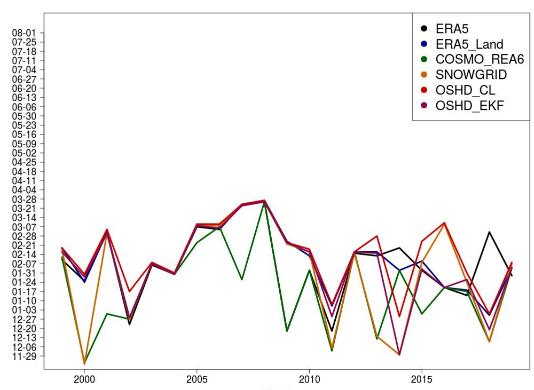

(e) Swiss Plateau

Figure 30: Climatology of the mean day of maximum snow for the period 1999-2019 for the regions (a) Engadine, (b) Valais, (c) North, (d) South, and (e) the Swiss Plateau.

When considering the correlation with OSHD_EKF, OSHD_CL has the highest correlation across all 11 regions. It is followed by SNOWGRID, ERA5-Land, ERA5, and COSMO-REA6. COSMO-REA6 has the largest range of correlation values, for half of the regions (e.g. central part of the southern flank) it is even negative. For the other regions, the correlation is positive, e.g. in the Jura the correlation attains 0.82. SNOWGRID fluctuates less than OSHD_CL, but still performs slightly worse across all regions. ERA5-Land and ERA5 have a correlation close to zero in the Engadine and Grisons, respectively. Whereas in the other regions it is positive.

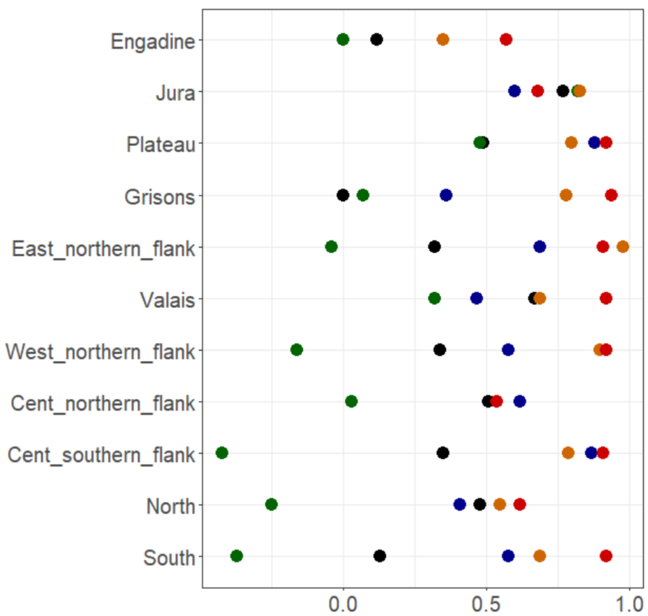

(a) Correlation

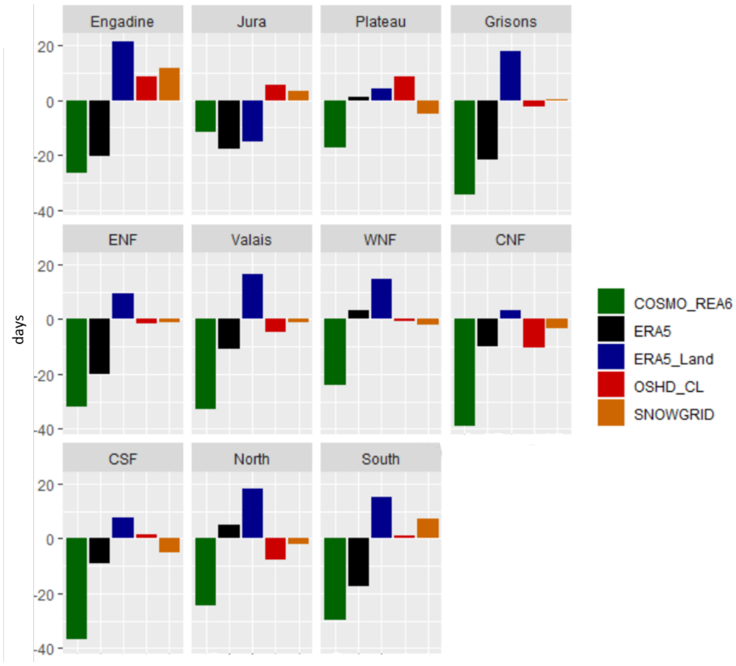

(b) Bias

Figure 31: On the left, the day of maximum snow correlation of ERA5 (black), ERA5-Land (blue), COSMO-REA6 (green), SNOWGRID (orange), and OSHD_CL (red) with OSHD_EKF are plotted. On the right, the bias to OSHD_EKF is displayed. Some regions areabbreviated: CNF denotes the central part of the northern flank, CSF the central part of the southern flank, ENF the eastern part of the northern flank, and WNF the western part of the northern flank.

4.3.2 Anomaly

At lower altitudes, such as the Swiss Plateau (Figure 32), the data sets correspond to the same deviation from the mean value in many years. However, in some years, e.g. 2000, 2009 or 2014, the deviations are larger. At higher elevations, the variability between the data sets is more pronounced, e.g., in the central part of the southern Alps, OSHD_CL and OSHD_EKF are consistent, but SNOWGRID shows a stronger deviation in 2005 and 2011. In addition, the coarse-resolution data sets show a large variability, especially COSMO-REA6, which deviates from the mean percentage of the other data sets in most years.

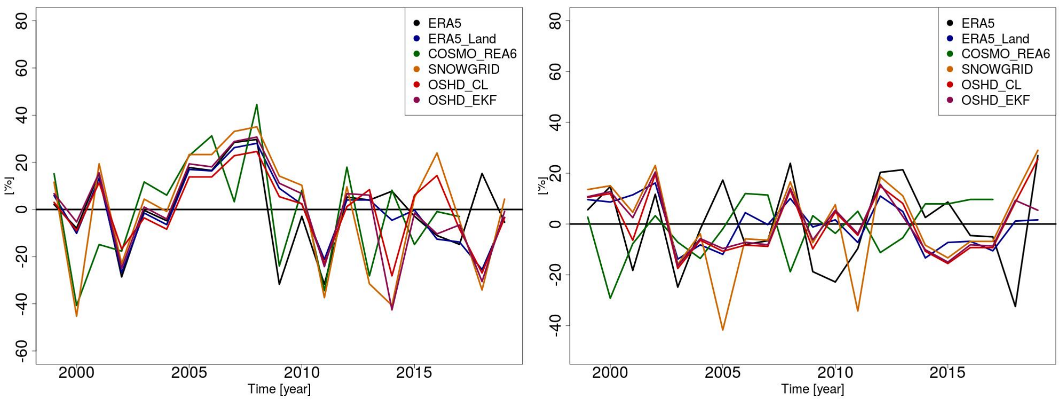

(a) Engadine

(b) Central Part of the southern flank

Figure 32: Percentage deviation from the mean of the day of maximum snow for (a) the Swiss Plateau and (b) the central part of the southern flank of the Alps. The data sets ERA5 (black), ERA5-Land (blue), COSMO-REA6 (green), SNOWGRID (orange), OSHD_CL (red), and OSHD_EKF (purple) are illustrated.

4.3.3 Deviation of products from the reference data set OSHD_EKF

The percentage deviation of the day of maximum to OSHD_EKF has a high variability between the data sets (not shown). The percentage deviations lie between -20% and 15% distributed over all regions with no region showing all data sets deviating in the same direction. COSMO-REA6 shows a negative deviation from OSHD_EKF and spans between -18 and -10% across all regions. ERA5 has negative deviation in most regions and a small positive deviation in some regions (range: between -10 and 4%). Whereas ERA5-Land shows a positive deviation, i.e. a maximum arriving later, in all regions except the Jura. Both 1 km data sets SNOWGRID and OSHD_CL have lower deviations (-4% to 5% and-5% to 8%, respectively) thereby underestimating or overestimating the timing in half of all regions. SNOWGRID has smaller deviations like OSHD_CL.

4.3.4 Trend

The results of the trend analysis are illustrated in Figure 33. It can be seen that all data sets in all regions, apart from the Jura and the Swiss Plateau, have a negative trend. The decadal trend of OSHD_CL in the Jura shows an arrival of the maximum 3 days earlier, whereas SNOWGRID shows almost no change (-0.07 days/decade). In the other regions, all data sets except ERA5 show an approximately equal negative trend. ERA5 shows either a much smaller or larger trend. It shows a very small decadal trend in the north, the central part of the southern and northern flank of the Alps.

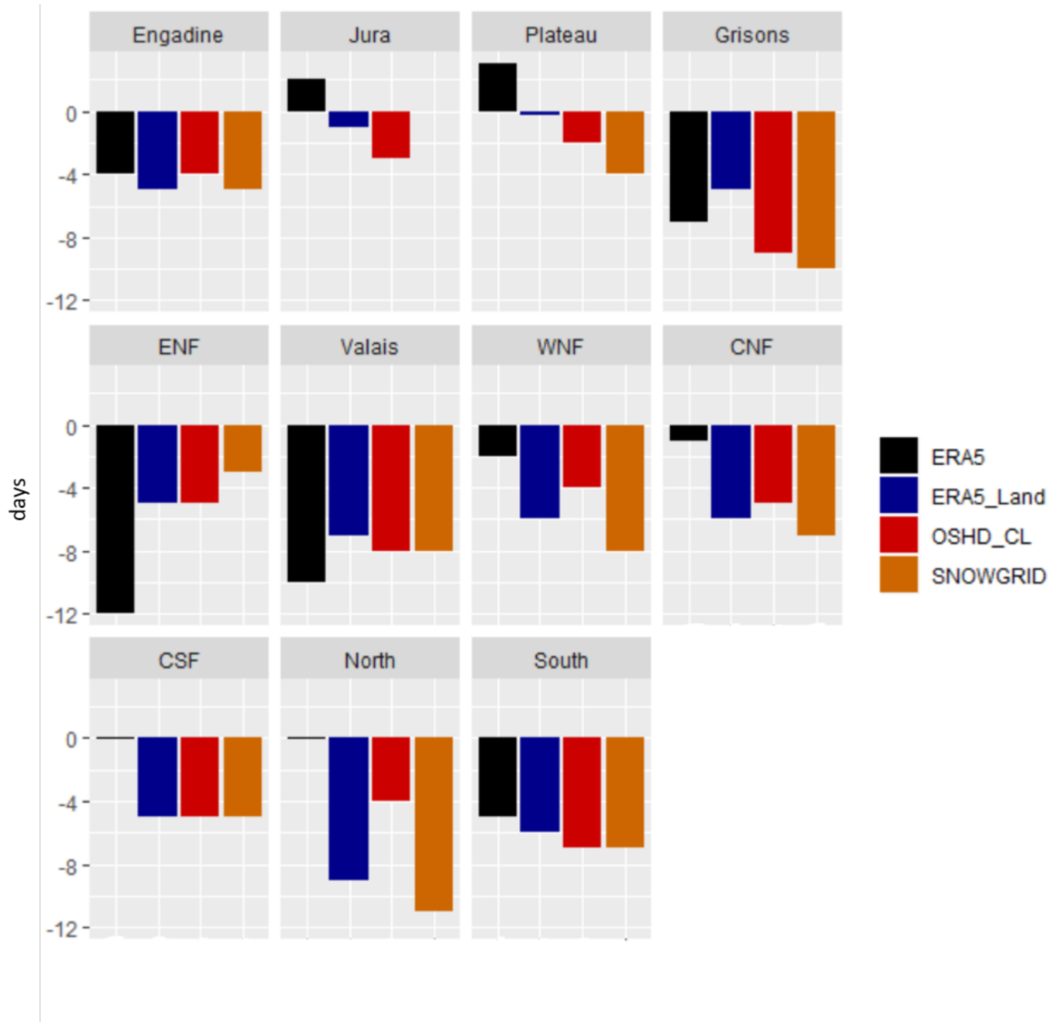

Figure 33: Decadal trend of day of maximum snow for all regions. The data sets ERA5 (black), ERA5-Land (blue), SNOWGRID (orange), and OSHD_CL (red) are displayed. A negative trend indicates a earlier occurrence of the maximum. Some regions are abbreviated: CNF denotes the central part of the northern flank, CSF the central part of the Southern flank, ENF the eastern part of the northern flank, and WNF the western part of the northern flank.

4.4 Snow cover fraction

In the following sections, different aspects of the snow cover fraction are described. First, the climatology and anomaly and then the the results of the trend analysis are shown.

4.4.1 Climatology

The mean snow cover fraction for the period 1999-2016 is shown in Figure 34. The coarse-resolution data sets display lower values than the high-resolution ones in regions with complex topography. While at the lower elevations, they show similar values. This indicator is also dependent on elevation. High elevations can be covered with snow throughout the year, while low elevations are covered with snow for a shorter period of time. Compared to the AVHRR satellite data set, the other 1 km data sets show a greater percentage of snow cover over the Jura Mountains. Furthermore, OSHD_CL shows a higher snow cover fraction over the Swiss Plateau than the other 1 km data sets.

In Table 6 the mean snow cover fraction over the period 1999-2016 is given. It shows that the 1 km data sets have similar snow cover fraction values in all regions. Considering all data sets, the regions with the highest values are the Engadine with a range between 54% and 68%, Grisons (45%-63%) and the Valais (51% -73%). The mean snow cover fraction for the eastern part of the northern flank ranges between 29% and 51%. Similar ranges are found for the Western and Central part of the northern flank, and the central part of the southern flank with 31%-57%, 30%-57%, and 26%-48%, respectively. In the lower lying regions the data sets simulate a smaller snow cover fraction: Jura with 10%-28% and the Swiss Plateau with 6%-20%. With a range of 23%-43%, the northern part of Switzerland shows lower values than the southern part with 41%-57%. Over the entire period, ERA5-Land shows the highest snow cover fraction over all regions except the Jura. The lowest snow cover fraction is shown by AVHRR and COSMO-REA6.

Table 6: Mean snow cover fraction over the period of 1999-2016 for all regions.

[%]	ERA5	ERA5-Land	COSMO-REA6	AVHRR	SNOWGRID	OSHD_CL	OSHD_EKF
Jura	10	18	15	12	20	28	22
Plateau	12	20	6	8	10	18	11
Engadine	55	68	63	54	61	59	60
Grisons	53	63	50	45	52	56	55
East. northern flank	41	51	31	29	37	43	42
West. northern flank	49	57	34	31	39	44	43
Cent. northern flank	51	57	34	30	42	46	44
Cent. southern flank	44	48	37	26	38	41	39
Valais	58	73	51	53	59	60	59
North	34	43	27	23	32	37	34
South	49	57	48	41	48	49	47

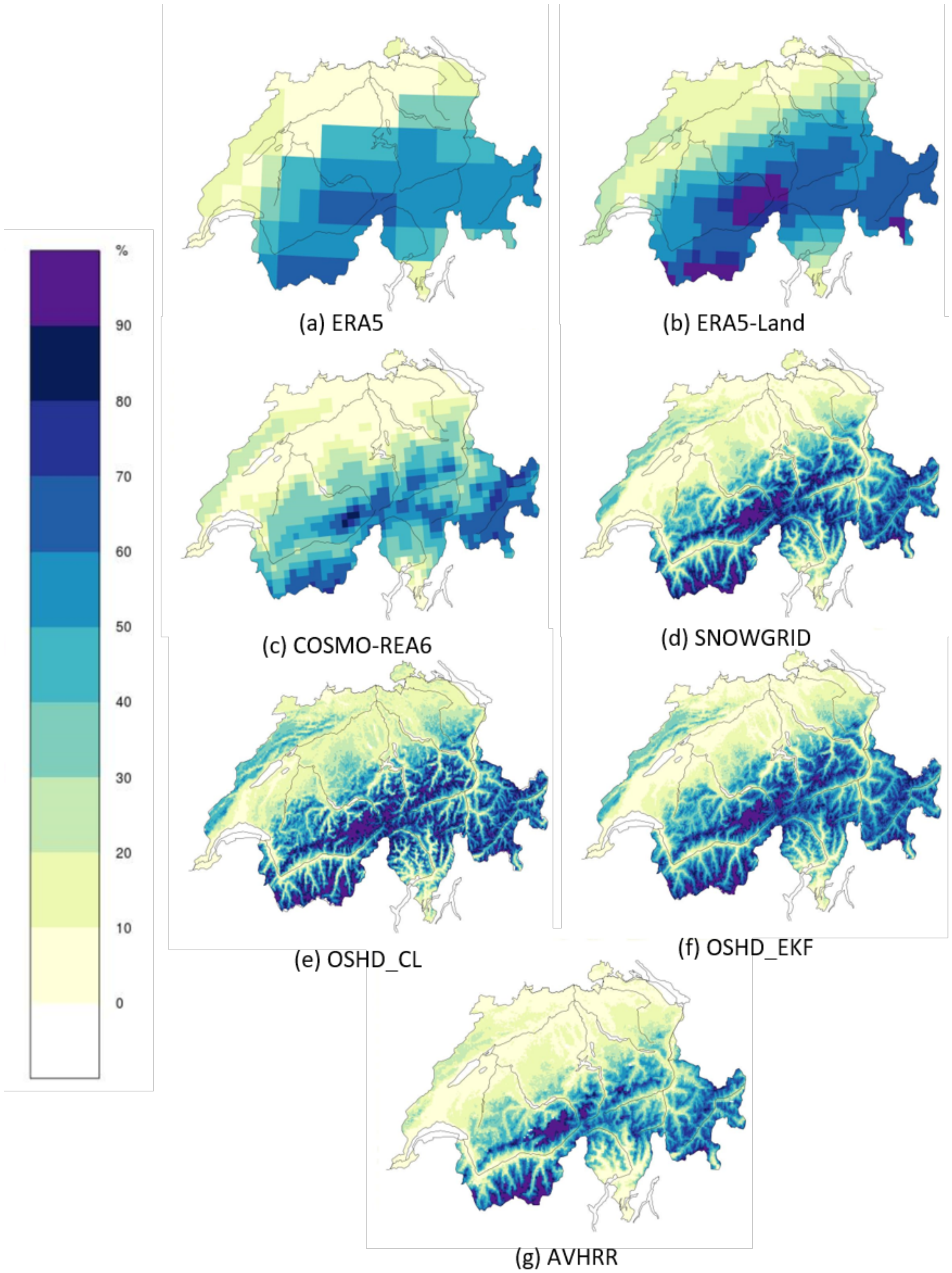

Figure 34: Climatology of snow cover fraction for the period 1999-2016 for (a) ERA5, (b) ERA5-Land, (c) COSMO-REA6, (d) SNOWGRID, (e) OSHD_CL, (f) OSHD_EKF, and (g) AVHRR.

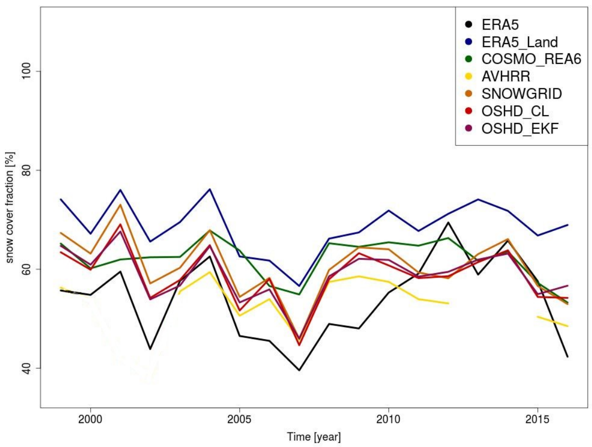

(a) Engadine

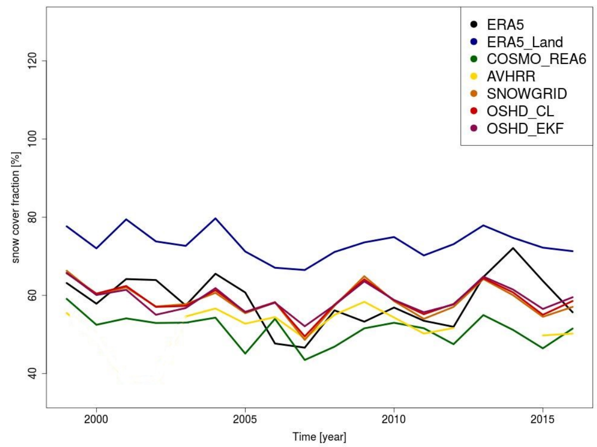

(b) Valais

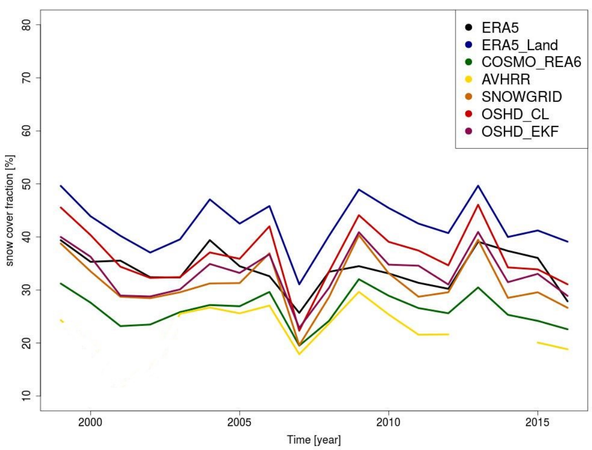

(c) North

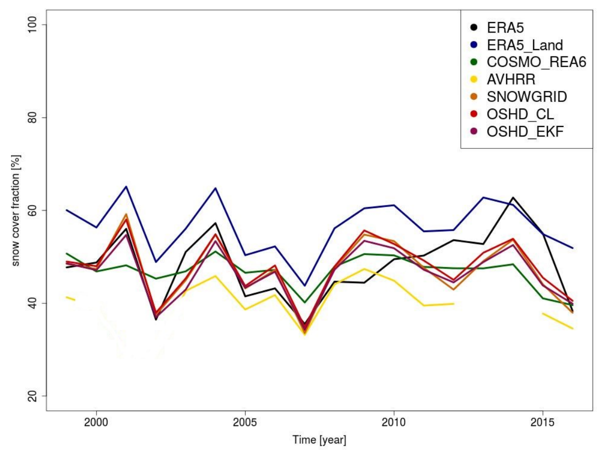

(d) South

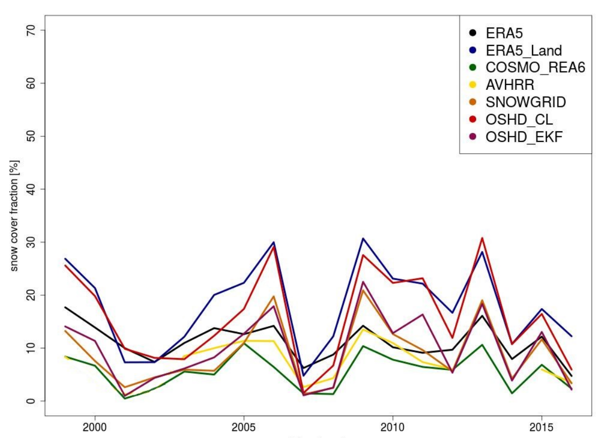

(e) Swiss Plateau

Figure 35: Climatology of the snow cover fraction in the regions (a) Engadine, (b) Valais, (c) Northern Switzerland, (d) Southern Switzerland, and (e) the Swiss Plateau. The data sets ERA5 (black), ERA5-Land (blue), COSMO-REA6 (green), SNOWGRID (orange), OSHD_CL (red), OSHD_EKF (purple), and AVHRR (yellow) are illustrated.

Figure 35 shows the climatology for the selected regions. The results show that ERA5-Land consistently records the highest snow cover fraction. In the Engadine the snow cover fraction is overestimated by all data sets except ERA5 compared to AVHRR. Furthermore, AVHRR shows a different year to year variability in the first years (2000, 2001) and the correlation over the entire period is strongest with SNOWGRID (correlation of 0.92), closely followed by OSHD_CL (0.91), OSHD_EKF (0.85), COSMO-REA6 (0.78), ERA5-Land (0.66) and finally ERA5 (0.46) (Figure 35).

In the Valais, the year-to-year variability is smaller and AVHRR shows a much smaller snow cover fraction in 2001 and 2002 than the other data sets. As in the Engadine, the best correlation is with SNOWGRID (0.71), OSHD_CL (0.67) and OSHD_EKF (0.62). Next come ERA5-Land (0.53), COSMO-REA6 (0.47), and ERA5 (0.21).

In the north and south, the behaviour of the data sets is quite similar: all show an overestimation. In the north, the variance between the 1 km data sets is larger. The correlation in the south is larger than in the north (see Figure 35). In the Swiss Plateau, the variability of the data sets is larger, and all data sets show a higher snow cover fraction than AVHRR. Further, a very similar correlation among the data sets is observed, the highest being SNOWGRID with 0.8 and the lowest being ERA5 with 0.61.

Looking at the bias in all regions, ERA5-Land shows the largest bias in all regions except the Jura. The remaining data sets show a similar bias as the differences between the data are of a rather small magnitude. The bias is mostly positve, only ERA5 underestimates the snow cover fraction in the Jura and COSMO-REA6 has a slight underestimation in the Valais and the Swiss Plateau. Out of the 1 km data sets, OSHD_CL has the largest positive bias in most regions, however, the difference is not substantial. Considering the correlation of all data sets with AVHRR is positive. SNOWGRID performs best with a correlation of 0.56-0.95, followed by COSMO-REA6, OSHD_CL, ERA5-Land, OSHD_EKF, and lastly ERA5. However, the correlation should be taken with caution as the time series is rather short.

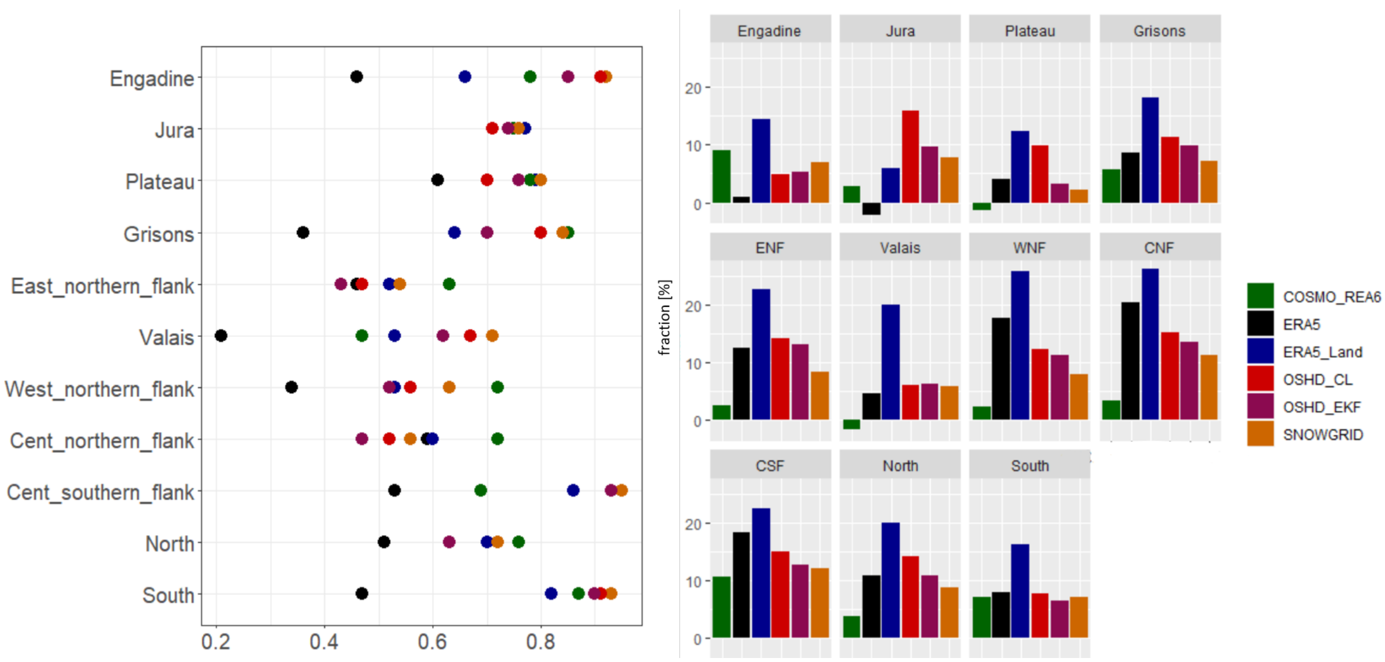

(a) Correlation (b) Bias

Figure 36: On the left, the snow cover fraction correlation during the period of 1999-2016 of the data sets ERA5 (black), ERA5-Land (blue), COSMO-REA6 (green), SNOWGRID (orange), OSHD_CL (red), OSHD_EKF (purple) with AVHRR are plotted. On the right, the bias to AVHRR is illustrated. Some regions are abbreviated: CNF denotes the central part of the northern flank, CSF the central part of the southern flank, ENF the eastern part of the northern flank, and WNF the western part of the northern flank.

4.4.2 Anomaly

As seen in Figure 37, the mean percentage deviation is smaller in the elevated regions than in the lower regions. The scatter is much larger among the data sets in the Swiss Plateau (Figure 37a) and ranges between -100% and 130%.

Furthermore, not all data sets deviate equally from the mean in all years, especially in the first 5 years the spread is larger, but all data sets indicate the same direction of deviation.

Whereas in the Valais (Figure 37b), the spread and the deviation are much smaller with a maximum of 24%. The behaviour of the low and high altitudes is also shown in the maps of the single years (Figure 37c and Figure 37d). The low-lying areas show stronger deviations from the mean compared to the higher regions. During the winter of 2009, which had a relatively high snowfall, the snow cover fraction was above the mean in the lower regions and below the mean during the winter of 2007, which had less heavy snowfall.

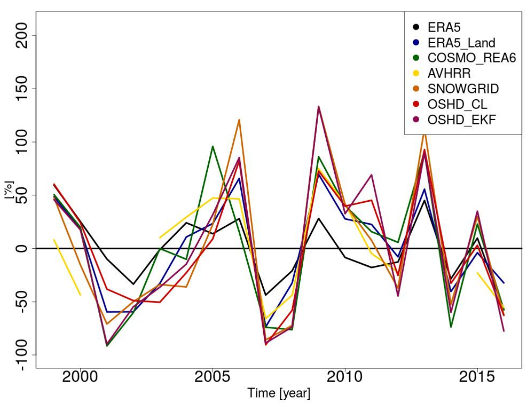

(a) Swiss Plateau

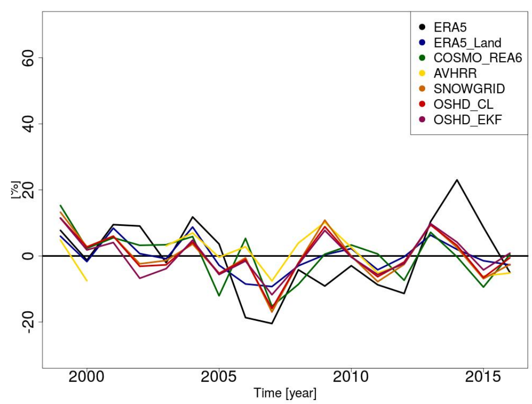

(b) Valais

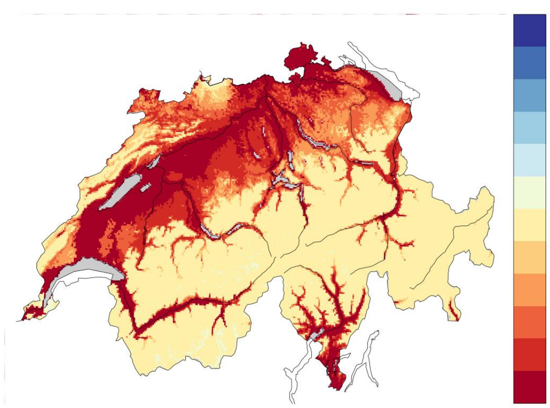

(c) 2007

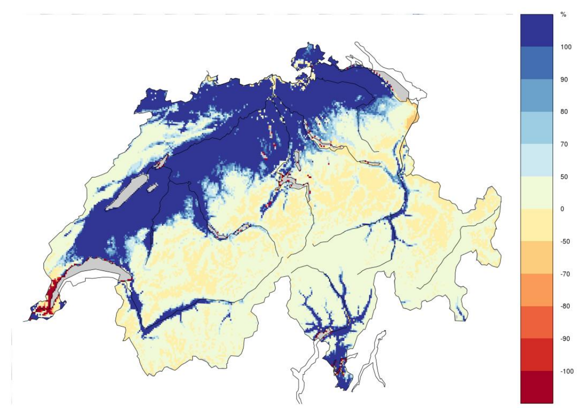

(d) 2009

Figure 37: Subfigures (a) and (b) show the percentage deviation of the snow cover fraction from the mean during the period of 1999-2019 for the Swiss Plateau and the Valais. The data sets ERA5 (black), ERA5-Land (blue), COSMO-REA6 (green), SNOWGRID (orange), OSHD_CL (red), OSHD_EKF (purple), and AVHRR (yellow) are illustrated. Subfigures (c) and (d) show the mean percentage deviation of OSHD_EKF for the years 2007 and 2009, respectively. Red indicates less and blue indicates a higher snow cover fraction than on average.

4.4.3 Trend

A negative relative trend is observed in all regions for each data set, and ERA5-Land shows the smallest trend in all regions (Figure 38 and Figure 39). For instance, in the Engadine, ERA5-Land with -6% shows only half the trend as the other data sets. In the Valais, ERA5 shows the largest trend with -17%, followed by OSHD_CL (-13%), SNOWGRID (-12%) and ERA5-Land (-10%), hence there are only minimal differences between the data sets. In the Swiss Plateau bigger differences between the data sets and the largest trend are found. Specifically, a decrease of -56% is shown by ERA5, -35% by SNOWGRID, -26% by OSHD_CL, and -5% by ERA5-Land.

Across all regions, the second strongest trend is seen in the eastern part of the northern flank with -11% to -42%. In the Jura, the third strongest trend is observed at a range of -4% to -30%. The other regions show similar trends, varying from -9% to -23%. SNOWGRID and OSHD_CL have minor differences in trend, with SNOWGRID showing a stronger trend more often.

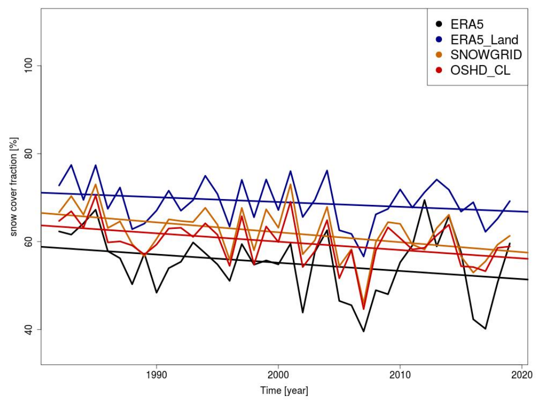

(a) Engadine

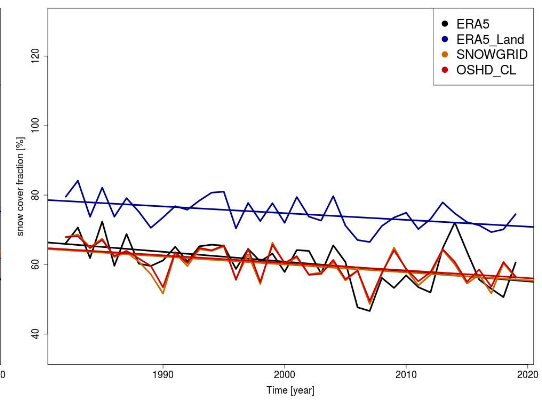

(b) Valais

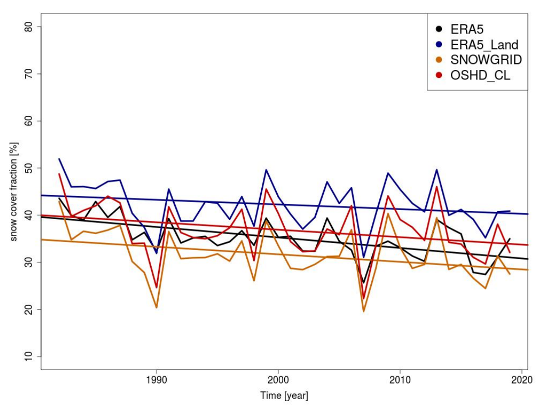

(c) North

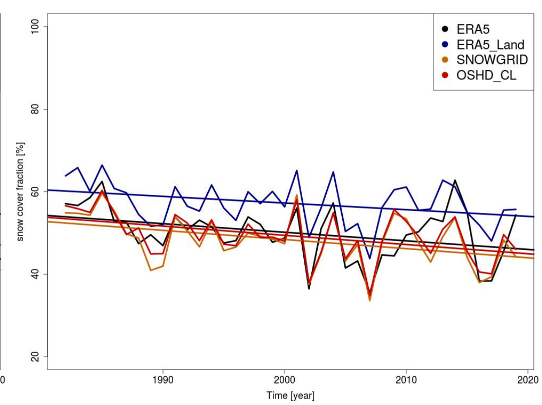

(d) South

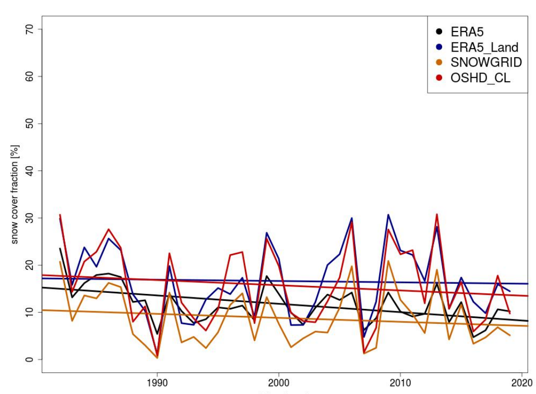

(e) Swiss Plateau

Figure 38: Trend of snow cover fraction for the period 1982-2019 for the regions (a) Engadine, (b) Valais, (c) North, (d) South, and (e) the Swiss Plateau. The data sets ERA5 (black), ERA5-Land (blue), SNOWGRID (orange), and OSHD_CL (red) are shown.

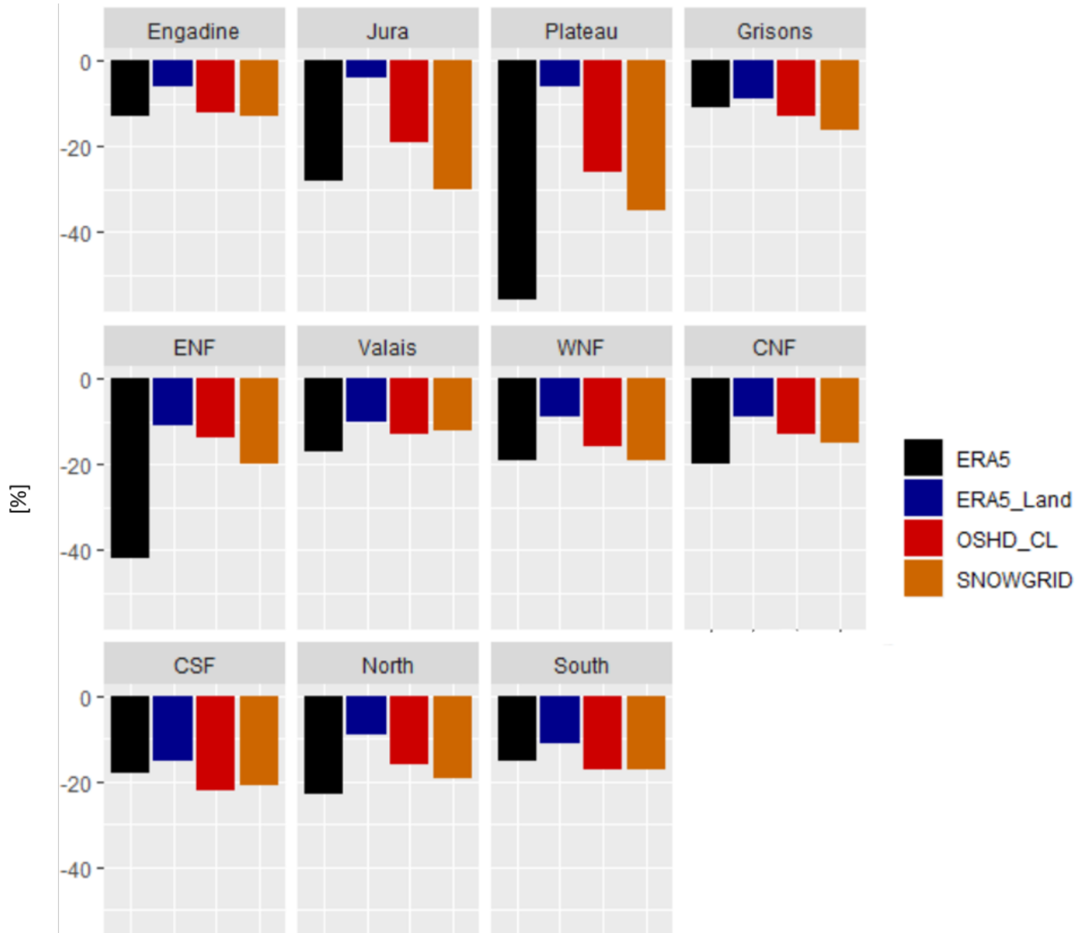

Figure 39: Relative trend of the snow cover fraction in percent over the period 1982-2019 is shown. ERA5 in black, ERA5-Land in blue, SNOWGRID in orange and, OSHD_CL in red. Some regions are abbreviated: CNF denotes the central part of the northern flank, CSF the central part of the southern flank, ENF the eastern part of the northern flank, and WNF the western part of the northern flank.

5 Discussion

SWE

The snow characteristics in Switzerland are described by various snow indicators. The mean SWE for the period 1999-2019 showed topographical features, higher (lower) elevations have higher (lower) SWE values. The reference data set OSHD_EKF shows a mean SWE of 0.194 m SWE in the Valais, 0.096 m SWE in the southern part of Switzerland, and 0.003 m SWE in the Swiss Plateau. Considering all regions, COSMO-REA6 has a very poor performance regarding the temporal correlation with OSHD_EKF. The correlation of other data sets with a lower spatial resolution such as ERA5 or ERA5-Land perform mostly better and have a higher correlation with the reference data set. ERA5-Land's correlation with the 1 km data sets is strong. However, it shows a positive SWE bias in most regions.

Looking at the snow distribution from the years 1982-2019 for the various regions of Switzerland showed that snow has not decreased to the same extent everywhere, but that large regional differences occur. Further, not all data sets show the same magnitude of decrease. We found, that the mean SWE has the strongest decline (range: -53% to -39%) in the northern regions of Switzerland. The analysis of altitude classes shows that the relative trend is strongest in the lower three altitude classes (0-500 m, 500-1000 m and 1000-1500 m) and weaker in the higher altitude classes (1500-2000 m, 2000-2500 m, >2500 m). Moreover, the magnitude of the trend varies between the data sets and the variation is stronger in the lower regions. The 1 km data sets show similar trends at all altitudes and ERA5-Land the weakest. Matiu et al. (2020) investigated the snow depth using in-situ measurements and they found similar behaviour for the altitude classes with stronger decreases of snow depth at lower elevations. Further, Laternser and Schneebeli (2003) also found the same elevation dependencies of trends. This coincides mostly with the results of this master's thesis, where the model data showed a stronger trend at lower elevations.

Comparing the station data with the nearest grid cells of the high resolution data, we find that SNOWGRID overestimates the amount of snow, especially in the central part of the northern and southern flank. OSHD_CL generally has a smaller bias than SNOWGRID in all regions expect in the Engadine. OSHD_EKF has the smallest bias, which is not surprising as the snow model assimilates these station observations. Overall, all 1 km data sets coincide well with the station data.

Number of snow days

The number of snow days is also dependent on the elevation. Higher lying regions experience more snow days throughout the year. For example, OSHD_EKF counts 221 snow days for the Valais, 184 days for the Southern part of Switzerland, and 31 days for the Swiss Plateau. Comparing all data sets with AVHRR reveals that most data sets correlate relatively well with the AVHRR data. Accross all regions, SNOWGRID shows the strongest and ERA5-Land the weakest correlation. For some regions (Valais and all parts of the northern flank (western, southern, and central)) a comparably low correlation (0-0.25) is found for all data sets. This could be caused by a lower performance of the AVHRR data for these regions.

The data sets mostly overestimate the number of snow days compared to AVHRR. This is likely related to the applied threshold of 1 cm SWE for determining a snow day. Increasing this value, whose exact numerical value is relatively uncertain, would enhance the overall agreement. Furthermore, the overestimation might also be due to the gaps in the AVHRR data.

The relative trend of this indicator showed a negative trend in all regions for all data sets. In the Valais, the trend of all data sets is of similar magnitude: ERA5 and OSHD_CL with -18%, ERA5-Land and SNOWGIRD with -14% and -16%, respectively. In the southern part, a relative trend of -14% is found for ERA5 and SNOWGRID. Smaller trend are found for OSHD_CL (-13%) and ERA5-Land (-9%). In the Swiss Plateau ERA5 shows a large trend of -83%, while the other data sets show a much smaller trend with -6% for ERA5-Land, -42% for SNOWGRID, and -27% for OSHD_CL.

Day of maximum snow

The results of this thesis showed that the day of maximum snow is found earlier in the regions with lower elevation. This thesis revealed that the high resolution data sets have very small differences among each other. For instance, in the Valais the 1 km data sets simulate the day of maximum snow at the beginning of April. A similar timing with the end of March is found in the southern part of Switzerland. In the Swiss Plateau, the day with maximum snow occurs at the beginning of February. For regions at high elevations, grid cells which only accumulate over a year and therefore reach their maximum at the end of the year, were masked out. So this might influence the results as not the same number of grid cells were taken out of the analysis.

The 1 km data sets have a strong temporal correlation with OSHD_EKF and the smallest bias across all regions.

This indicator clearly benefits from high spatial resolution. I.e. a high resolution seems to be important to accurately predict the timing of maximum SWE. This is important for snow hydrology and connected sectors like hydropower production, agriculture, etc.

The trend analysis revealed mostly negative trends, meaning that the timing of the maximum snow is shifted forward in time over the last 30 years. In the Valais and the southern part of Switzerland, the data sets ERA5, ERA5-Land, OSHD_CL, and SNOWGRID have a trend around -8 days/decade. In the Swiss Plateau, the decadal trends are weaker. ERA5 shows a positive trend of 3 days/decade, ERA5-Land shows almost no trend, OSHD_CL and SNOWGIRD have a trend of -2 days/decade, and -4 days/decade, respectively.

Snow cover fraction

The mean snow cover fraction shows that coarse-resolution data sets display lower values than the high-resolution ones in regions with complex topography. For example, OSHD_EKF has a snow cover fraction of 59% in the Valais, 47% in the southern part of Switzerland, and 11% in the Swiss Plateau. In comparison with the AVHRR data, a positive bias is found in most regions. The high resolution data sets show a similar bias in most regions and SNOWGRID also has the highest temporal correlation with AVHRR. As previously with the snow indicator number of snow days, the results might be improved by choosing a higher threshold for determining the snow cover fraction.

A negative trend is found in all regions for all data sets. For instance, in the Valais, the trend is -17% for ERA5, -10% for ERA5-Land, -12% for SNOWGRID, and -13% for OSHD_CL. At lower regions like the Swiss Plateau, ERA5 shows a stronger trend of -56% and ERA5-Land shows a weaker trend of -6%. The differences between the 1 km data sets SNOWGRID (-35%) and OSHD_CL (-12%) are larger in this region.

In the following, the research questions are discussed:

- **Do certain products reveal superiorities or weaknesses in specific geographical regions, elevations, or seasons (e.g. during accumulation/ablation) in representing snow cover?**

  The data sets demonstrated different SWE climatologies for the period 1999-2019. COSMO-REA6 overestimates the SWE amount in the Engadine, OSHD_CL in the Swiss Plateau, and ERA5 underestimates the SWE in most regions. The data revealed year-to-year variability and in general, the high-resolution data sets OSHD_EKF, OSHD_CL and SNOWGRID show similar snow amounts and a strong correlation with each other. Compared to OSHD_EKF, OSHD_CL and SNOWGRID slightly overestimate the snow amount in all regions, where SNOWGRID has a larger bias. The data sets with lower resolution show larger biases, whereby ERA5-Land overestimates the mean SWE in most regions, and COSMO-REA6 and ERA5 show an underestimation in many regions. ERA5-Land shows a correlation with OSHD_EKF almost as large as the 1 km data sets, whereas ERA5 and COSMO-REA6 show much weaker correlations. The differences among the data sets can be attributed to horizontal resolution, forcing data, and the complexity of the model.

  Several data sets show weaknesses in certain regions and elevations as well. In the Valais and Engadine, ERA5 Land provides an incomplete spatial coverage because some grid cells had to be masked out and consequently less snow is accumulated. Furthermore, we see that in elevation classes 3 (1000-1500 m) and 4 (1500-2000 m), ERA5-Land strongly overestimates the amount of snow. COSMO-REA6 shows deficiencies in the Engadine, here it overestimates the SWE amount and has a low correlation with the remaining data sets. Considering the different elevations, these weaknesses are also observable in the altitude classes 5 (2000-2500 m) and 6 (>2500 m) for the regions Engadine, Grisons and the eastern part of the northern flank. Moreover, COSMO-REA6 shows an earlier maximum of SWE. The fact that COSMO-REA6 is driven by ERA-Interim and differences in model physics might explain part of the observed differences.

- **Do the existing data sets represent the spatio-temporal variability of Swiss snow cover, and to what extent do they agree or disagree with each other?**

  The gridded snow data sets agree on the snow climatology on different levels. The highest agreement is found among the 1 km data sets for all snow indicators. Considering the indicator SWE, the temporal correlation with the reference data set OSHD_EKF is strong for all data sets except COSMO-REA6 and ERA5. COSMO-REA6 does not represent the variability in the Engadine well.

  Looking at the number of snow days and the snow cover fraction, AVHRR shows substantially less snow days and a smaller snow cover fraction compared to the other data sets. For the snow days, the correlation is weak for the western and central parts of the northern flank. However, the chosen threshold of the snow day definition and the short time series may be responsible for this. Regarding the snow cover fraction, ERA5 shows a very small correlation with AVHRR, whereas the other data sets show medium to large correlation. All data sets show positive biases with the reference data set, whereby COSMO-REA6 has the smallest bias. All data sets show the deviation from the mean in the same years in all regions.

For the day of maximum snow, the correlation of COSMO-REA6 with OSHD_EKF is weak and displays a high negative bias in all regions. ERA5 also has a low correlation with OSHD_EKF and a small bias. The 1 km data sets show a high correlation and a small bias with OSHD_EKF. ERA5-Land has a medium to high correlation with the reference data set, however the biases are large in many regions. The 1 km data sets show the anomalies in the same year, and the coarse resolution data sets are more variable.

- **Are high-resolution reanalyses suitable for snow monitoring in the alpine region in Switzerland?**

  Depending on the region and snow indicator, COSMO-REA6 is suitable for snow monitoring. Considering the SWE, COSMO-REA6 shows a small bias and a good correlation in all regions expect the Engadine. In all regions, COSMO-REA6 detects the peak earlier and starts to melt earlier. For the number of snowdays, it has a small bias and a good correlation in all regions expect the central part of the northern flank. For the day of maximum snow, the correlation with the reference data set is small and the bias rather large. For the snow cover fraction a small bias and a medium correlation with AVHRR was found.

  ERA5-Land has a high correlation with the 1 km data sets and a small bias considering the snow indicator SWE. It is suitable for monitoring in all regions except the Valais as many grid cells are masked out in this region. For the number of snow days, the correlation with AVHRR is small in many regions (Valais, western and central part of the northern flank, and the northern part of Switzerland). For the other regions, the correlation is higher, but the bias is large in all regions. However, this depends on the chosen threshold for the definition of a snow day. ERA5-Land has small biases for the day of maximum snow in the regions Swiss Plateau, eastern and central part of the northern flank, and in the central part of the southern flank. In these regions, ERA5-Land can be used for monitoring.

To sum up, in the following the advantages and disadvantages of the data sets are shortly listed in the tables below.

Table 7: Advantages and disadvantages of ERA5

Advantages	**Disadvantages**
Long time period, suitable for trend analysis	Coarse resolution
Similar trend compared to other data sets in many regions	Low correlation with AVHRR
	No gridcells above 2000 m

Table 8: Advantages and disadvantages of ERA5-Land

Advantages	**Disadvantages**
Long time period, suitable for trend analysis	Coarse resolution
Good correlation with OSHD_EKF	Not suitable for high elevation regions like the Valais
medium correlation with AVHRR	Overestimates the amount of snow compared to OSHD_EKF

Table 9: Advantages and disadvantages of COSMO-REA6

Advantages	**Disadvantages**
Good correlation with AVHRR	Intermediate resolution
	Seasonal cycle shows earlier peak
	Overestimates snow in the Engadine and has little correlation
	Overestimates the SWE at altitude classes 5 and 6
	Weak/negative correlation with OSHD_EKF

Table 10: Advantages and disadvantages of SNOWGRID

Advantages	Disadvantages
High resolution	Overestimates snow in all regions, especially in the Valais
Long time period, suitable for trend analysis	Shows larger station bias than OSHD_CL
Shows similar trend as OSHD_EKF	
Good correlation with OSHD_EKF and AVHRR	
suitable for analysing elevation dependent snow distribution	

Table 11: Advantages and disadvantages of OSHD_CL

Advantages	Disadvantages
Long time period, suitable for trend analysis	Overestimates snow in all regions, especially in the Swiss Plateau
High resolution	Medium correlation with AVHRR
Shows similar trend as OSHD_EKF	
Shows small station bias	
Good correlation with OSHD_EKF	
suitable for analysing elevation dependent snow distribution	

Table 12: Advantages and disadvantages of OSHD_EKF

Advantages	Disadvantages
High resolution	Short time period
Reference data set including assimilation of snow observations	Medium to low correlation with AVHRR
Shows smallest station bias	
suitable for analysing elevation dependent snow distribution	

Table 13: Advantages and disadvantages of AVHRR

Advantages	Disadvantages
High resolution	Short time period with missing data points
Reference data set	Medium to low correlation with OSHD_EKF
suitable for analysing elevation dependent snow distribution	binary data and no information about snow quantity

6 Conclusion and outlook

In this thesis, an analysis of the Swiss snow climatology for the two time periods 1999-2019 and 1982-2019 of various data sets was presented. Further, a trend analysis was conducted for the longer time period. The data sets were used to derive snow indicators such as the mean SWE, number of snow days, day of maximum snow, and snow cover fraction in eleven regions of Switzerland. The data sets were validated against the reference data sets OSHD_EKF (high resolution snow model with assimilation of snow observations), AVHRR (remote sensing product), and station data.

The data reveals a high year-to-year variability and the data sets agree well on the Swiss snow climatology with small biases for the 1 km data sets. Strong seasonal cycles were found in all regions and data sets. The highest agreement is found for the indicator mean SWE, here the bias ranges from -0.03 m SWE to 0.03 m SWE among all data sets. The performance of the data sets varies, COSMO-REA6 does not represent the snow climatology in the Engadine, and ERA5-Land has a poor representation of the mean SWE in the Engadine and the Valais. In addition, when considering the day of maximum snow, many regions do not compare well because many grid cells are masked out.

The trend analysis showed a decrease in mean SWE, snow cover fraction, number of snowdays, and an earlier occurrence of the day with maximum snow. The magnitude of the trends is highly dependent on the region (respectively the orography) and altitude. The results of the trend of the mean SWE showed a higher decrease for the lower elevations and lower decrease for the higher elevations. This behaviour of the trend was found in all data sets. For example, in the northern part of Switzerland the relative trend of SNOWGRID ranges from -78% (0-500 m) to -31% (>2500 m).

This thesis has shown the spatial and temporal variability of the Swiss snow climatology for different data sets. There are further approaches to extend this analysis. It would generally be desirable to include more data sets with long time periods, high resolution, or more observational data. Moreover, it would be interesting to analyse additional snow indicators such as onset, duration, and end of the continuous snow cover, changing the threshold for the number of snow days, analysing all indicators for the different altitude classes, and choosing a smaller time period (e.g. winter months) for the trend analysis. Furthermore, it would be interesting to see if a Theil-Sen trend yields different results than the linear regression. This would lead to better understanding of the distribution of snow for the different regions. Another interesting aspect would be to look at the forcing data of the models such as temperature or precipitation to make statements about their influences. This might help to understand what causes the behaviour of COSMO-REA6 in the Engadine and the higher altitude classes in the regions of Grisons or eastern part of the northern flank. Further, large scale phenomena like the NAO could also be included in the analysis to understand its influence. The development of a reliable spatial and temporal snow climatology and the results of this analysis is of relevance for various sectors such as winter tourism, hydrology and ecological purposes.

Acknowledgements

First, I would like to thank Dr. Stefanie Gubler and Dr. Christian Steger for the support throughout this master's thesis. Furthermore, I would like to thank Dr. Sven Kotlarski, Dr. Simon Scherrer and Prof. Dr. Christoph Schär for valuable comments and inputs. Additionally, I would like to thank Dr. Tobias Jonas for providing the SWE in-situ data for this study.

References

Abegg, B., Agrawala, S., Crick, F. and Montfalcon, A.. (2007): Climate change impacts and adaptation in winter tourism. Climate Change in the European Alps. Adapting Winter Tourism and Natural Hazards Management. 25-60.

Anghileri, D., Botter, M., Castelletti, A., Weigt, H., and Burlando, P. (2018) A Comparative Assessment of the Impact of Climate Change and Energy Policies on Alpine Hydropower, Water Resources Research, 54(11), 9144–9161, doi: https://doi.org/10.1029/2017WR022289

Beniston M. (1997) Variations of Snow Depth and Duration in the Swiss Alps Over the Last 50 Years: Links to Changes in Large-Scale Climatic Forcings. In: Diaz H.F., Beniston M., Bradley R.S. (eds) Climatic Change at High Elevation Sites. Springer, Dordrecht. https://doi.org/10.1007/978-94-015-8905-5_3

Bundesamt für Energie (2020) Wasserkraft; https://www.bfe.admin.ch/bfe/de/home/forschung-und-cleantech/forschungsprogramme/wasserkraft.html ; Date accessed: 16.04.2020.

CH2018 (2018), CH2018 – Climate Scenarios for Switzerland, Technical Report, National Centre for Climate Services, Zurich, 271 pp. ISBN: 978-3-9525031-4-0

Copernicus Climate Change Service (2018). ERA 5 data; https://cds.climate.copernicus.eu/cdsapp#!/dataset/reanalysis-era5-single-levels?tab=overview ; Date accessed: 16.04.2020.

Copernicus Climate Change Service (2019). ERA5-Land; https://cds.climate.copernicus.eu/cdsapp#!/dataset/reanalysis-era5-land?tab=overview ; Date accessed: 16.04.2020.

ECMWF (2020) Climate reanalysis; https://www.ecmwf.int/en/research/climate-reanalysis ; Date accessed: 30.05.2020.

Eidgenössische Forschungsanstalt WSL (2012). Alpine Schnee- und Wasserressourcen gestern, heute, morgen. Technical report.

Elsasser, H. and Bürki, R. (2002) Climate change as a threat to tourism in the Alps, Climate Research, 20,253–257, doi:10.3354/cr020253

Foppa, N. and Seiz, G. (2012). Inter-annual variations of snow days over Switzerland from 2000-2010 derived from MODIS satellite data. Cryosphere, 6(2):331–342.

Grünewald, T., Bühler, Y., and Lehning, M. (2014). Elevation dependency of mountain snow depth. Cryosphere, 8(6):2381–2394.

Hüsler, F., Jonas, T., Riffler, M., Musial, J. P., and Wunderle, S. (2014) A satellite-based snow cover climatology (1985–2011) for the European Alps derived from AVHRR data, The Cryosphere, 8, 73–90, https://doi.org/10.5194/tc-8-73-2014

IPCC (2013). Climate Change 2013: The Physical Science Basis. Contribution of Working Group I to the Fifth Assessment Report of the Intergovernmental Panel on Climate Change [Stocker, T.F., D. Qin, G.-K. Plattner, M.Tignor, S.K. Allen, J. Boschung, A. Nauels, Y. Xia, V. Bex and P.M. Midgley (eds.)] Cambridge University Press, Cambridge, United Kingdom and New York, NY, USA, 1535 pp.

Koenig, U. and Abegg, B. (1997) Impacts of Climate Change on Winter Tourism in the Swiss Alps, Journal of Sustainable Tourism, 5(1), 46–58

Laternser M., Schneebeli M. (2003) Long-term snow climate trends of the Swiss Alps (1931–99). Int J Climatol 23:733–750, doi: https://doi.org/10.1002/joc.912

Luetschg, M., Lehning, M., and Haeberli, W. (2008). A sensitivity study of factors influencing warm/thin permafrost in the Swiss Alps. Journal of Glaciology, 54(187):696–704.

Marty, C. (2008) Regime shift of snow days in Switzerland, Geophys. Res. Lett., 35, L12501, doi: https://doi.org/10.1029/2008GL033998

Marty, C., Tilg, A., & Jonas, T. (2017). Recent Evidence of Large-Scale Receding Snow Water Equivalents in the European Alps, *Journal of Hydrometeorology*, *18*(4), 1021-1031. Retrieved Apr 7, 2021, from https://journals.ametsoc.org/view/journals/hydr/18/4/jhm-d-16-0188_1.xml

Matiu, M., Crespi, A., Bertoldi, G., Carmagnola, C. M., Marty, C., Morin, S., Schöner, W., Cat Berro, D., Chiogna, G., De Gregorio, L., Kotlarski, S., Majone, B., Resch, G., Terzago, S., Valt, M., Beozzo, W., Cianfarra, P., Gouttevin, I., Marcolini, G., Notarnicola, C., Petitta, M., Scherrer, S. C., Strasser, U., Winkler, M., Zebisch, M., Cicogna, A., Cremonini, R., Debernardi, A., Faletto, M., Gaddo, M., Giovannini, L., Mercalli, L., Soubeyroux, J.-M., Sušnik, A., Trenti, A., Urbani, S., and Weilguni, V.: Observed snow depth trends in the European Alps: 1971 to 2019, (2021): The Cryosphere, 15, 1343–1382, https://doi.org/10.5194/tc-15-1343-2021, 2021.

Olefs, M. (2019). SNOWGRID CL Dokumentation. Technical report.

Pettorelli, N., Pelletier, F., von Hardenberg, A., Festa-Bianchet, M., and Coteal, S. D.(2007) Early onset of vegetation growth vs. rapid green-up: impacts on juvenile mountain ungulates, Ecology, 88, 381–390, doi:10.1890/06-0875

Scherrer S.C., Appenzeller C., Laternser M.C. (2004) Trends in Swiss Alpine snow days—the role of local- and largescale climate variability, Geophys Res Lett 31:L13215, doi:10.1029/2004GL02025

Scherrer, S. C. and Appenzeller, C. (2006) Swiss alpine snow pack variability: major patterns and links to local climate and large-scale flow, Clim. Res., 32, 187–199, https://doi.org/10.3354/cr032187

Scherrer, S. C., Ceppi, P., Croci-Maspoli, M., and Appenzeller, C. (2012). Snow-albedo feedback and Swiss spring temperature trends. Theoretical and Applied Climatology, 110(4):509–516.

Scherrer, S.C., Wüthrich, C., Croci-Maspoli, M., Weingartner, R. and Appenzeller, C. (2013), Snow variability in the Swiss Alps 1864–2009. Int. J. Climatol., 33: 3162-3173. https://doi.org/10.1002/joc.3653

Sippel, S., Fischer, E. M., Scherrer, S. C., Meinshausen, N., and Knutti, R. (2020). Late 1980s abrupt climatic change in Europe consistent with circulation variability and long-term warming. Manuscript submitted for publication. Environmental Research Letters.

SLF (2020). Operationelle schneehydrologische Modelle des SLF; https://www.slf.ch/de/schnee/schnee-als-wasserressource/schneehydrologische-vorhersagen/oshd-modelle.html ; Date accessed: 07.05.2020.

Stähli, M. and Gustafsson, D. (2006). Long-term investigations of the snow cover in a subalpine semi-forested catchment. Hydrological Processes, 20(2):411–428.

Steger, C., Kotlarski, S., Jonas, T., and Schär, C. (2013). Alpine snow cover in a changing climate: A regional climate model perspective. Climate Dynamics, 41(3-4):735–754.

Steiger R (2010) The impact of climate change on ski season length and snowmaking requirements in Tyrol, Austria. Clim Res 43:251-262. https://doi.org/10.3354/cr00941

Terzago, S., Von Hardenberg, J., Palazzi, E., and Provenzale, A. (2017). Snow water equivalent in the Alps as seen by gridded data sets, CMIP5 and CORDEX climate models. Cryosphere, 11(4):1625–1645.

Trachsel, J., Zweifel, B., Techel, f., Marty, C.; Stucki, T., (2020): Schnee und Lawinen in den Schweizer Alpen. Hydrologisches Jahr 2019/20. WSL Ber. 101: 76 S.

Whiteman, C. (2000). Mountain Meteorology: Fundamentals and Applications. : Oxford University; retrieved from https://oxford.universitypressscholarship.com/view/10.1093/oso/9780195132717.001.0001/isbn-9780195132717.

Wirz, V., Schirmer, M., Gruber, S., and Lehning, M. (2011). Spatio-temporal measurements and analysis of snow depth in a rock face. Cryosphere, 5(4):893–905.

Wu, W.-Y., Lan C.-W., Lo M.-H., Reager J. T., and Famiglietti J. S. (2015): Increases in the annual range of soil water storage at northern middle and high latitudes under global warming, Geophys. Res.Lett., 42,3903–3910, doi:10.1002/2015GL064110

7 Appendix

7.1 SWE

7.1.1 Climatology

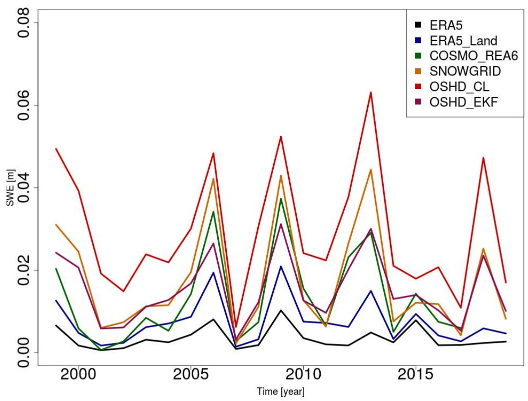

(a) Jura

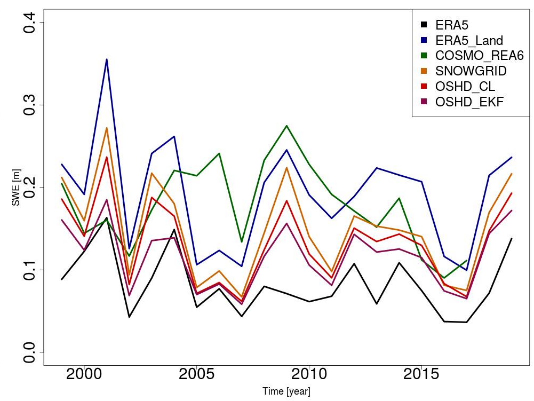

(b) Grisons

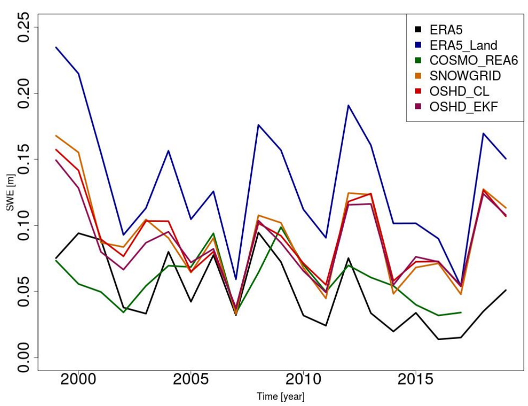

(c) Eastern part of the northern flank

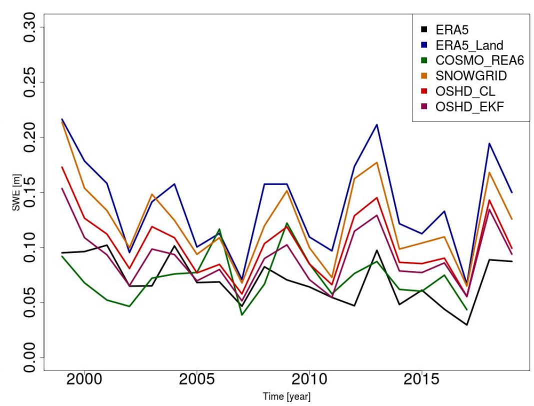

(d) Western part of the northern flank

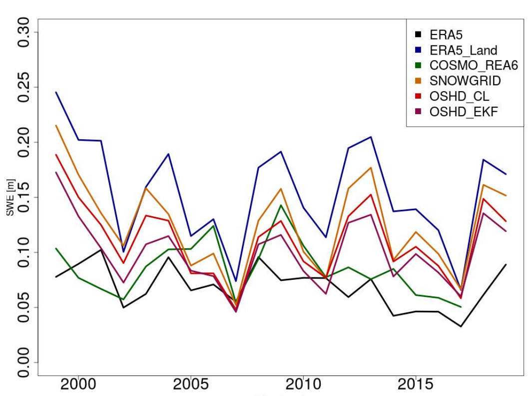

(e) Central part of the northern flank

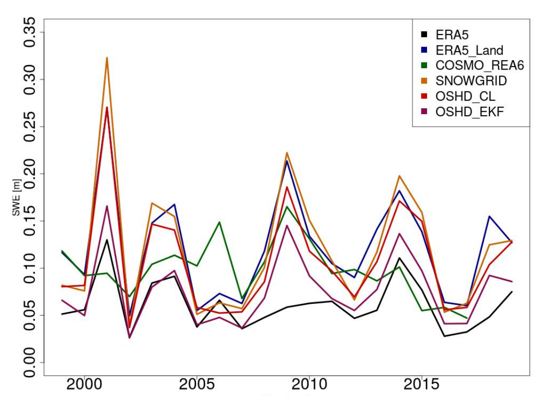

(f) Central part of the southern flank

Figure 40: Mean SWE for the period 1999-2019 for the regions (a) Jura, (b) Grisons, (c) Eastern part of the northern flank, (d) Western part of the northern flank, (e) Central part of the northern flank, and (f) Central part of the southern flank. Each color represents a data set and note the variable y-axis range.

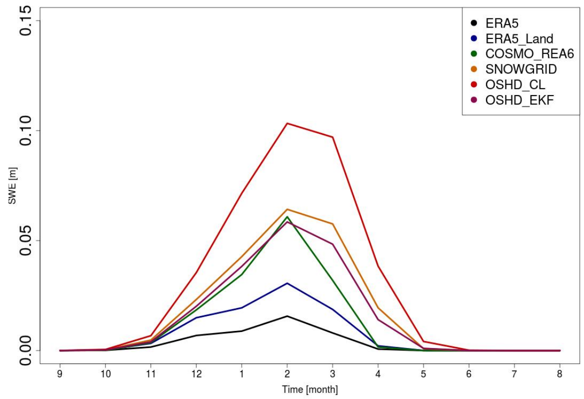

(a) Jura

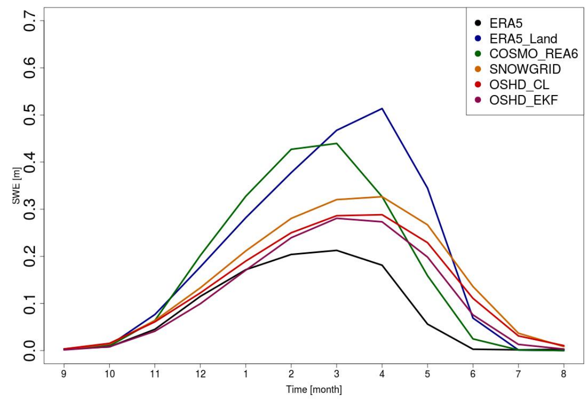

(b) Grisons

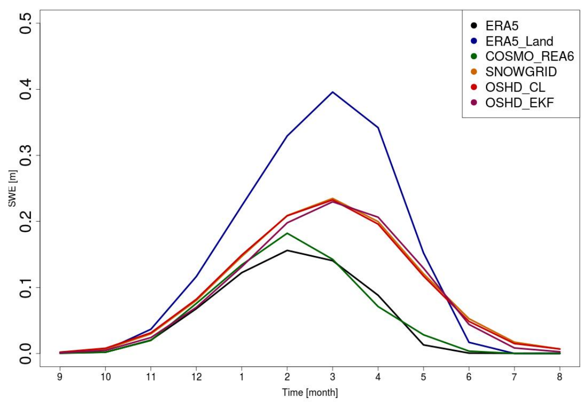

(c) Eastern part of the northern flank

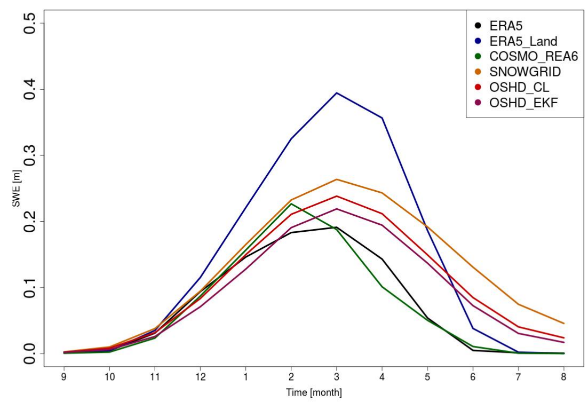

(d) Western part of the northern flank

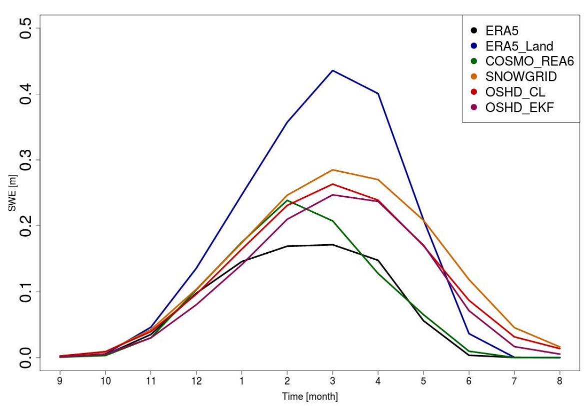

(e) Central part of the northern flank

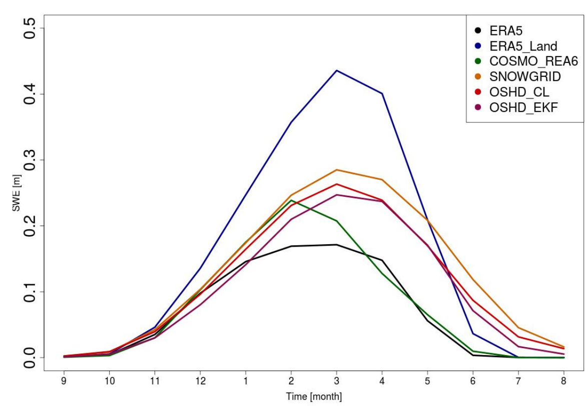

(f) Central part of the southern flank

Figure 41: Monthly Climatology over the period of 1999-2019 for the regions (a) Jura, (b) Grisons, (c) Eastern part of the northern flank, (d) Western part of the northern flank, (e) Central part of the northern flank, and (f) Central part of the southern flank. The data sets ERA5 (black), ERA5-Land (blue), COSMO-REA6 (green), SNOWGRID (orange), OSHD_CL (red), and OSHD_EKF (purple) are illustrated.

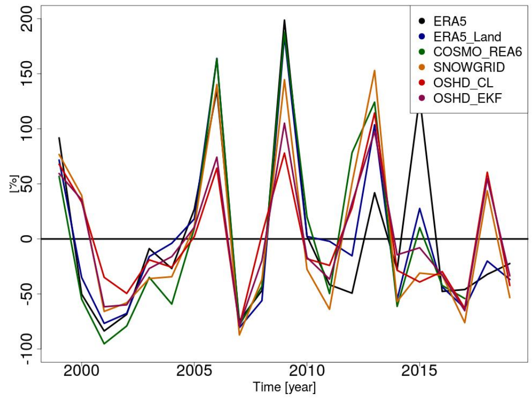

(a) Jura

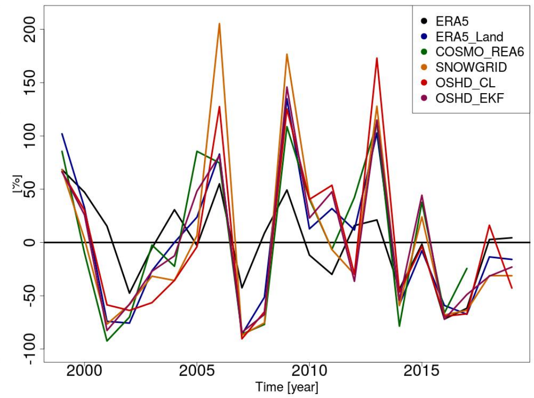

(b) Swiss Plateau

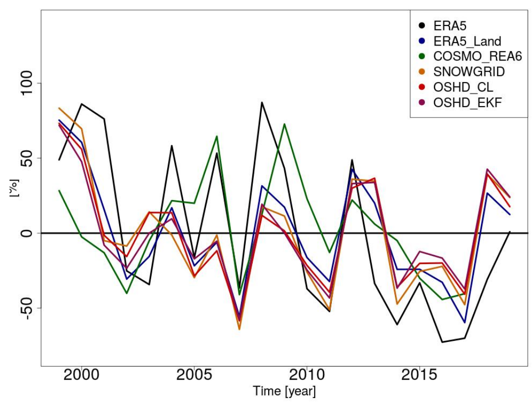

(c) Eastern part of the northern flank

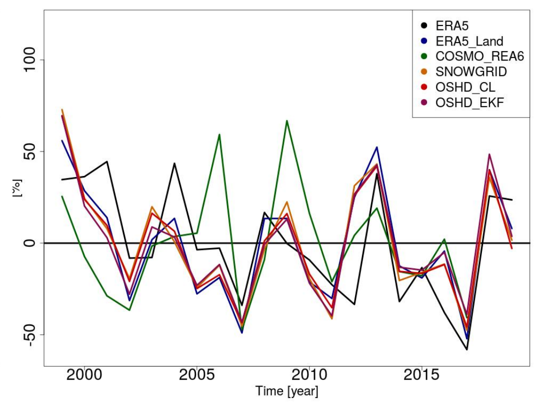

(d) Western part of the northern flank

Figure 42: Percentage deviation of SWE from the mean (1999-2019) for (a) Jura, (b) the Swiss Plateau, (c) Eastern part of the northern flank, (d) Western part of the northern flank. The data sets ERA5 (black), ERA5-Land (blue), COSMO-REA6 (green), SNOWGRID (orange), OSHD_CL (red), and OSHD_EKF (purple) are illustrated. Note the variable y-axis range.

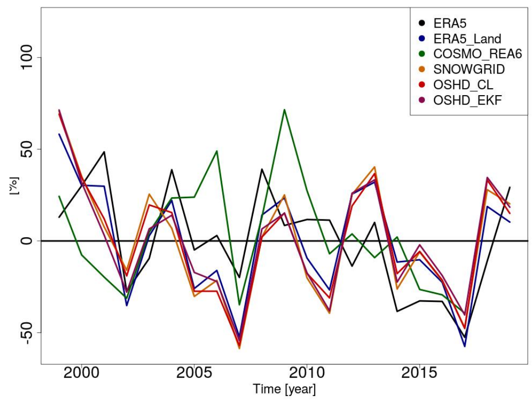

(a) Central part of the northern flank

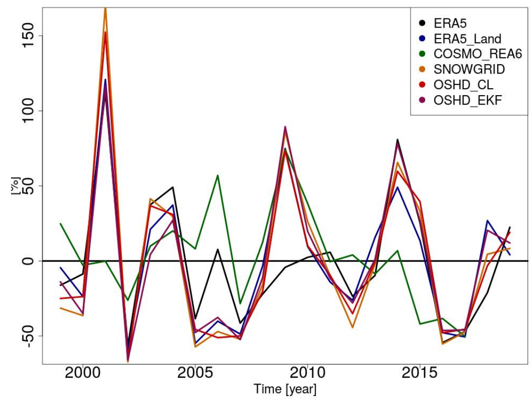

(b) Central part of the southern flank

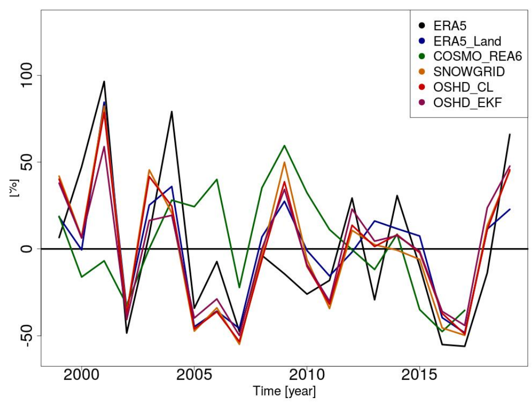

(c) Grisons

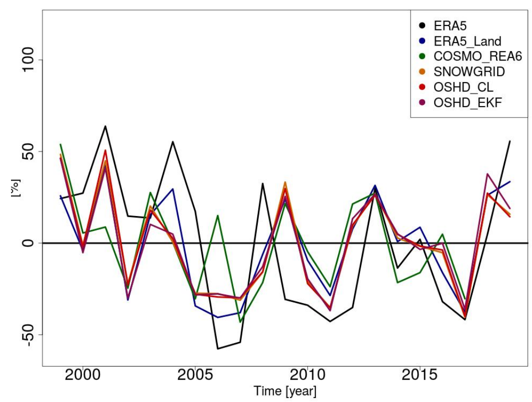

(d) Valais

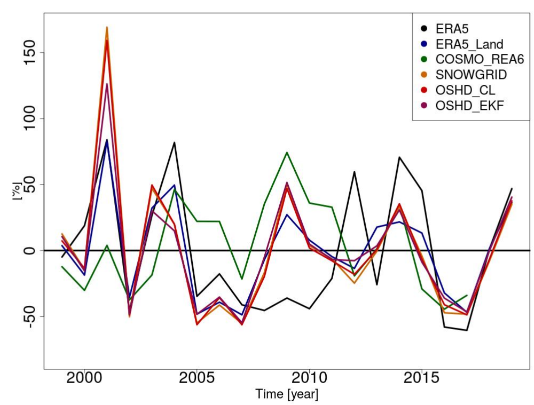

(e) Engadine

Figure 43: Percentage deviation of SWE from the mean (1999-2019) for (a) Central part of the northern flank, (b) Central part of the southern flank, (c) Grisons, and (d) the Engadine. The data sets ERA5 (black), ERA5-Land (blue), COSMO-REA6 (green), SNOWGRID (orange), OSHD_CL (red), and OSHD_EKF (purple) are illustrated. Note the variable y-axis range.

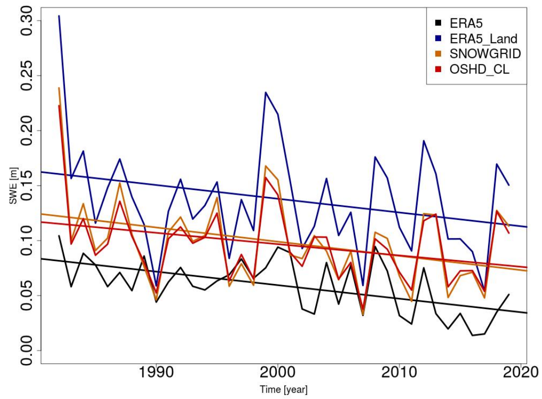

(a) Eastern part of the northern flank

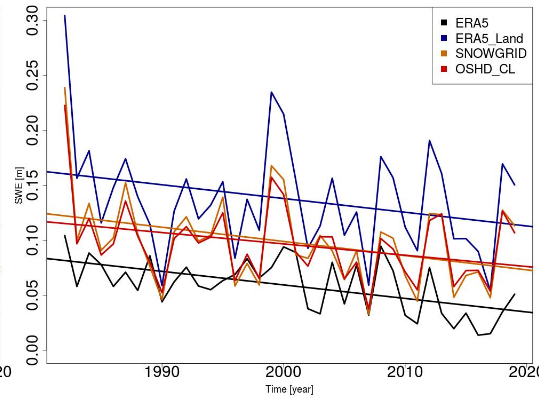

(b) Western part of the northern flank

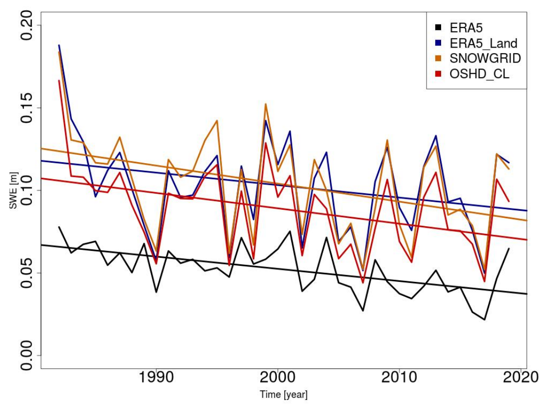

(c) North

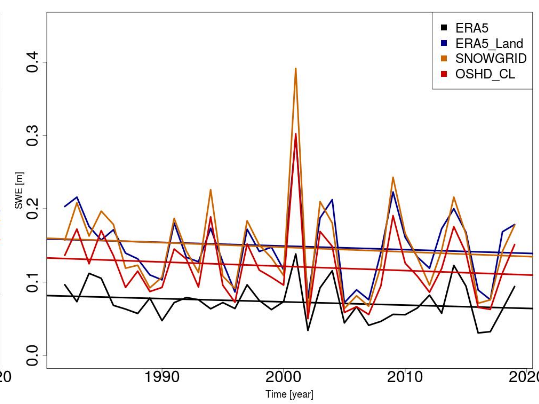

(d) South

Figure 44: Mean SWE with calculated trend line for the period 1982-2019 for the regions regions (a) Eastern part of the northern flank, (b) Western part of the northern flank, (c) Northern, and (d) Southern part of Switzerland. The data sets ERA5 (black), ERA5-Land (blue), SNOWGRID (orange), and OSHD_CL (red) are shown.

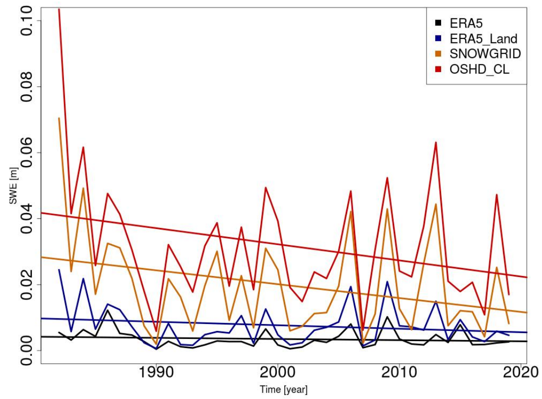

(a) Jura

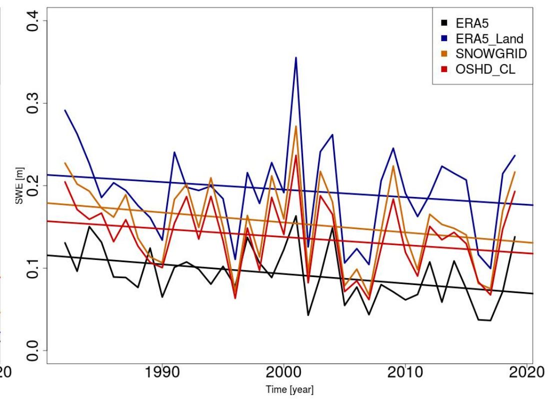

(b) Grisons

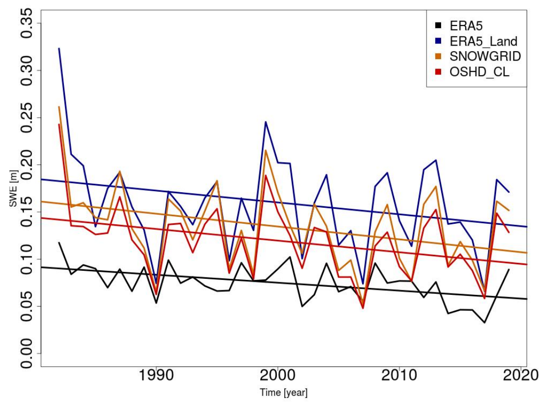

(c) Central part of the northern flank

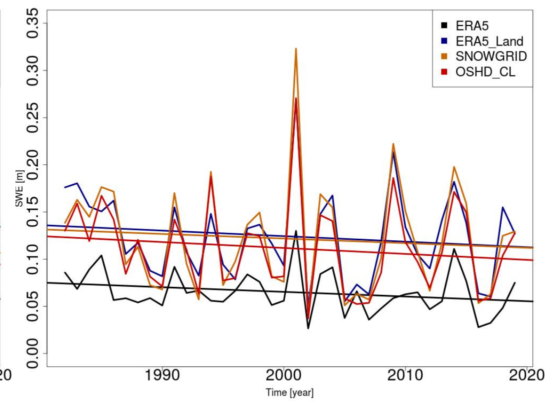

(d) Central part of the southern flank

Figure 45: Mean SWE with calculated trend line for the period 1982-2019 for the regions regions (a) Jura, (b) Grisons, (c) Central part of the northern flank, and (d) Central part of the southern flank. The data sets ERA5 (black), ERA5-Land (blue), SNOWGRID (orange), and OSHD_CL (red) are shown.

7.1.2 Trend at different elevation classes

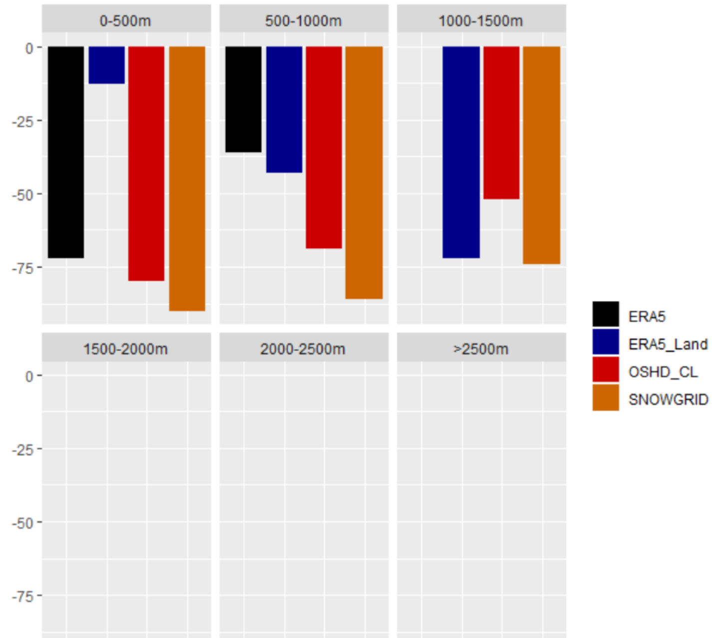

Figure 46: Trend at different altitudes in the Jura for the period 1999-2019. The unit is m SWE.

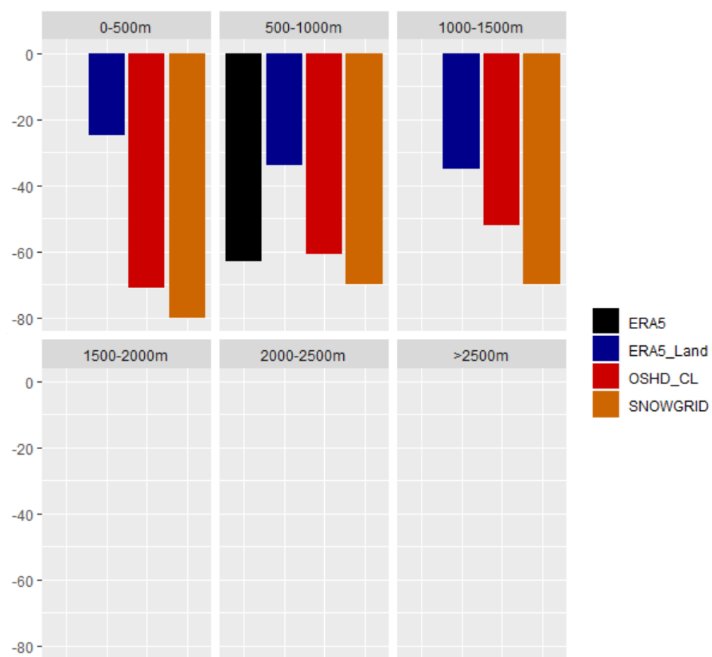

Figure 47: Trend at different altitudes in the Swiss Plateau for the period 1999-2019. The unit is m SWE.

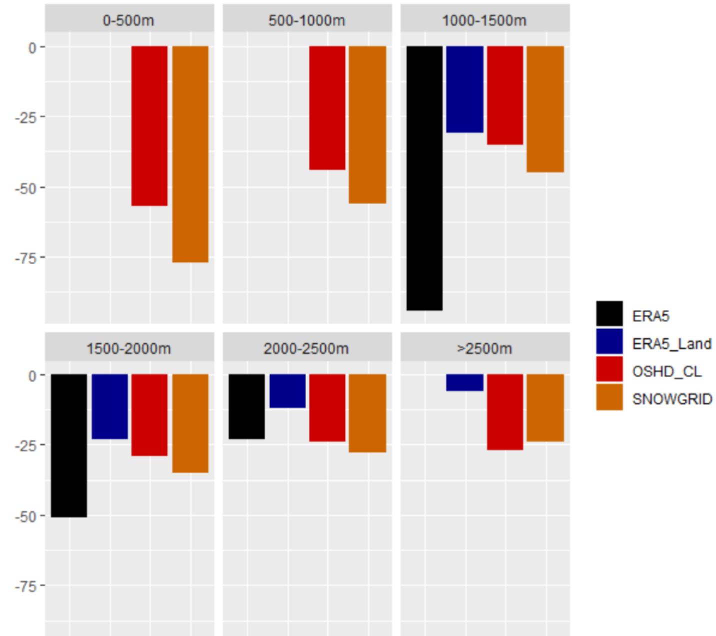

Figure 48: Trend at different altitudes in the Grisons for the period 1999-2019. The unit is m SWE.

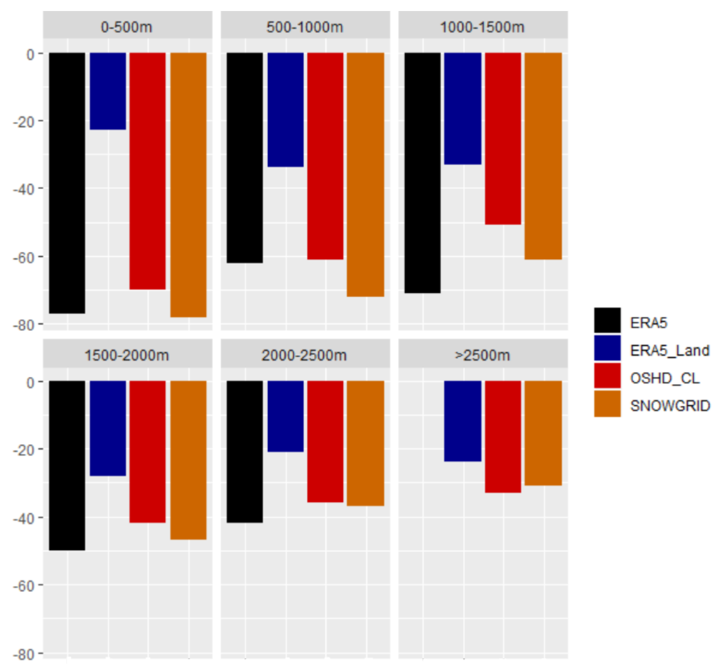

Figure 49: Trend at different altitudes in the Northern part of Switzerland for the period 1999-2019. The unit is m SWE.

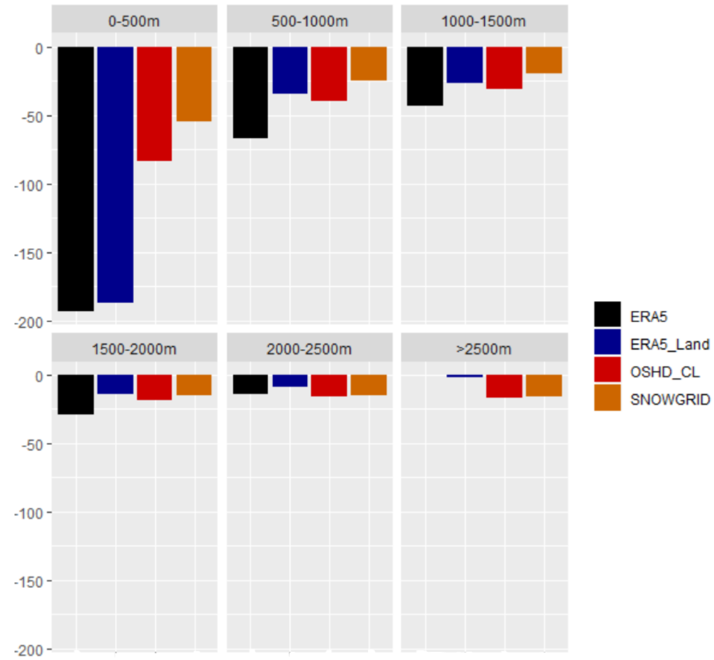

Figure 50: Trend at different altitudes in the Southern part of Switzerland for the period 1999-2019. The unit is m SWE.

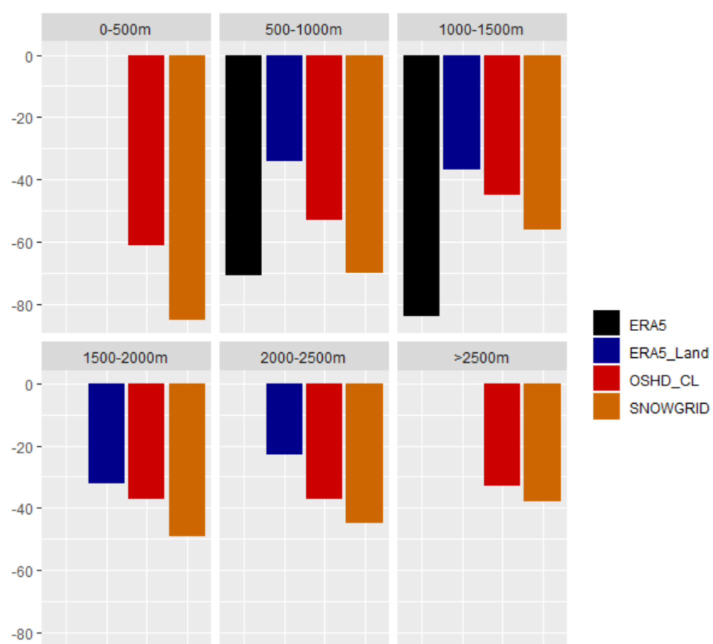

Figure 51: Trend at different altitudes in the eastern part of the northern flank of Switzerland for the period 1999-2019. The unit is m SWE.

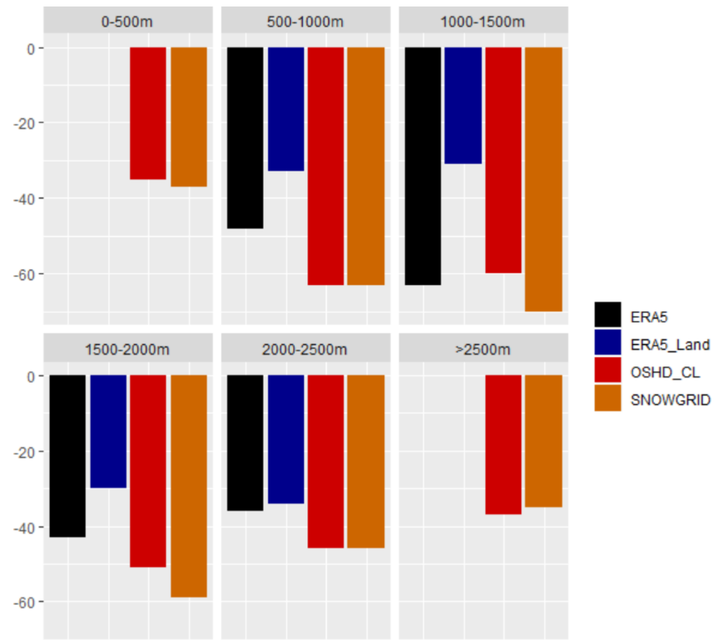

Figure 52: Trend at different altitudes in the western part of the northern flank of Switzerland for the period 1999-2019. The unit is m SWE.

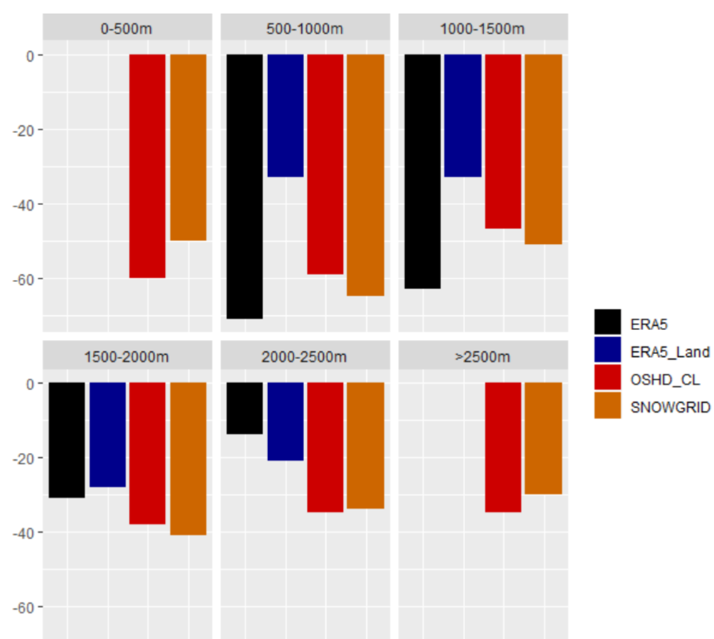

Figure 53: Trend at different altitudes in the central part of the northern flank of Switzerland for the period 1999-2019. The unit is m SWE.

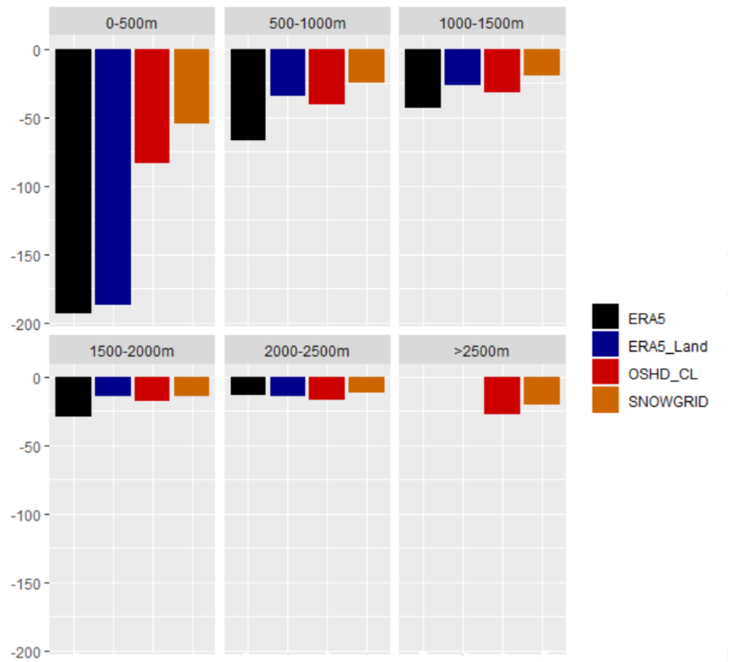

Figure 54: Trend at different altitudes in the central part of the southern flank of Switzerland for the period 1999-2019. The unit is m SWE.

7.2 Number of snow days

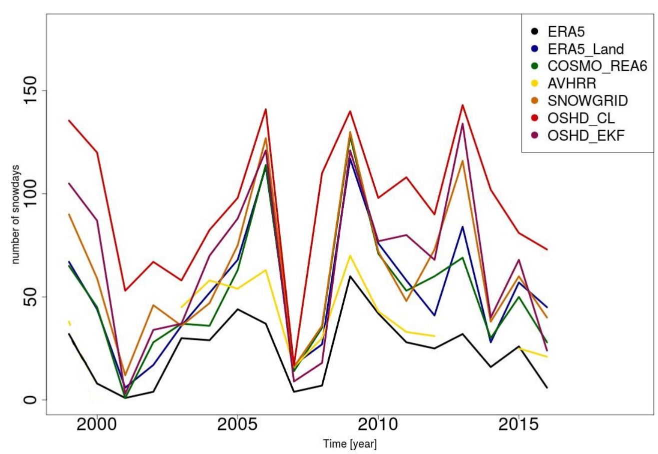

Figure 55: The climatology of the number of snow days in the Jura.

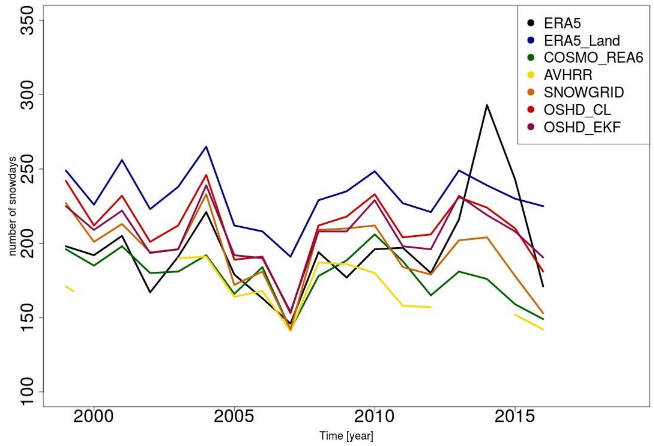

Figure 56: The climatology of the number of snow days in Grisons.

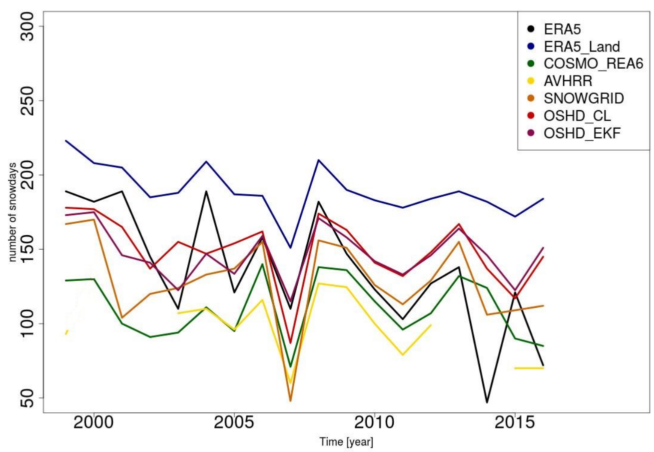

Figure 57: The climatology of the number of snow days in the eastern part of the northern flank of the Alps.

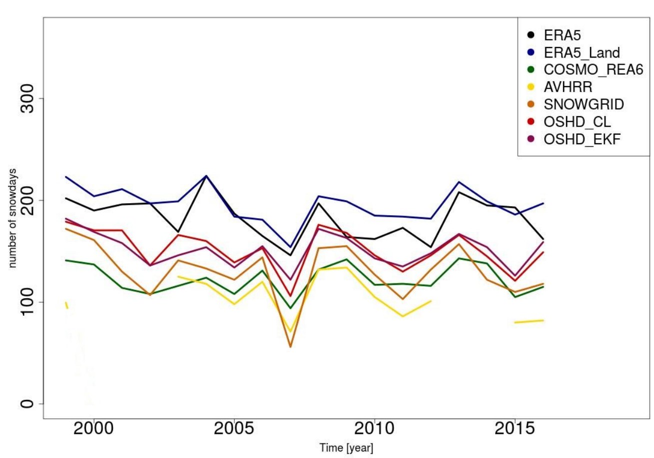

Figure 58: The climatology of the number of snow days in the western part of the northern flank of the Alps.

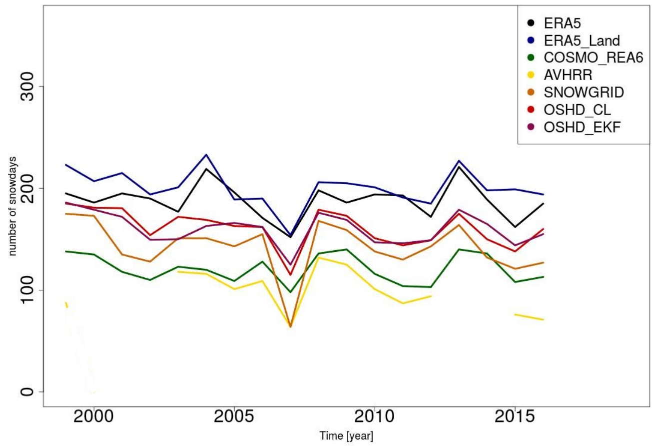

Figure 59: The climatology of the number of snow days in the central part of the northern flank of the Alps.

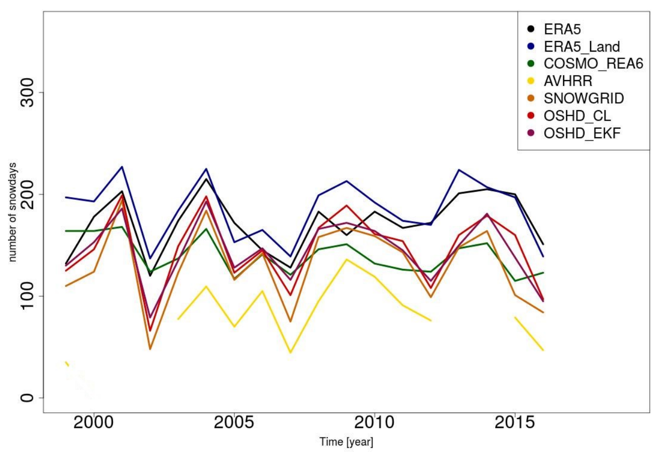

Figure 60: The climatology of the number of snow days in the central part of the southern flank of the Alps.

7.3 Snow cover fraction

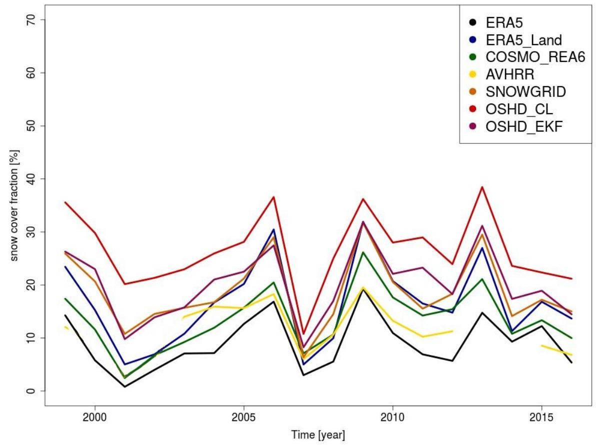

Figure 61: The climatology of the snow cover fraction in the Jura.

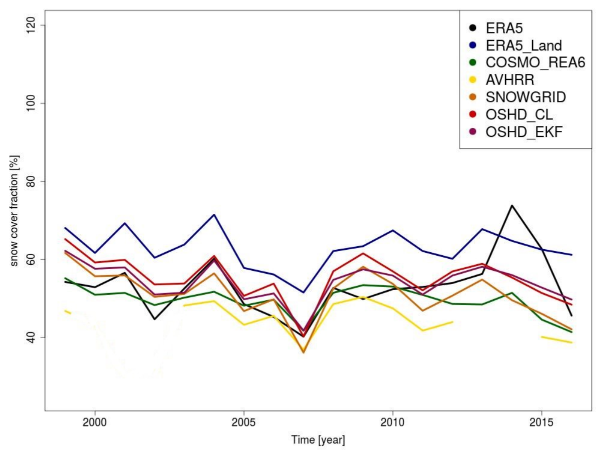

Figure 62: The climatology of the snow cover fraction in Grisons.

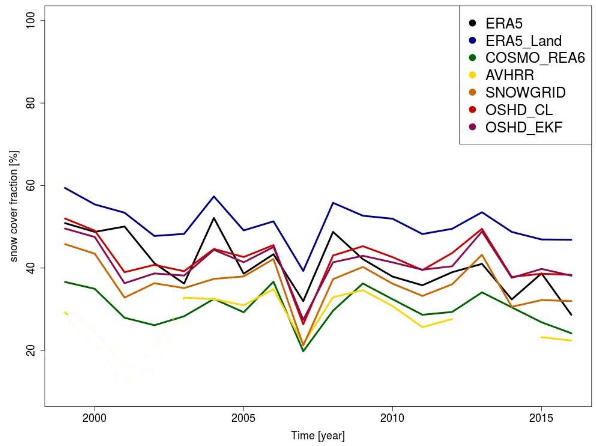

Figure 63: The climatology of the snow cover fraction in the eastern part of the northern flank of the Alps.

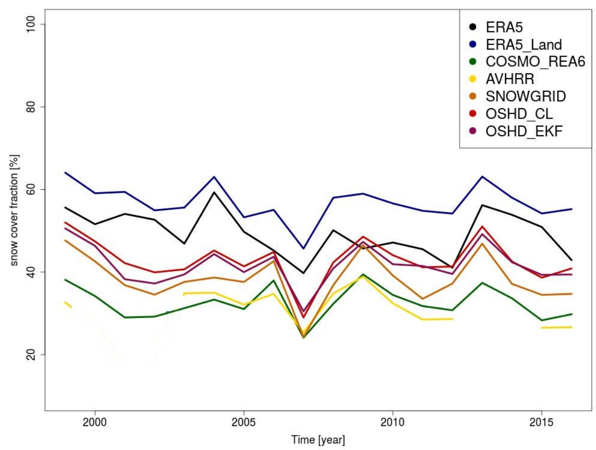

Figure 64: The climatology of the snow cover fraction in the western part of the northern flank of the Alps.

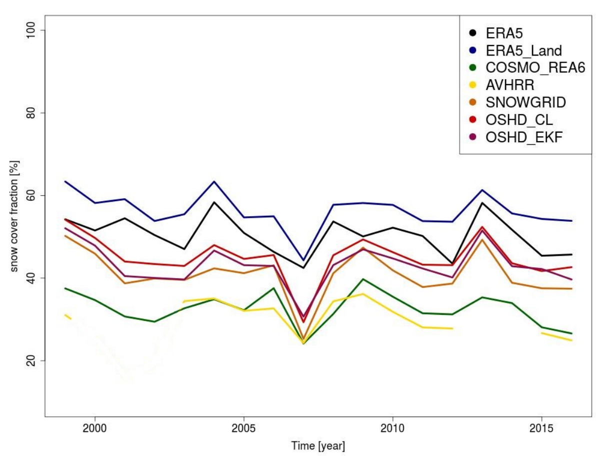

Figure 65: The climatology of the snow cover fraction in the central part of the northern flank of the Alps.

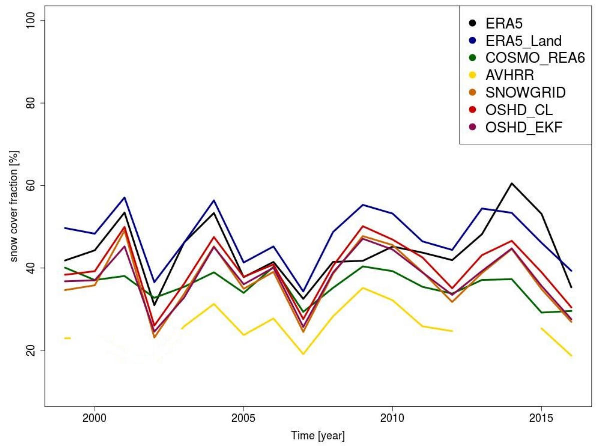

Figure 66: The climatology of the snow cover fraction in the central part of the southern flank of the Alps.

7.4 Day of maximum snow

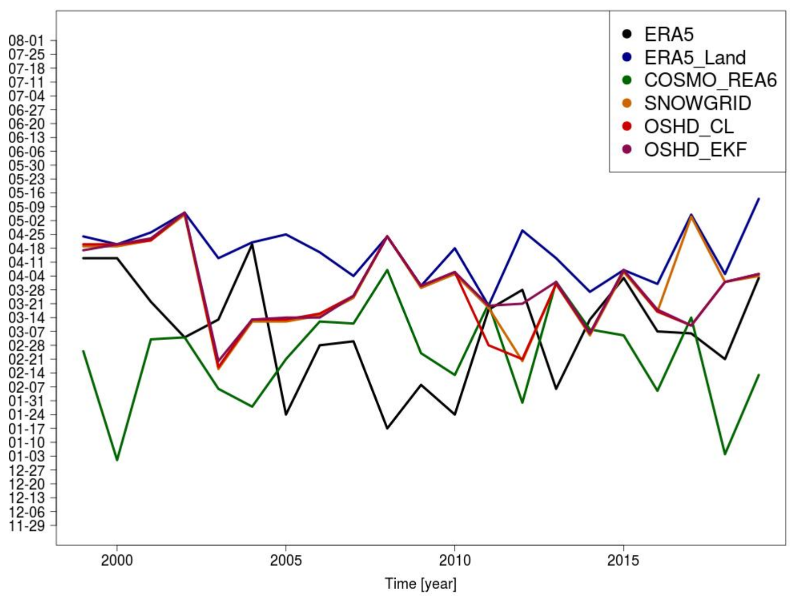

Figure 67: The climatology of the day of maximum snow in Grisons.

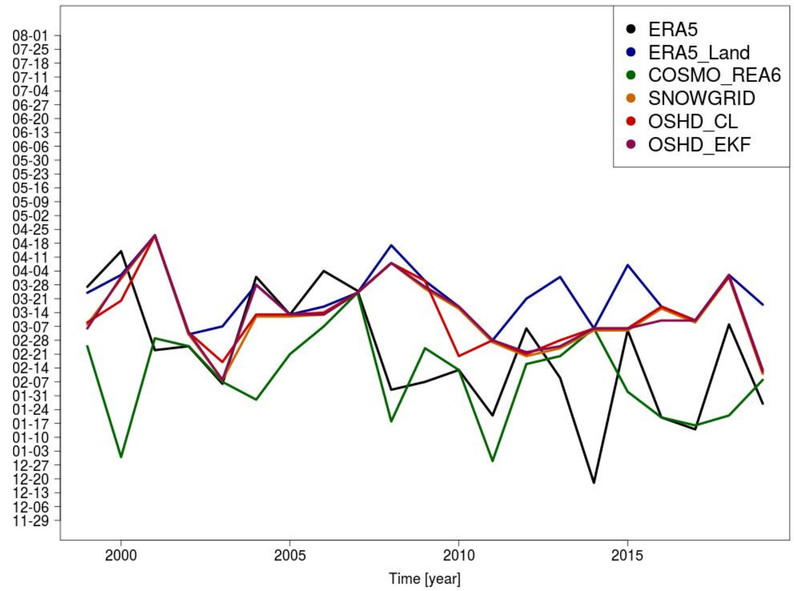

Figure 68: The climatology of the day of maximum snow in the eastern part of the northern flank of the Alps.

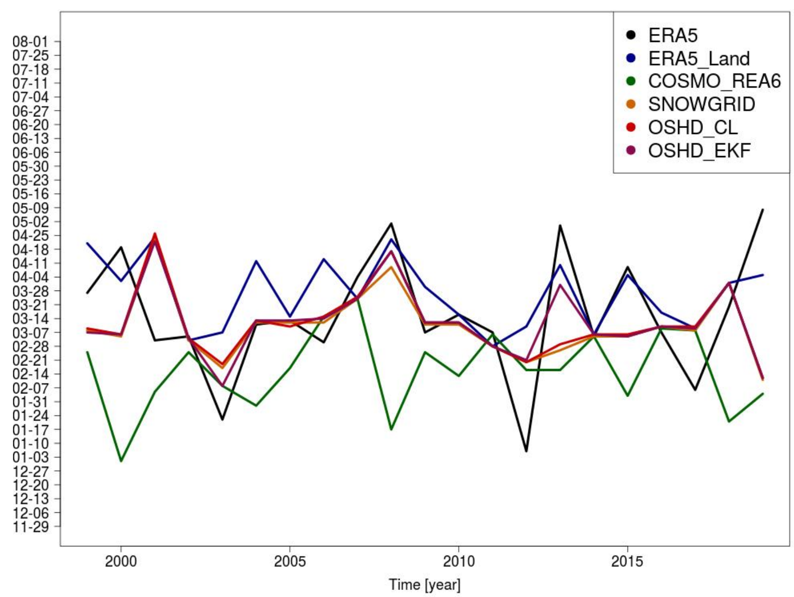

Figure 69: The climatology of the day of maximum snow in the western part of the northern flank of the Alps.

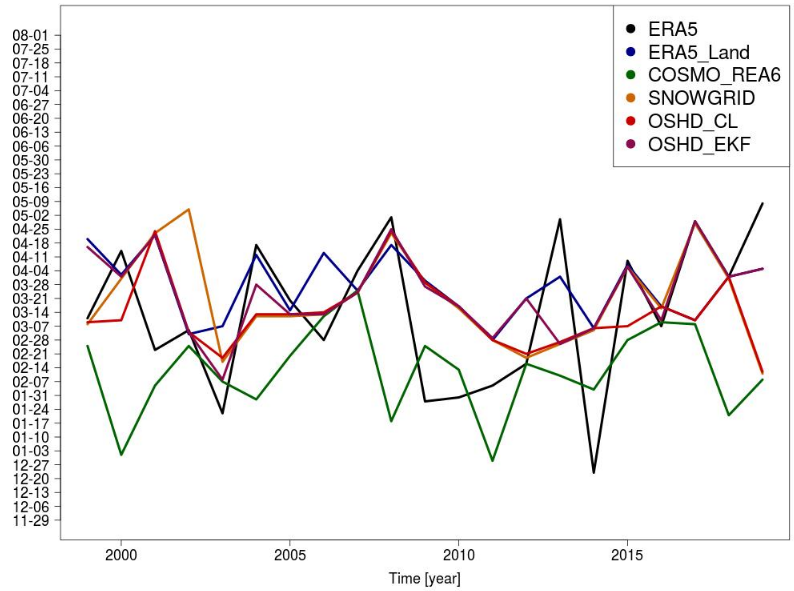

Figure 70: The climatology of the day of maximum snow in the central part of the northern flank of the Alps.

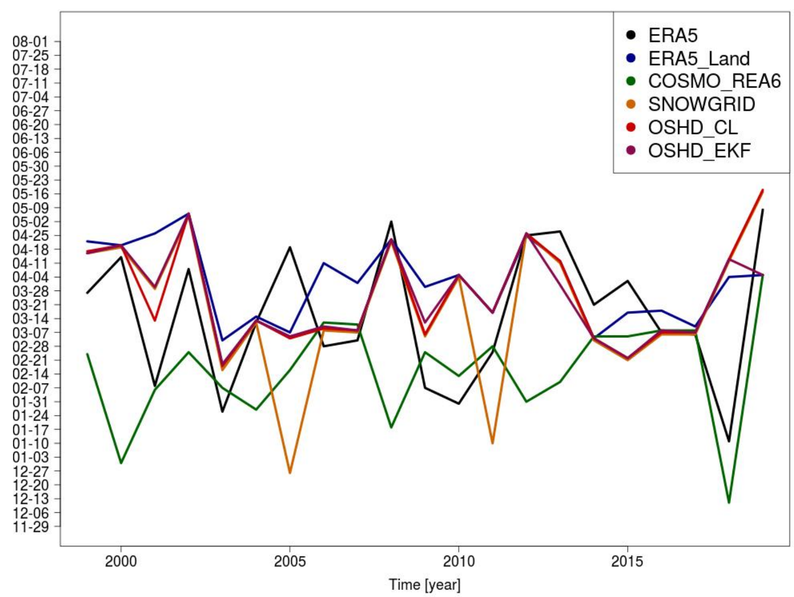

Figure 71: The climatology of the day of maximum snow in the central part of the southern flank of the Alps.

7.5 Climatology of SWE at different elevations

7.5.1 Elevation class 1

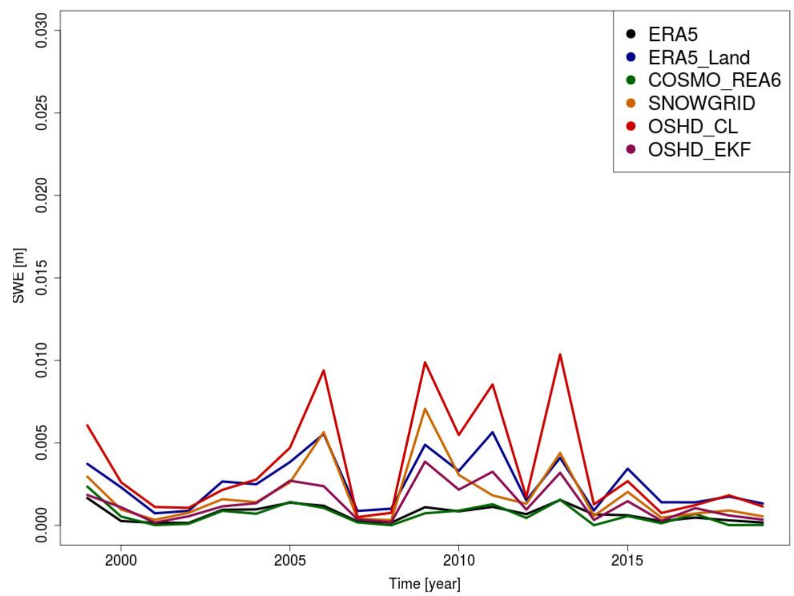

Figure 72: The climatology of SWE at elevation 0-500m from 1999-2019 in the Jura.

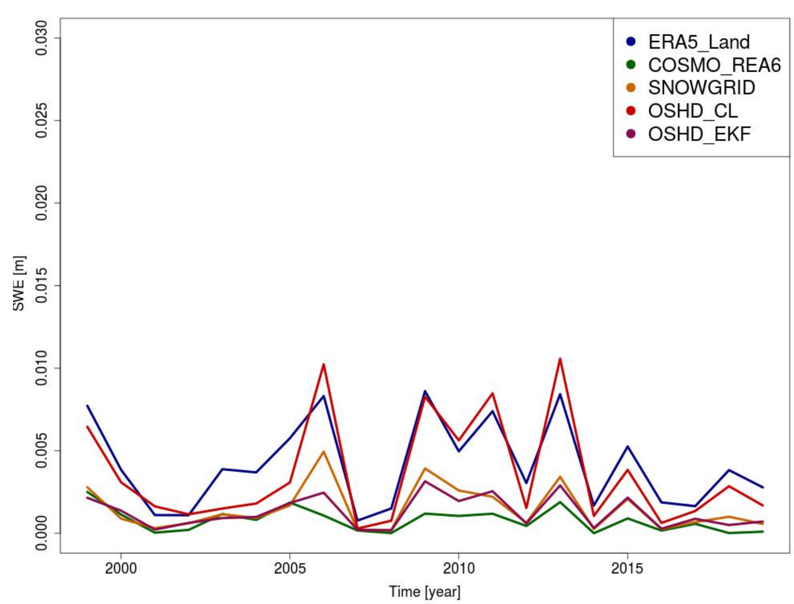

Figure 73: The climatology of SWE at elevation 0-500m from 1999-2019 in the Swiss Plateau.

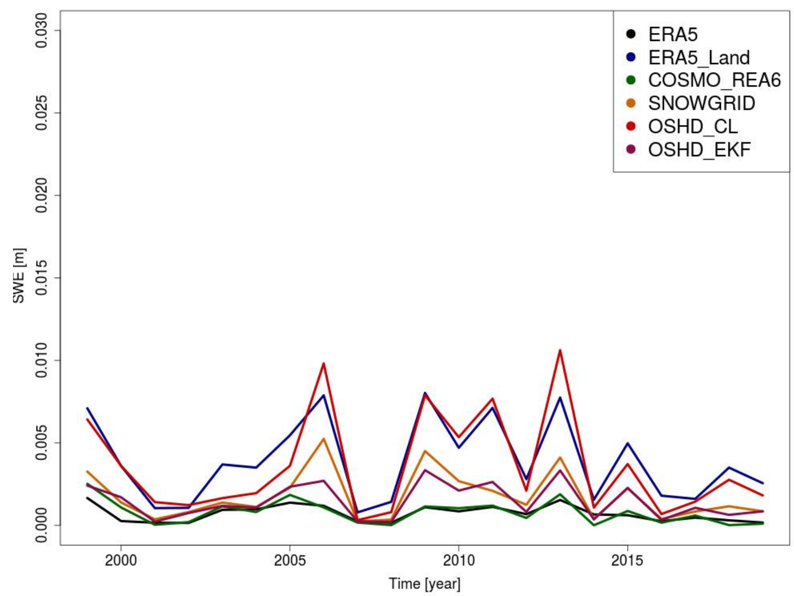

Figure 74: The climatology of SWE at elevation 0-500m from 1999-2019 in northern Switzerland.

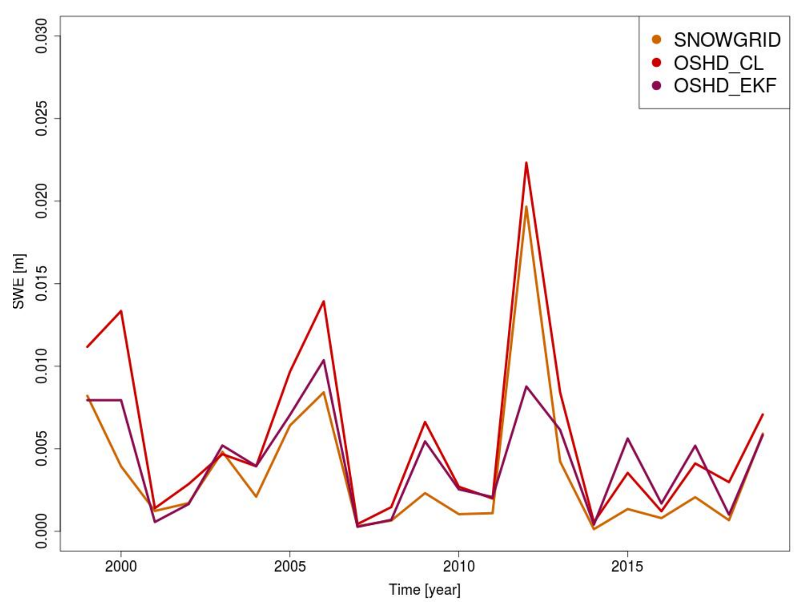

Figure 75: The climatology of SWE at elevation 0-500m from 1999-2019 in the Grisons.

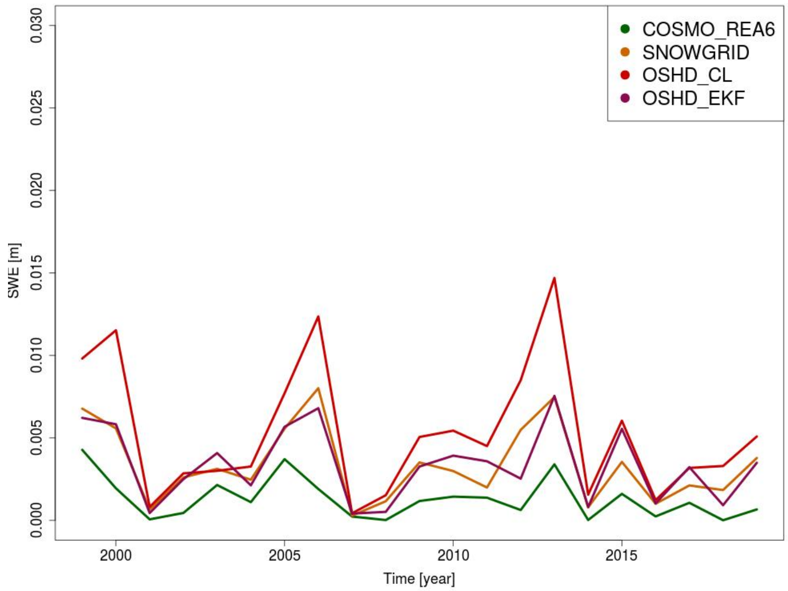

Figure 76: The climatology of SWE at elevation 0-500m from 1999-2019 in the eastern part of the northern flank of the Alps.

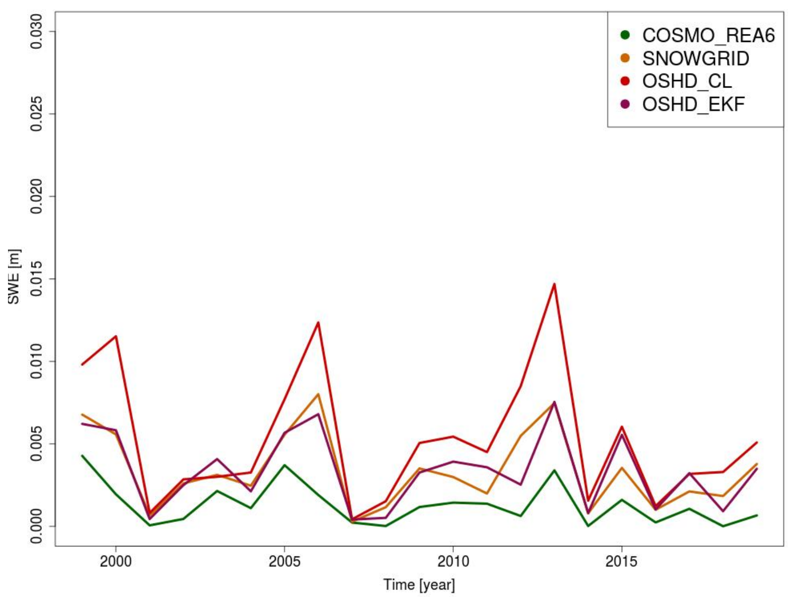

Figure 77: The climatology of SWE at elevation 0-500m from 1999-2019 in the eastern part of the northern flank of the Alps.

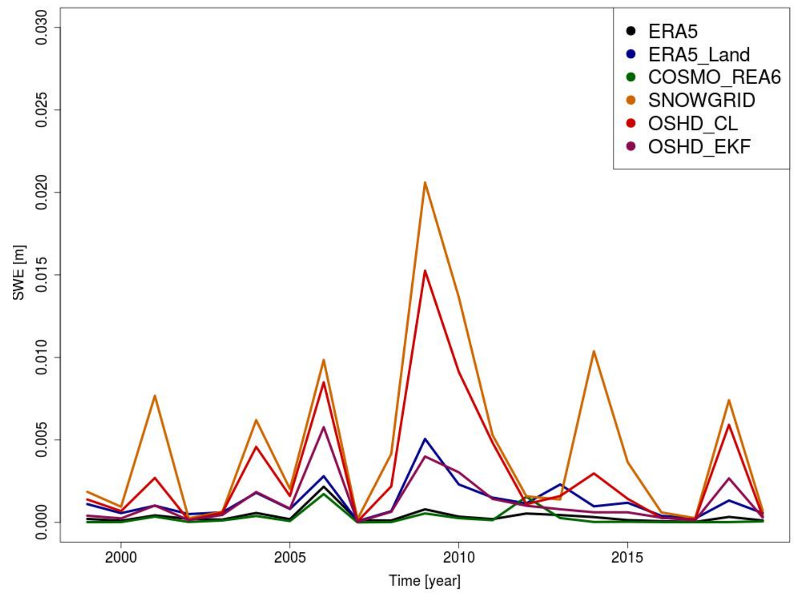

Figure 78: The climatology of SWE at elevation 0-500m from 1999-2019 in southern Switzerland.

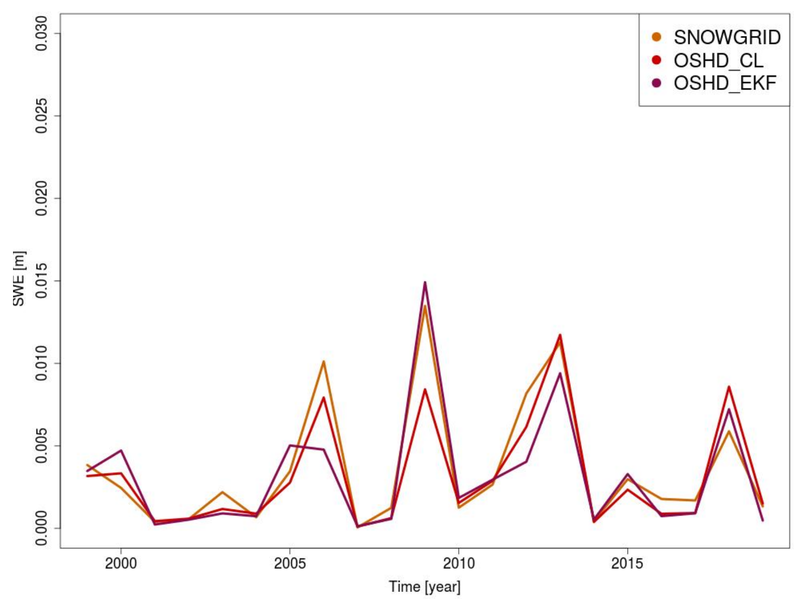

Figure 79: The climatology of SWE at elevation 0-500m from 1999-2019 in the Valais.

7.5.2 Elevation class 2

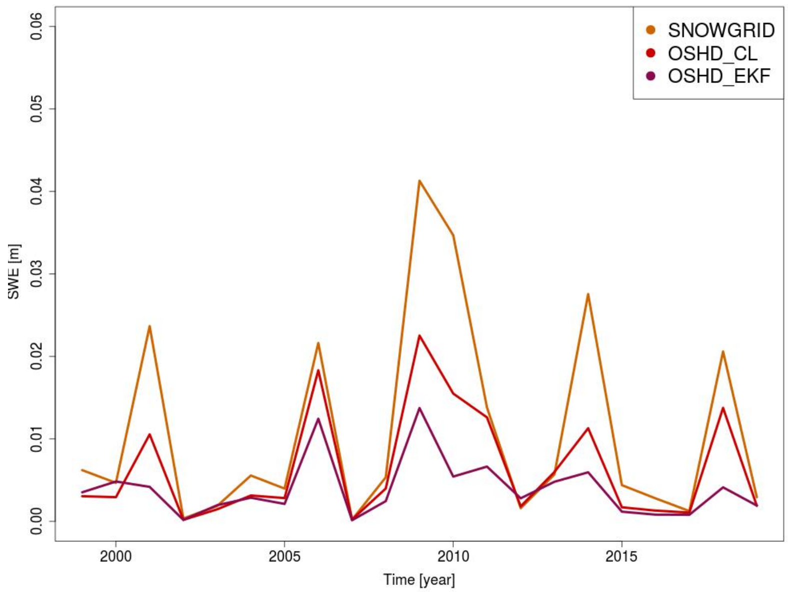

Figure 80: The climatology of SWE at elevation 500-1000m from 1999-2019 in the Engadine.

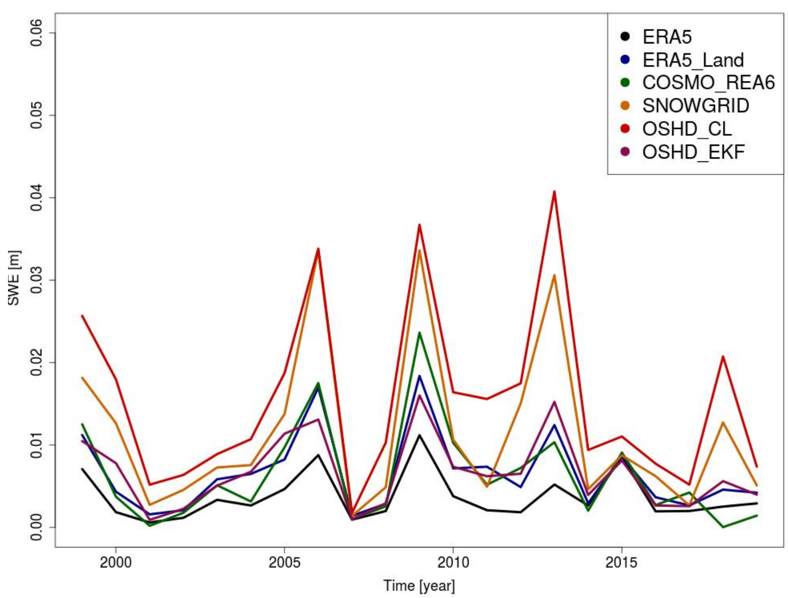

Figure 81: The climatology of SWE at elevation 500-1000m from 1999-2019 in the Jura.

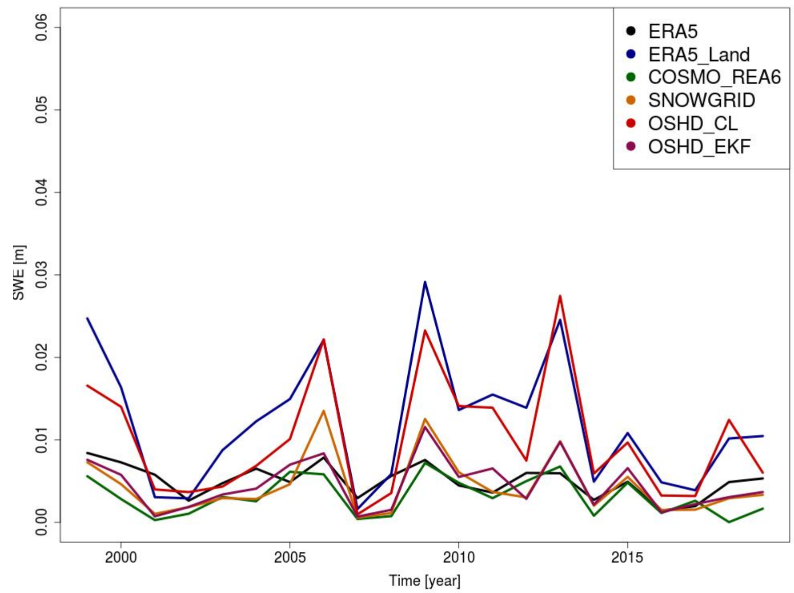

Figure 82: The climatology of SWE at elevation 500-1000m from 1999-2019 in the Swiss Plateau.

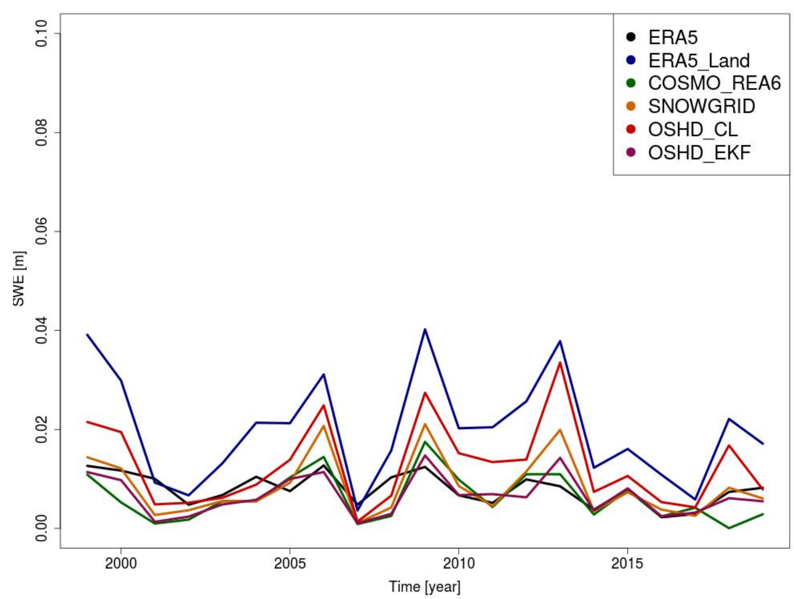

Figure 83: The climatology of SWE at elevation 500-1000m from 1999-2019 in northern Switzerland.

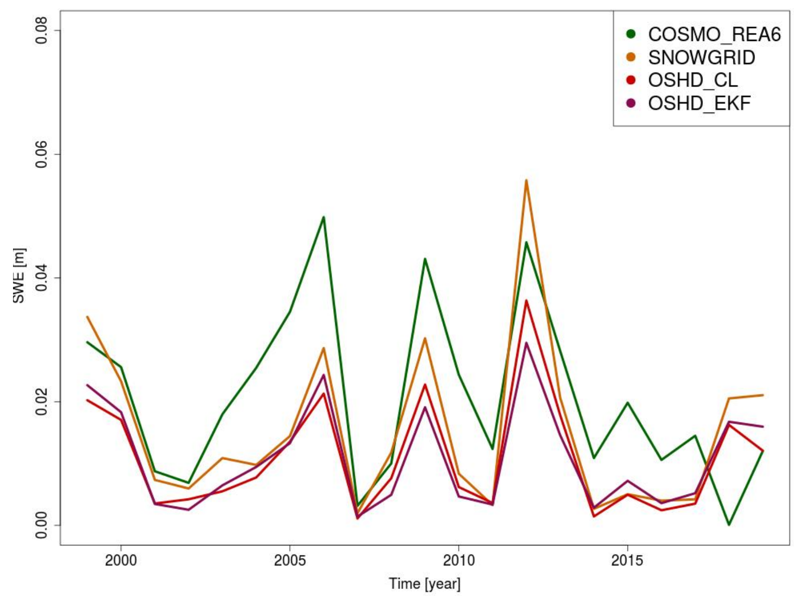

Figure 84: The climatology of SWE at elevation 500-1000m from 1999-2019 in Grisons.

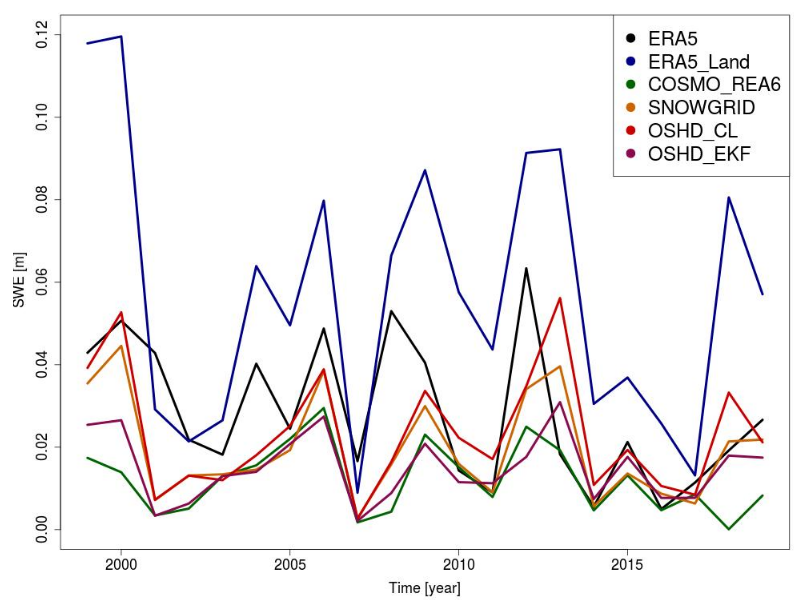

Figure 85: The climatology of SWE at elevation 500-1000m from 1999-2019 in the eastern part of the northern flank of the Alps.

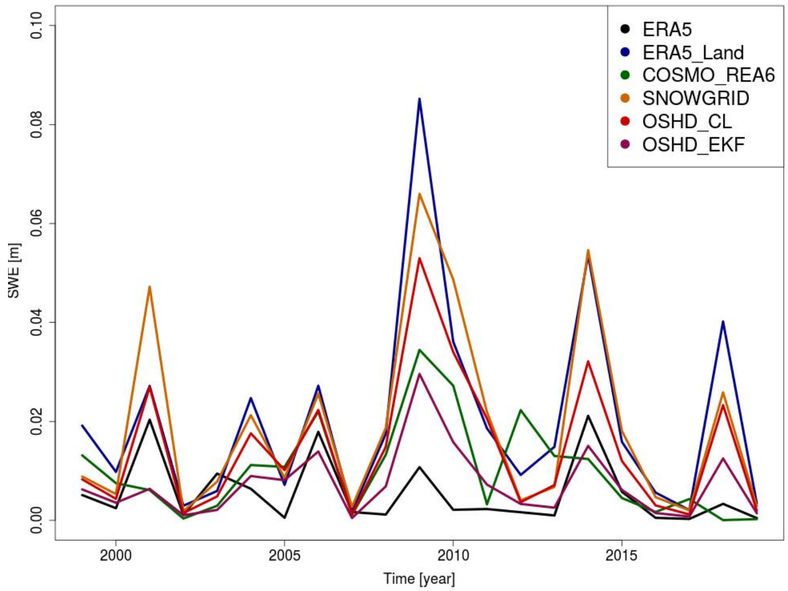

Figure 86: The climatology of SWE at elevation 500-1000m from 1999-2019 in southern Switzerland.

7.5.3 Elevation class 3

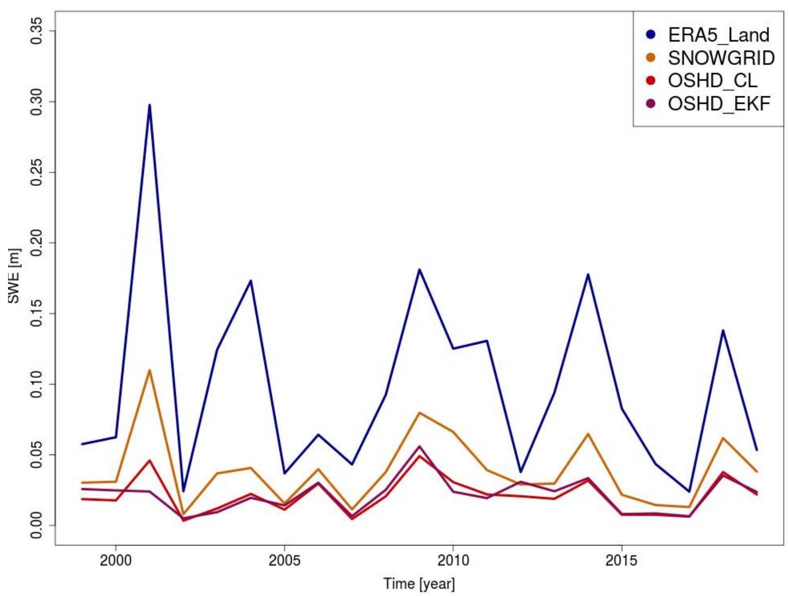

Figure 87: The climatology of SWE at elevation 1000-1500m from 1999-2019 in the Engadine.

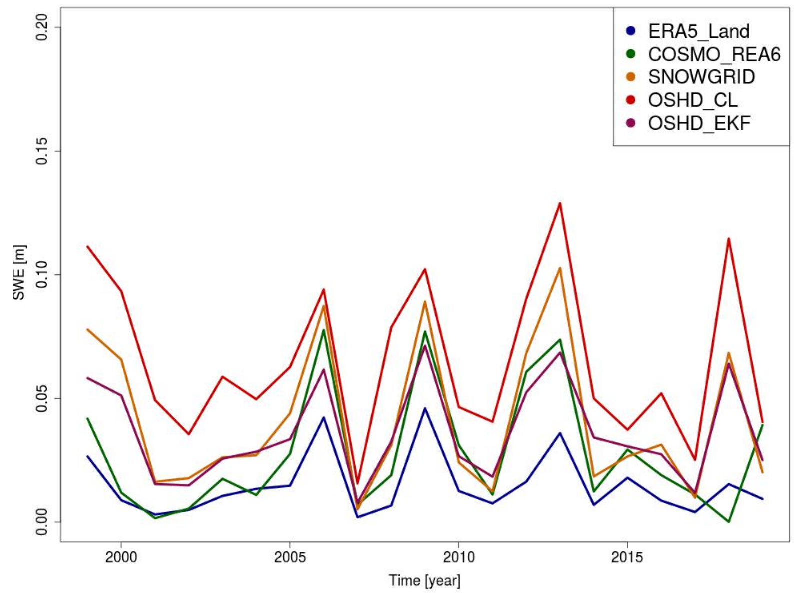

Figure 88: The climatology of SWE at elevation 1000-1500m from 1999-2019 in the Jura.

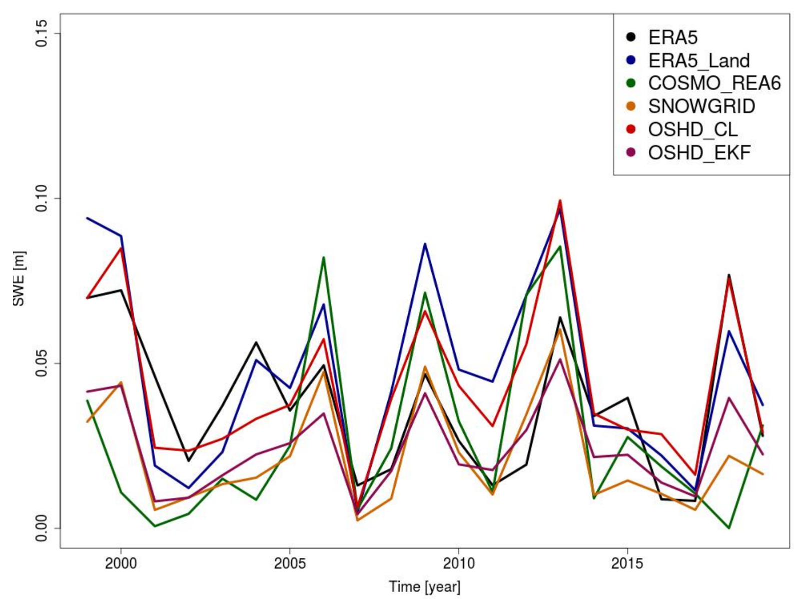

Figure 89: The climatology of SWE at elevation 1000-1500m from 1999-2019 in the Swiss Plateau.

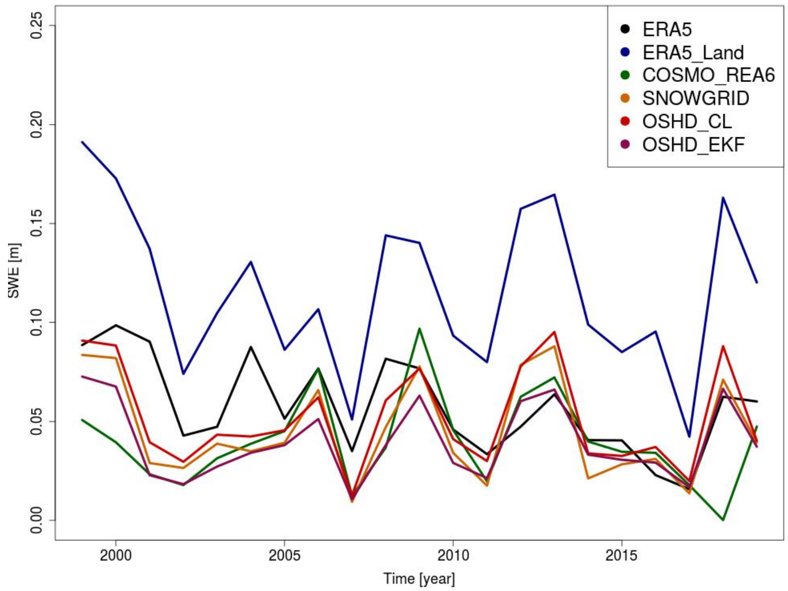

Figure 90: The climatology of SWE at elevation 1000-1500m from 1999-2019 in northern Switzerland.

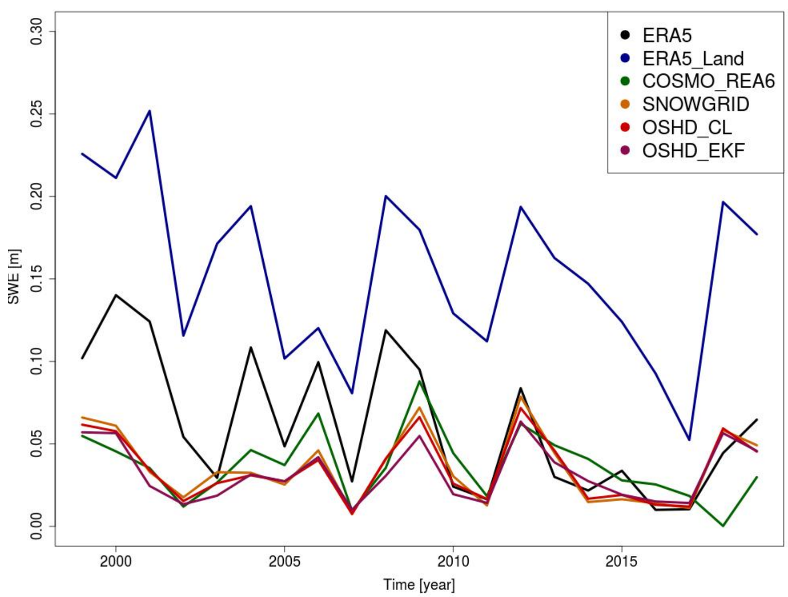

Figure 91: The climatology of SWE at elevation 1000-1500m from 1999-2019 in Grisons.

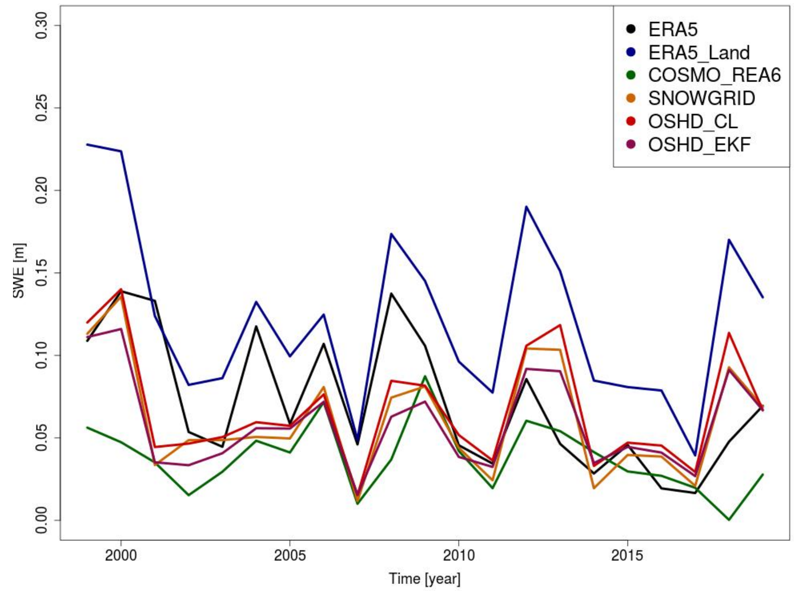

Figure 92: The climatology of SWE at elevation 1000-1500m from 1999-2019 in the eastern part of the northern flank of the Alps.

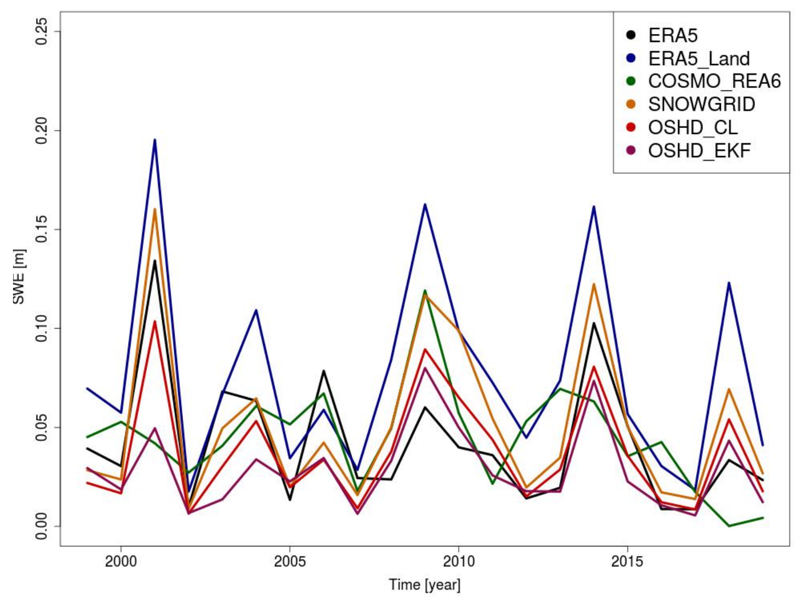

Figure 93: The climatology of SWE at elevation 1000-1500m from 1999-2019 in southern Switzerland.

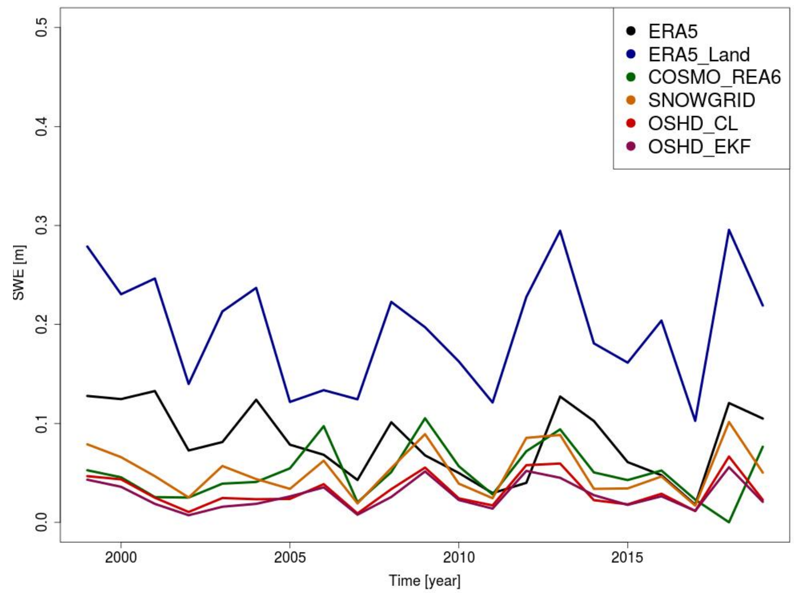

Figure 94: The climatology of SWE at elevation 1000-1500m from 1999-2019 in the Valais.

7.5.4 Elevation class 4

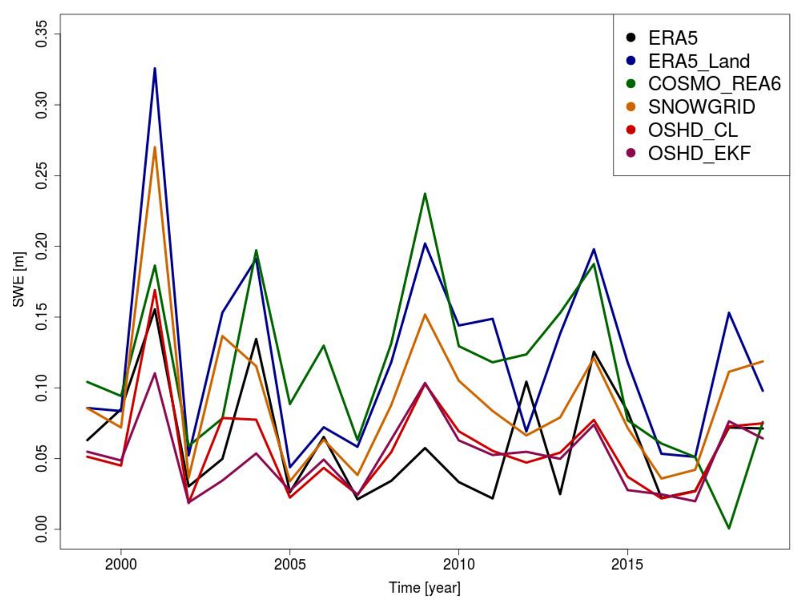

Figure 95: The climatology of SWE at elevation 1500-2000m from 1999-2019 in the Engadine.

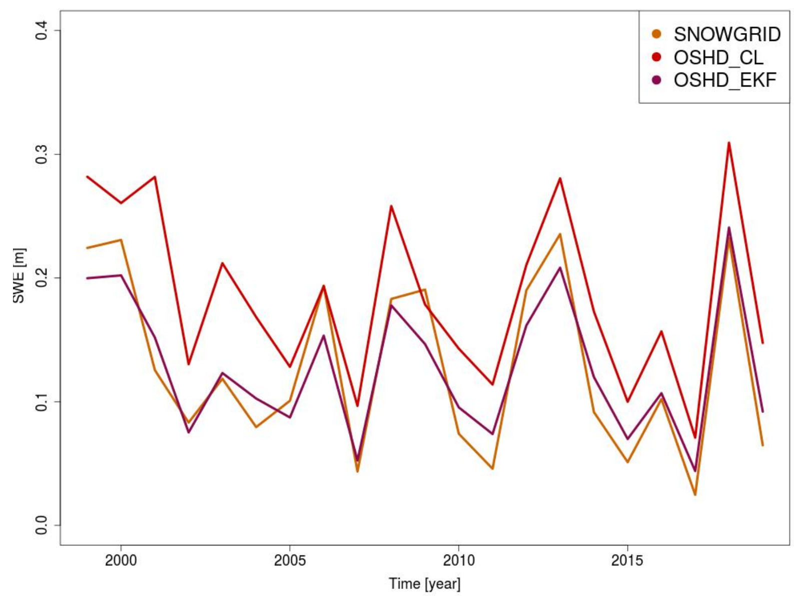

Figure 96: The climatology of SWE at elevation 1500-2000m from 1999-2019 in the Jura.

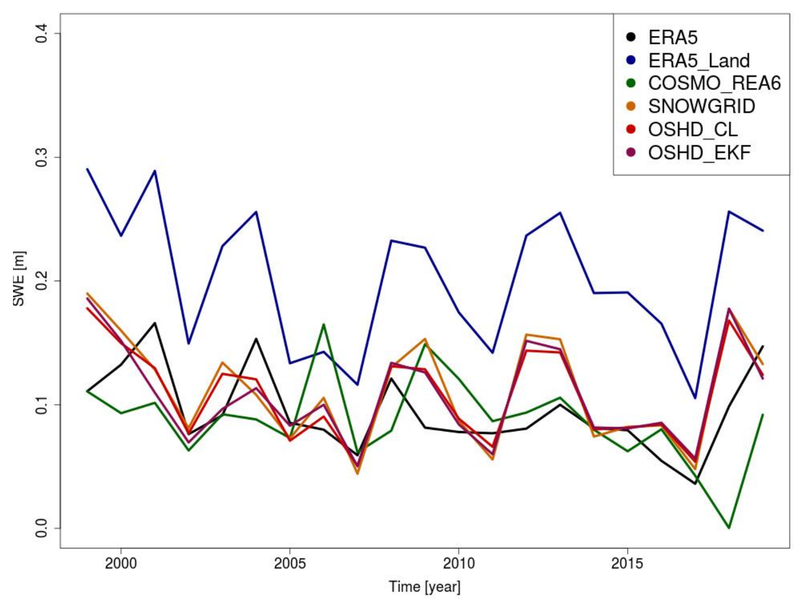

Figure 97: The climatology of SWE at elevation 1500-2000m from 1999-2019 in northern Switzerland.

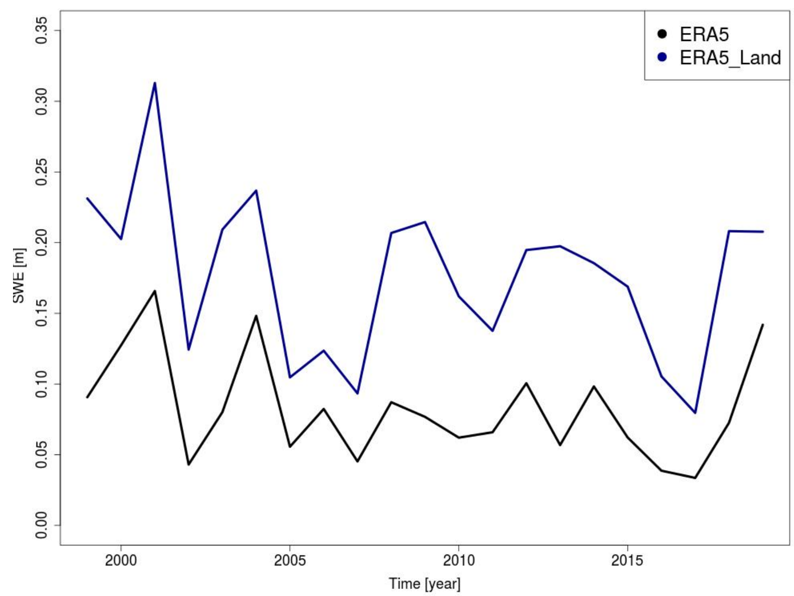

Figure 98: The climatology of SWE at elevation 1500-2000m from 1999-2019 in Grisons.

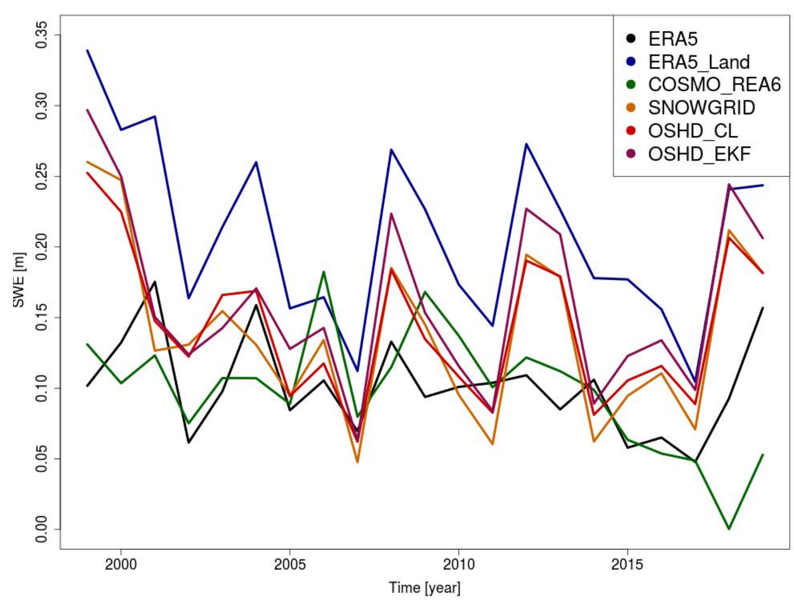

Figure 99: The climatology of SWE at elevation 1500-2000m from 1999-2019 in eastern part of the northern flank of the Alps.

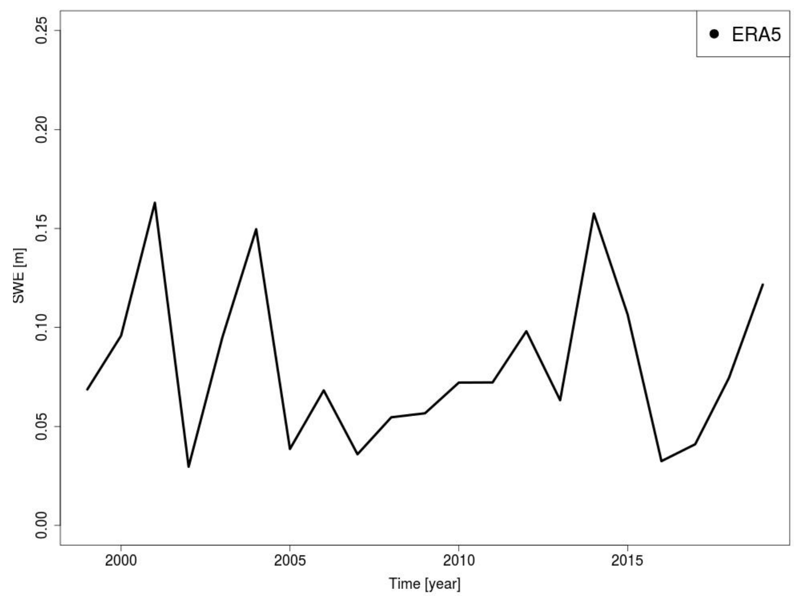

Figure 100: The climatology of SWE at elevation 1500-2000m from 1999-2019 in southern Switzerland.

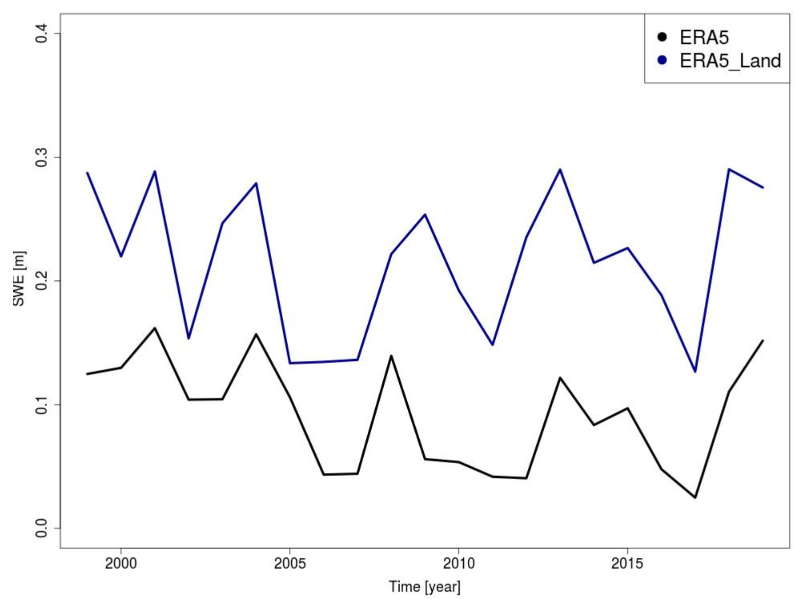

Figure 101: The climatology of SWE at elevation 1500-2000m from 1999-2019 in the Valais.

7.5.5 Elevation class 5

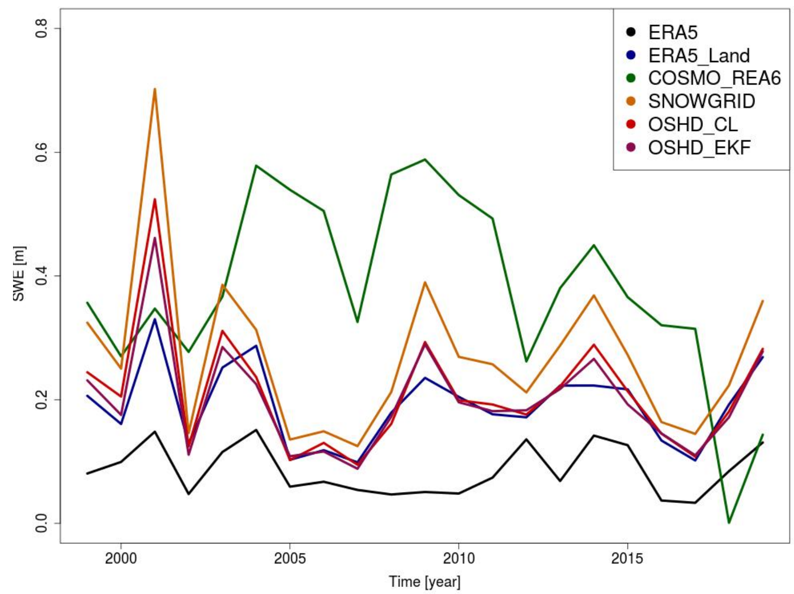

Figure 102: The climatology of SWE at elevation 2000-2500m from 1999-2019 in the Engadine.

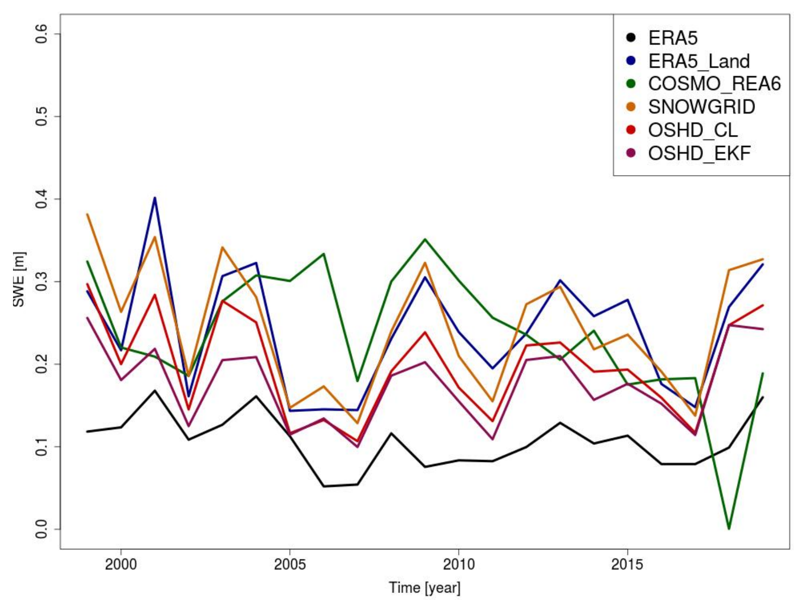

Figure 103: The climatology of SWE at elevation 2000-2500m from 1999-2019 in northern Switzerland.

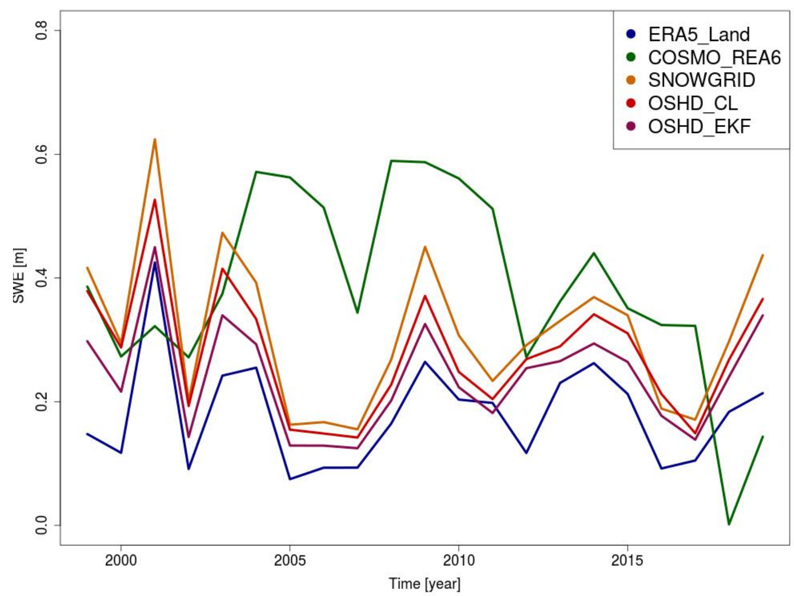

Figure 104: The climatology of SWE at elevation 2000-2500m from 1999-2019 in Grisons.

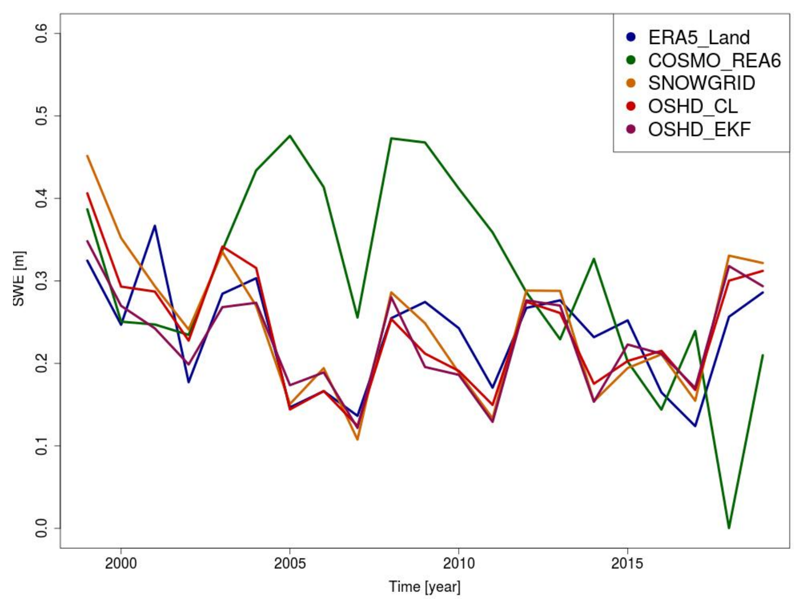

Figure 105: The climatology of SWE at elevation 2000-2500m from 1999-2019 in the eastern part of the northern flank of the Alps.

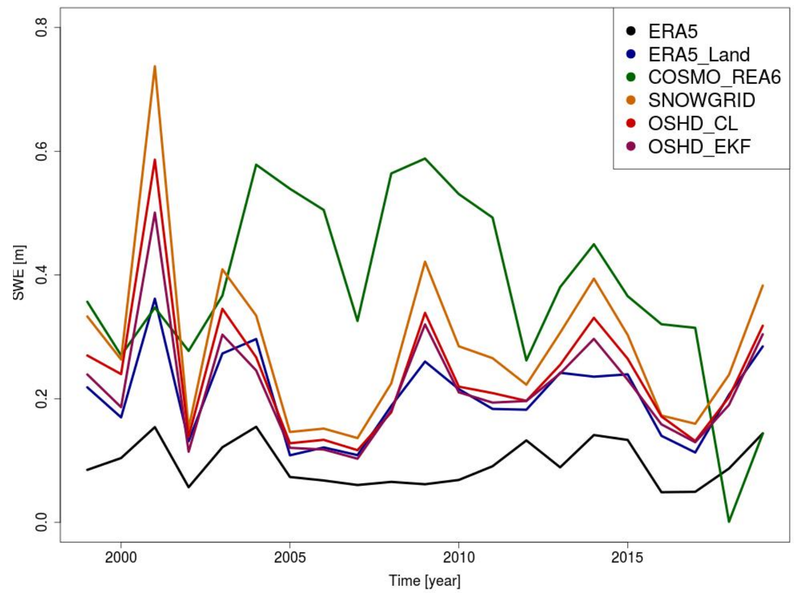

Figure 106: The climatology of SWE at elevation 2000-2500m from 1999-2019 in southern Switzerland.

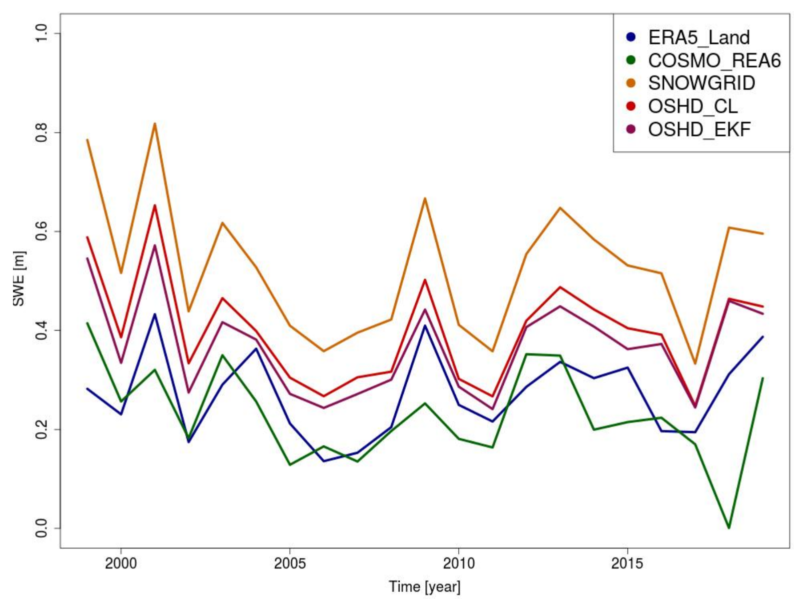

Figure 107: The climatology of SWE at elevation 2000-2500m from 1999-2019 in the Valais.

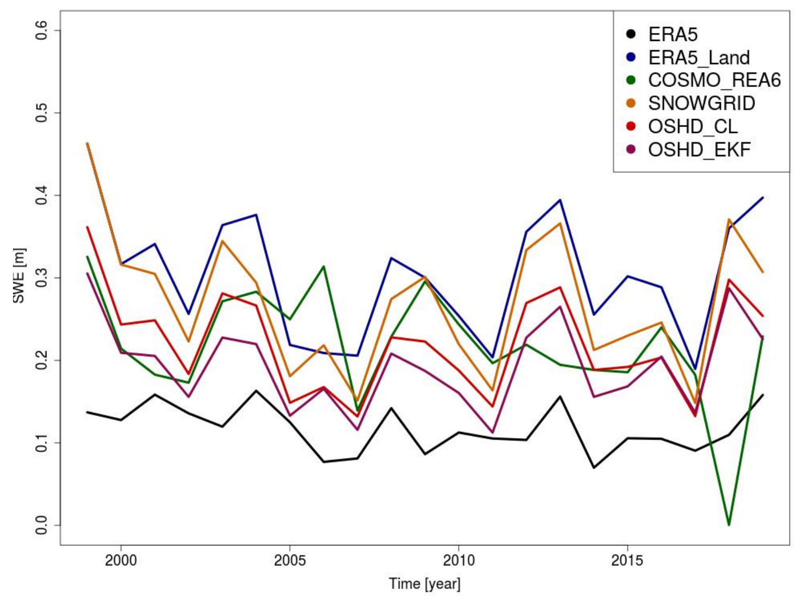

Figure 108: The climatology of SWE at elevation 2000-2500m from 1999-2019 in the western part of the northern flank of the Alps.

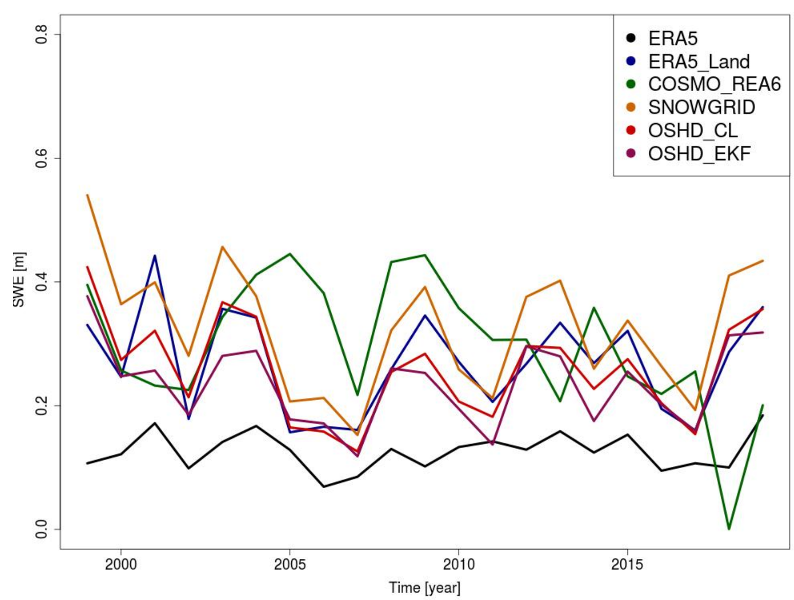

Figure 109: The climatology of SWE at elevation 2000-2500m from 1999-2019 in the central part of the northern flank of the Alps.

7.5.6 Elevation class 6

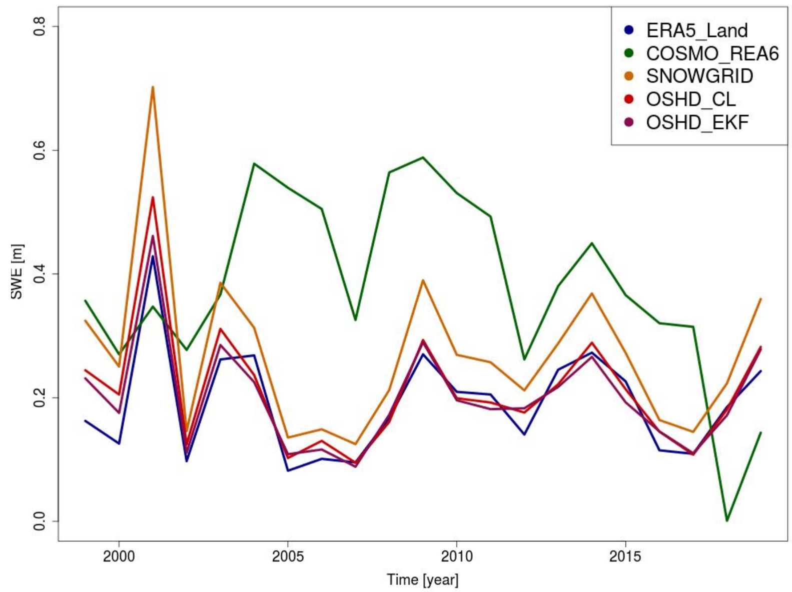

Figure 110: The climatology of SWE at elevation >2500m from 1999-2019 in the Engadine.

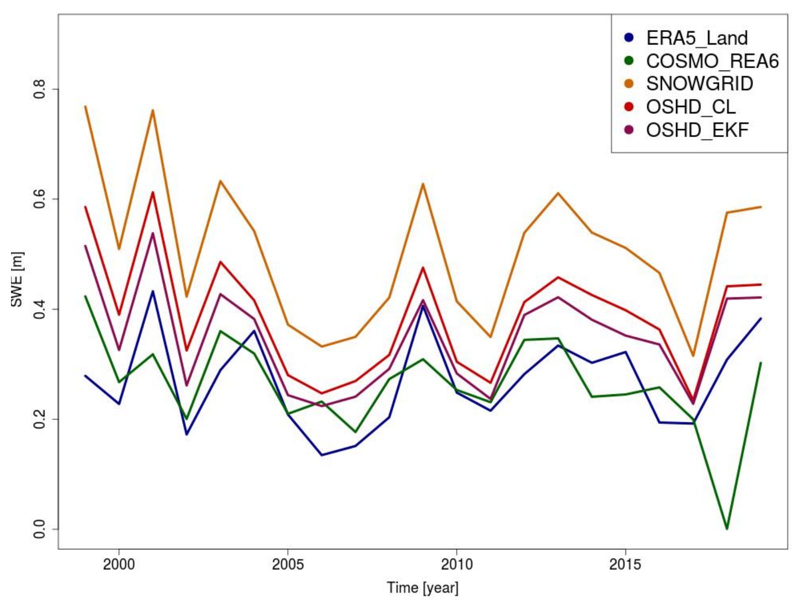

Figure 111: The climatology of SWE at elevation >2500m from 1999-2019 in northern Switzerland.

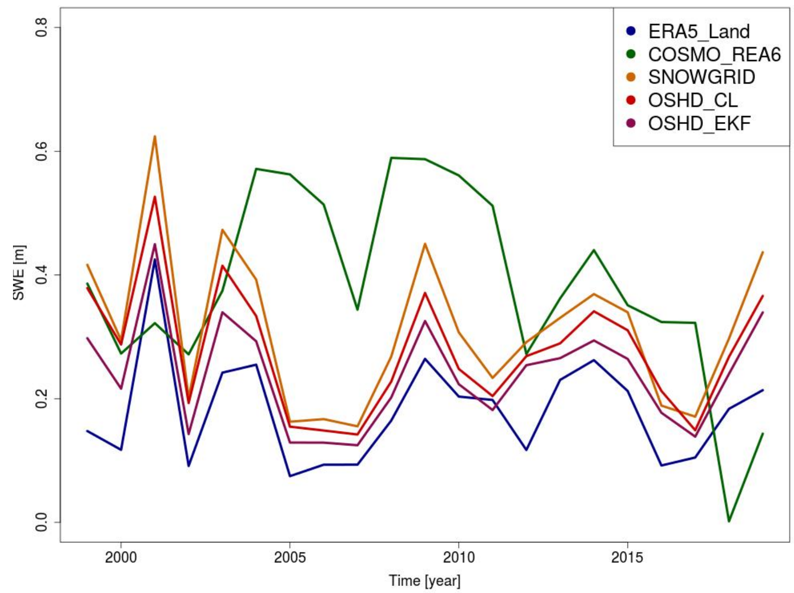

Figure 112: The climatology of SWE at elevation >2500m from 1999-2019 in Grisons.

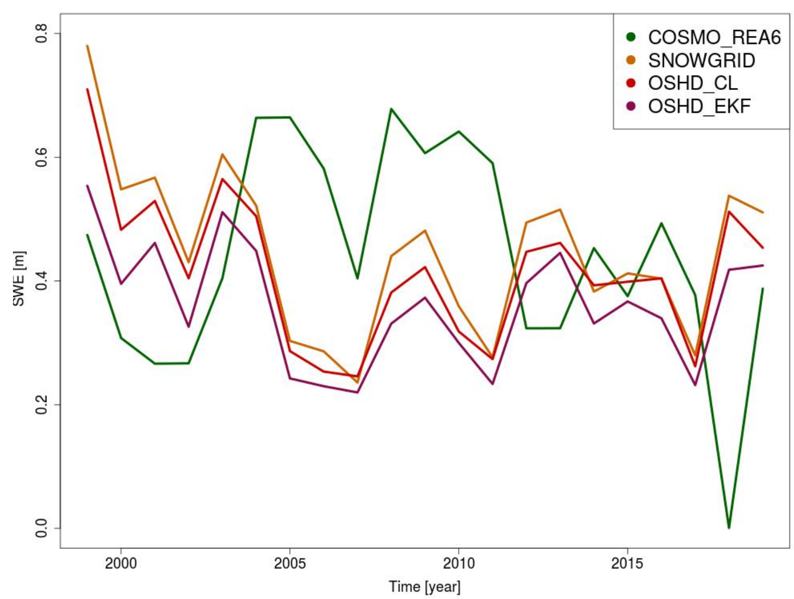

Figure 113: The climatology of SWE at elevation >2500m from 1999-2019 in the eastern part of the northern flank of the Alps.

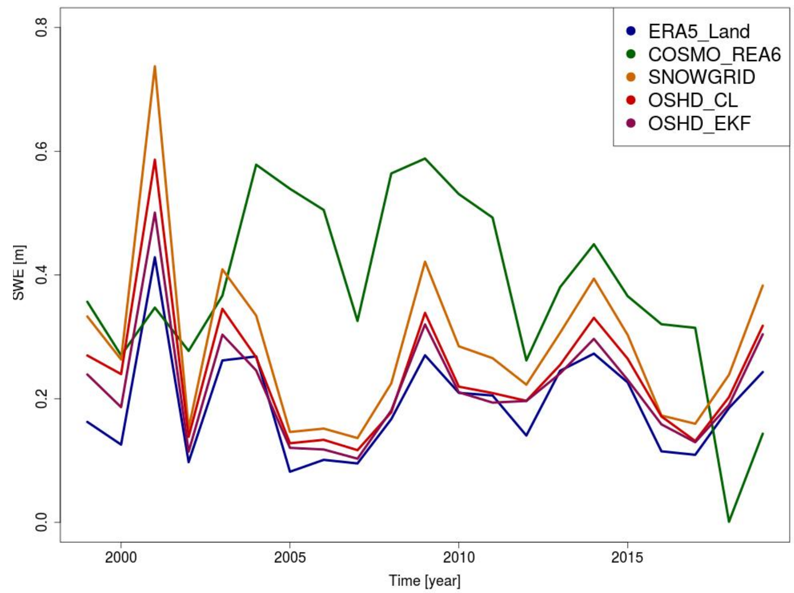

Figure 114: The climatology of SWE at elevation >2500m from 1999-2019 in southern Switzerland.

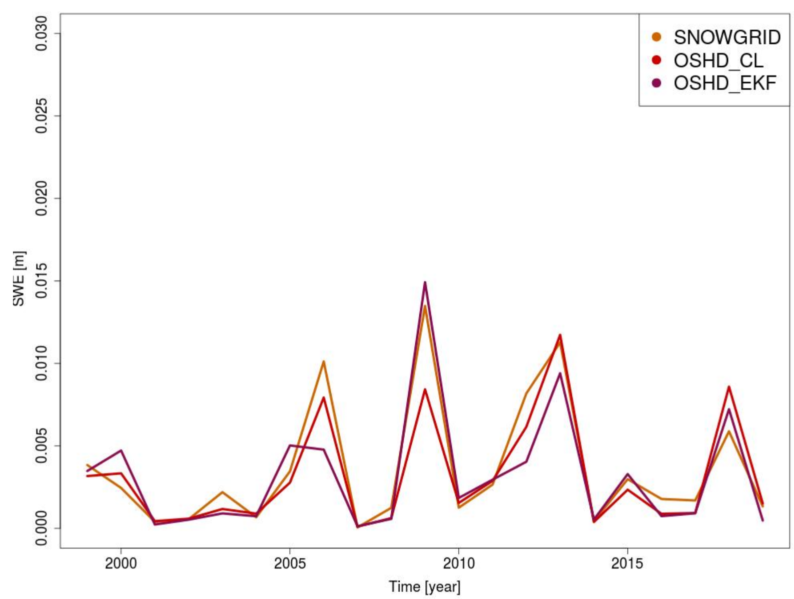

Figure 115: The climatology of SWE at elevation >2500m from 1999-2019 in the Valais.

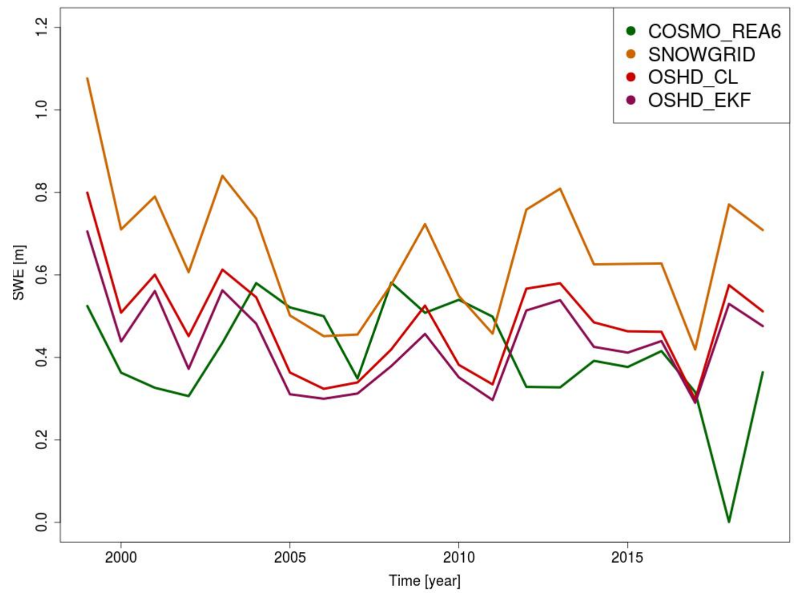

Figure 116: The climatology of SWE at elevation >2500m from 1999-2019 in the western part of the northern flank of the Alps.

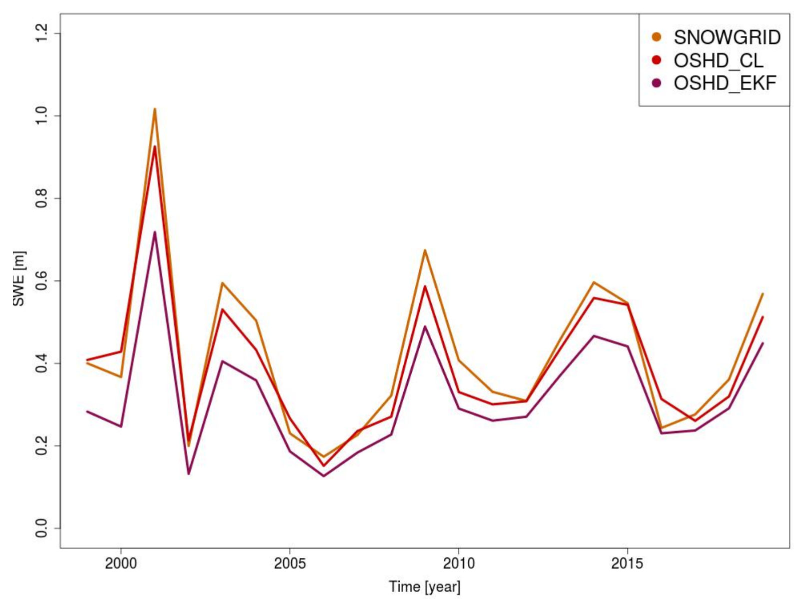

Figure 117: The climatology of SWE at elevation >2500m from 1999-2019 in the central part of the southern flank of the Alps.

Eidgenössische Technische Hochschule Zürich
Swiss Federal Institute of Technology Zurich

Declaration of originality

The signed declaration of originality is a component of every semester paper, Bachelor's thesis, Master's thesis and any other degree paper undertaken during the course of studies, including the respective electronic versions.

Lecturers may also require a declaration of originality for other written papers compiled for their courses.

I hereby confirm that I am the sole author of the written work here enclosed and that I have compiled it in my own words. Parts excepted are corrections of form and content by the supervisor.

Title of work (in block letters):

Spatial snow climatologies for Switzerland: Intercomparison and validation

Authored by (in block letters):
For papers written by groups the names of all authors are required.

Name(s):	**First name(s):**
Göldi	Monika

With my signature I confirm that
- I have committed none of the forms of plagiarism described in the 'Citation etiquette' information sheet.
- I have documented all methods, data and processes truthfully.
- I have not manipulated any data.
- I have mentioned all persons who were significant facilitators of the work.

I am aware that the work may be screened electronically for plagiarism.

Place, date	**Signature(s)**
St.Gallen, 7.4.2021	M.Göldi

For papers written by groups the names of all authors are required. Their signatures collectively guarantee the entire content of the written paper.